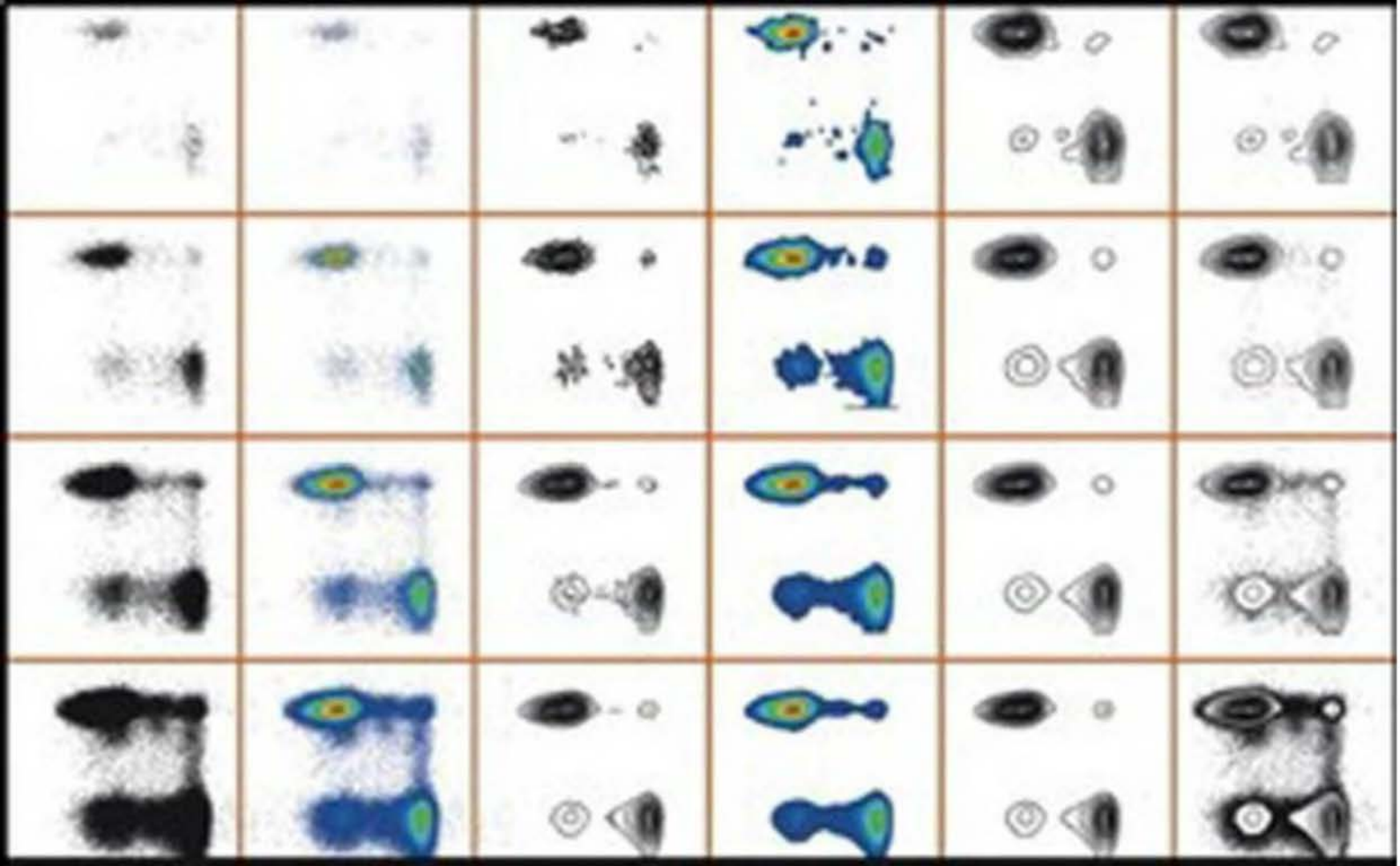


PRACTICAL FLOW CYTOMETRY

FOURTH EDITION

HOWARD M. SHAPIRO

CYTEK V. BECKMAN
PGR2025-00088
BECKMAN 2029
Part 1 of 2

PRACTICAL FLOW CYTOMETRY

Fourth Edition

HOWARD M. SHAPIRO

WILEY-LISS

A JOHN WILEY & SONS, INC., PUBLICATION

Copyright © 2003 by John Wiley & Sons, Inc. All rights reserved.

Published by John Wiley & Sons, Inc., Hoboken, New Jersey.

No part of this publication may be reproduced, stored in a retrieval system or transmitted in any form or by any means, electronic, mechanical, photocopying, recording, scanning or otherwise, except as permitted under Section 107 or 108 of the 1976 United States Copyright Act, without either the prior written permission of the Publisher, or authorization through payment of the appropriate per-copy fee to the Copyright Clearance Center, Inc., 222 Rosewood Drive, Danvers, MA 01923, (978) 750-8400, fax (978) 750-4470, or on the web at www.copyright.com. Requests to the Publisher for permission should be addressed to the Permissions Department, John Wiley & Sons, Inc., 111 River Street, Hoboken, NJ 07030, (201) 748-6011, fax (201) 748-6008, e-mail: permreq@wiley.com.

Limit of Liability/Disclaimer of Warranty: While the publisher and author have used their best efforts in preparing this book, they make no representation or warranties with respect to the accuracy or completeness of the contents of this book and specifically disclaim any implied warranties of merchantability or fitness for a particular purpose. No warranty may be created or extended by sales representatives or written sales materials. The advice and strategies contained herein may not be suitable for your situation. You should consult with a professional where appropriate. Neither the publisher nor author shall be liable for any loss of profit or any other commercial damages, including but not limited to special, incidental, consequential, or other damages.

For general information on our other products and services please contact our Customer Care Department within the U.S. at 877-762-2974, outside the U.S. at 317-572-3993 or fax 317-572-4002.

Wiley also publishes its books in a variety of electronic formats. Some content that appears in print, however, may not be available in electronic format.

Library of Congress Cataloging-in-Publication Data:

Shapiro, Howard M. (Howard Maurice), 1941
Practical flow cytometry / Howard M. Shapiro. 4th ed.
Includes bibliographical references and index.
ISBN 0-471-41125-6 (alk. paper)
1. Flow cytometry.
[DNLM: 1. Flow Cytometry. QH 585.5.F56 S529p 2002] I. Title.
QH585.5.F56 S48 2002
571.6'0287—dc21 2002002969

Printed in the United States of America.

10 9 8 7 6 5 4 3

CONTENTS

LIST OF TABLES AND FIGURES xxvii

PREFACE TO THE FOURTH EDITION: WHY YOU SHOULD READ THIS BOOK – OR NOT xxxiii

FOREWORD TO THE THIRD EDITION by Leonard A. Herzenberg xxxix

PREFACE TO THE THIRD EDITION xli

PREFACE TO THE SECOND EDITION xlv

FOREWORD TO THE FIRST EDITION by Louis A. Kamentsky xlvii

PREFACE TO THE FIRST EDITION xlix

1. OVERTURE 1

1.1 What (And What Good) Is Flow Cytometry? 1

Tasks and Techniques of Cytometry 1

Some Notable Applications 1

What is Measured: Parameters and Probes 2

1.2 Beginnings: Microscopy And Cytometry 2

A Little Light Music 4

Making Mountains out of Molehills: Microscopy 6

Why Cytometry? Motivation and Machinery 9

Flow Cytometry and Sorting: Why and How 10

Fluorescence and Flow: Love at First Light 11

Conflict: Resolution 12

1.3 Problem Number One: Finding The Cell(s) 14

Flow Cytometry: Quick on the Trigger 16

The Main Event 17

The Pulse Quickens, the Plot Thickens 17

1.4 Flow Cytometry: Problems, Parameters, Probes, and Principles 18

Counting Cells: Precision I (Mean, S.D., CV) 18

Poisson Statistics and Precision in Counting 19

Rare Event Analysis: The Fundamental Things Apply as Cells Go By 19

Count Constant Numbers for Constant Precision 20

Alternative Counting Aids: The Venerable Bead 20

And Now to See with Eye Serene the Very Pulse of the Machine: Display, Digitization, and Distributions 21

DNA Content Analysis: Precision II (Variance) 21

The Normal Distribution: Does the Word "Gaussian" Ring a Bell? 22

1.4 Flow Cytometry: Problems, Parameters, Probes, and Principles (continued)
Binned Data: Navigating the Channels ... 22
DNA Content: Problem, Parameter, Probes ... 23
One-Parameter Displays: Pulse Height Distributions ... 24
Mathematical Analysis of DNA Histograms: If It's Worth Doing, It's Worth Doing Well ... 25
Linear Thinking ... 26
Lineage Thinking: Sperm Sorting ... 26
Two-Parameter Displays: Dot Plots and Histograms ... 26
Multiparameter Analysis Without Computers: Gates Before Gates ... 27
Two-Parameter Histograms: Enter the Computer ... 29
Modern Multiparameter Analysis: List Mode ... 30
Three-Dimensional Displays: Can We Look at Clouds from Both Sides? No ... 32
Identifying Cells in Heterogeneous Populations: Lift Up Your Heads, Oh Ye Gates! ... 33
Cluster Headaches ... 34
Painting and White- (or Gray-) Washing Gates ... 34
The Quad Rant: Are You Positive? Negative! ... 35
Deals With the Devil: Logarithmic Amplifiers and Fluorescence Compensation ... 35
Evils of Axes: Truth in Labeling Cells and Plots ... 38
When Bad Flow Happens to Good Journals ... 40
Sorting Sorting Out ... 40
Parameters and Probes II: What is Measured and Why ... 42
Probes versus Labels ... 42
Living and Dyeing: Stains, Vital and Otherwise ... 43
Nucleic Acid (DNA and RNA) Stains ... 43
Fluorescence and Fluorescent Labels ... 44
Binary Fishin': Tracking Dyes Through Generations ... 45
Membrane Perturbation: A Matter of Life and Death? ... 46
Cytoplasmic/Mitochondrial Membrane Potential ... 46
Indicators of Cytoplasmic [Ca^{++}]: Advantages of Ratiometric Measurements ... 47
Finding Antigen-Specific Cells Using Tetramers ... 47
Hip, Hip Arrays: Multiplexing on Slides and in Bead Suspensions ... 48
GFP and its Relatives: Mild Mannered Reporters ... 48
Beyond Positive and Negative; Putting the –Metry in Cytometry ... 48
1.5 What's In the Box: Flow Cytometer Anatomy, Physiology, and Pathology ... 49
Light Sources for Microscopy and Flow Cytometry ... 49
Instrument Configurations: The Orthogonal Geometry ... 50
Laser Beam Geometry and Illumination Optics ... 50
Flow Chamber and Forward Scatter Collection Optics ... 51
Fluorescence and Orthogonal Scatter Optics ... 52
Optical Filters for Spectral Separation ... 52
Multistation Flow Cytometers ... 54
Photomultipliers and Detector Electronics ... 54
Putting the Flow in Flow Cytometry ... 55
Signal Processing Electronics ... 57
Is It Bigger than a Breadbox? ... 57
Flow Cytometer Pathology and Diagnostics ... 58
1.6 Alternatives to Flow Cytometry; Cytometer Ecology ... 59
1.7 The Rest Of The Book ... 60
Lis(z)t Mode ... 60

2. LEARNING FLOW CYTOMETRY ... 61
Learning from History: Take One ... 61
Who Should Read this Book? ... 62
2.1 Information Sources and Resources ... 62
Books on Flow Cytometry in General ... 62
Books on Flow Cytometric Methodology and Protocols ... 62

2.1 Information Sources and Resources (continued)
Clinical Flow Cytometry Books 63
Other Flow Cytometry Books 63
Flow's Golden Oldies 63
2.2 The Reader's Guide To Periodical Literature 64
2.3 Resources And Courses 66
Flow Cytometer Manufacturers 66
The International Society for Analytical Cytology 66
The Clinical Cytometry Society 66
The National Flow Cytometry Resource 66
"The Annual Courses" and Others 67
Other Societies and Programs 67
The Purdue Mailing List, Web Site, and CD-ROMs 68
2.4 Exploring The Foundations 68
Optics and Microscopy 68
Electronics69
Computers: Hardware and Software 69
Digital Signal Processing 70
Data Presentation and Display 70
Spectroscopy, Fluorescence and Dye Chemistry 71
Cell and Molecular Biology and Immunology 71
2.5 Alternatives To Flow Cytometry 71

3. HISTORY 73
3.1 Ancient History 73
Flow Cytometry: Conception and Birth 73
Staining Before and After Paul Ehrlich 74
Origins of Modern Microscopy 75
Making Cytology Quantitative: Caspersson et al 75
Origins of Cancer Cytology: The Pap Smear 76
The Fluorescent Antibody Method 77
Blood Cell Counting: Theory and Practice 77
Video and Electron Microscopy 78
Optical Cell Counters and the Coulter Orifice 78
3.2 Classical History 79
Analytical Cytology in the 1950's 79
The Cytoanalyzer 79
Acridine Orange as an RNA Stain: Round One 79
How I Got Into this Mess 79
The Rise of Computers 80
Computers in Diagnosis: A Central Problem 80
Diagnosis and Classification: Statistical Methods 80
Cytology Automation in the 1960's 81
First Steps toward Automated Differentials 81
Pattern Recognition Tasks in Cell Identification 82
Differential Leukocyte Counting: An Early Flow Systems Approach 83
Kamentsky's Rapid Cell Spectrophotometer 84
Fulwyler's Cell Sorter 85
3.3 Modern History 85
Cell Cycle Analysis: Scanning versus Flow Systems 85
Cancer Cytology: Scanning versus Flow Cytometry 86
Early Commercial Flow Cytometers 87
Not Quite Commercial: The Block Projects 89
The Evolution of Flow Cytometers in the 1970's 90
Dog Days: The Genesis of Cytomutts 93
The 1980's: Little Things Mean a Lot 94

3.3 Modern History (continued)
Measurements in the Main Stream ... 95
Immunofluorescence Comes of Age ... 95
Developments in DNA Content Analysis ... 96
Flow Cytometry of RNA Content ... 96
Measurements of Functional Parameters ... 97
Clinical Uses of Fluorescence Flow Cytometry ... 98
The End of History? ... 99

4. HOW FLOW CYTOMETERS WORK ... 101
4.1 Light and Matter ... 101
Introduction ... 101
Photometry versus Radiometry: What's in a Name? ... 101
Physical Measurement Units ... 101
Light in Different Lights ... 102
It's All Done With Photons ... 102
A Few Warm Bodies ... 103
Polarization and Phase; Interference ... 104
Light Meets Matter: Rayleigh and Mie Scattering ... 105
A Time for Reflection - and Refraction: Snell's Law ... 107
Polarization by Reflection; Brewster's Angle ... 107
Dispersion: Glass Walls May Well a Prism Make ... 108
Interference in Thin Films ... 108
Interference and Diffraction; Gratings ... 108
Optical Activity and Birefringence ... 109
Matter Eats Light: Absorption ... 109
Absorption: Counting the Calories ... 110
A Selective Diet ... 110
The Chance of a Lifetime ... 110
Spinning a Tale of Degeneracy ... 111
Facing Extinction: Cross Section and Optical Density ... 111
Unexciting Times: Emigrating from the Excited States ... 112
Fluorescence: Working the Stokes Shift ... 112
Phosphorescence ... 113
Fluorescence Polarization ... 114
Stimulated Emission ... 114
Resonance Energy Transfer ... 115
Quenching, Bleaching, and Photon Saturation ... 115
Quantum Flotsam and Jetsam ... 118
Inelastic Scattering and Doppler Measurements ... 118
Raman Scattering ... 118
Nonlinear Optics and Harmonic Generation ... 118
Two-Photon and Multiphoton Excitation ... 118
4.2 Optical Systems ... 119
Light Propagation and Vergence ... 119
Image Formation by Optical Systems: Magnification ... 119
Lens Types and Lens Aberrations ... 120
Numerical Aperture and Lens Performance ... 121
Gradient Index, Fresnel, and Cylindrical Lenses ... 122
The Helmholtz Invariant and Throughput ... 123
Photons in Lenses: See How They Run ... 123
Aperture and Field Stops: The f Number ... 124
Depth of Field and Focus and Resolution of Lenses ... 124
4.3 Light Sources ... 124
The Best and the Brightest ... 124

4.3 Light Sources (continued)
Harc, Harc, the Arc! 126
Quartz Halogen Lamps 127
Light Emitting Diodes (LEDs) 127
Illumination Optics for Lamps and LEDs 127
Arc Source Epiillumination for Flow Cytometry 128
Lasers as Light Sources for Flow Cytometers 129
Laser Illumination: Going to Spot 130
Shedding Light on Cells: Lasers, Lamps, and LEDs 131
Lasers: The Basic Physics 133
Einstein on the Beam: Stimulated Emission 133
Look, Ma, One Cavity: Optical Resonators 133
Laser Action à la Mode 134
Pumping Ions 135
Laser Efficiency: Your Mileage May Vary 135
Mirrors and Prisms for Wavelength Selection 135
Brewster Windows for Polarized Output 135
Laser Power Regulation: Current and Light Control 136
Beam Profiles and Beam Quality 136
Puttin' on My Top Hat? 138
Harmonic Generation and Modulation 138
Lasers Used and Usable in Cytometry 138
Argon and Krypton Ion Lasers 138
Dye Lasers 141
Helium-Neon Lasers 141
Helium-Cadmium and Helium-Selenium Lasers 142
Diode Lasers: Red, Infrared, Violet, and UV 142
Solid-State Lasers: Like, YAG Me! 145
Laser and Light Source Noise and Noise Compensation 147
Fifty Ways to Lose Your Laser 148
Danger!!! Laser!!! Hazards and Haze 148
4.4 Light Collection 149
Microscope Objectives 149
Looking at the Observation Point 150
Stops versus Blockers 150
Signal versus Noise: To See or Not to See 150
Spectral Selection: Monochromators versus Filters 152
Monochromators and Polychromatic Detection 152
Interference Filters: Coatings of Many Colors 153
Absorptive Filters versus Interference Filters 153
Filter Transmission Characteristics 154
Dichroics 155
Neutral Density Filters 156
Beamsplitters; Ghosts and Ghostbusters 156
Optics for Polarization Measurements 156
Tunable Filters 157
Fiber Optics and Optical Waveguides 157
Through a Glass Darkly: Light Lost (and Found) in Optical Components 158
Collection Optics for Forward Scatter Signals 159
4.5 Detectors 160
Silicon Photodiodes 160
Photomultiplier Tubes (PMTs) 161
Sensitivity Training: Photodiode versus PMT 163
Single Photon Counting 164
Avalanche Photodiodes (APDs) 164
PMTs: Picking a Winner 165

4.5 Detectors (continued)
Photomultipliers: Inexact Science ... 166
Charge Transfer Devices: CCDs, CIDs, Etc. ... 166
4.6 Flow Systems ... 166
Flow System Basics ... 167
Gently Down the Stream: Laminar Flow ... 167
Flow Chambers; Backflushes, Boosts, and Burps ... 169
Cuvettes versus Streams for Analysis and Sorting ... 170
Light Collection from Streams and Cuvettes ... 171
When You've a Jet ... 174
Core and Sheath: Practical Details ... 175
Grace Under Pressure: Driving the Sheath and Core ... 175
Perfect Timing: Fluidics for Kinetic Experiments ... 177
Oriented and Disoriented Cells ... 178
Matchmaker, Matchmaker, Make Me a(n) Index Match! ... 178
Flow Unsheathed ... 178
Flow Systems: Garbage In, Garbage Out ... 178
4.7 Electronic Measurements ... 180
Electricity and Electronics 101 ... 180
Charge Separation, Electric Fields, and Current ... 180
Resistance, Voltage, and Power; Ohm's Law ... 181
Alternating and Direct Current; Magnetism ... 181
Inductance, Reactance, Capacitance, Impedance ... 182
The Coulter Principle: Electronic Cell Sizing ... 182
Electrical Opacity: AC Impedance Measurement ... 183
4.8 Analog Signal Processing ... 183
Beam Geometry and Pulse Characteristics ... 183
Electronics 102: Real Live Circuits ... 184
Circuits: Current Sources and Loads ... 184
Ground Rules ... 185
Couplings, Casual and Otherwise; Transformers ... 186
Power Supplies ... 187
Active Electronics: Tubes, Transistors, ICs ... 188
Analog Nirvana: Operational Amplifiers ... 189
Detector Preamplifiers and Baseline Restoration ... 190
Analog Pulse Processing: Front Ends and Triggering ... 191
Peak Detectors ... 192
Pulse Integral or Area Measurements ... 194
Pulse Width Measurement Circuits ... 195
Analog Pulse Processing: The Bottom Line ... 195
Dead Times, Doublets, and Problem Pulses ... 196
Trigger Happy? ... 196
Analog Linear, Log and Ratio Circuits ... 197
Linear Circuits; Fluorescence Compensation ... 197
Logarithmic Amplifiers and Dynamic Range ... 199
Twin Peaks: Distributions on Linear and Log Scales ... 200
Falling Off a Log: Log Amps Behaving Badly ... 201
Limits to Dynamic Range ... 202
Ratio Circuits ... 204
4.9 Digital Signal Processing ... 204
Analog-to-Digital Conversion ... 204
Free Samples? Hold it! ... 205
Quantization: When Are Two Bits Worth a Nickel? ... 205
Analog-to-Digital Converters (ADCs) (and Digital-to-Analog Converters (DACs)) ... 208
Digital Pulse Processing and DSP Chips ... 209

4.9 Digital Signal Processing (continued)
The Screwy Decibel System....211
Pulse Slicing: Déjà Vu All Over Again....212
In Defense of dc Fence....213
Digitization: Tying it All Together....214
4.10 Performance: Precision, Sensitivity, and Accuracy....214
Precision; Coefficient of Variation (CV)....214
Sensitivity I: Minimum Detectable Signal....215
Sensitivity II: MESF Units....216
Accuracy I: Linearity and Nonlinearity....217
Sensitivity III: What's All the Noise About?....217
Sensitivity IV: More Photons Give Better Precision....218
Sensitivity V: Background Effects....218
Sensitivity VI: Electrons Have Statistics, Too....218
Source Noise Fluctuations and Performance....219
I Blurred It Through the Baseline....219
Restoration Comedy: The Case of the Disappearing Leukocytes....220
Top 40 Noise Sources....221
Sensitivity 007: Q and B (Dye Another Day?)....221

5. DATA ANALYSIS....225
5.1 Goals and Methods in Data Analysis....225
Cell Counting....225
Characterization of Pure Cell Populations....226
Identification of Cells in Mixed Populations....226
Characterization of Cell Subpopulations....226
Data Analysis Hardware and Software Evolve....226
5.2 Computer Systems for Flow Cytometry....227
The Beginning....227
The End of the Beginning....227
Data Rates and Data Acquisition Systems....228
PC Data Acquisition Boards....229
Preprocessors for Data Acquisition....230
5.3 Primary Data: Frequency Distributions....231
You Say You Want a Distribution....231
Gauss Out of Uniform....231
About Binomial Theorem, I'm Teeming With a Lot o' News....232
Distributions Have Their Moments....233
Statistical versus Cytometric Parameters....233
Mean, Variance, and Standard Deviation....233
With Many Cheerful Facts About the Square of the Hypotenuse: Euclidean Distance....234
Higher Moments; Skewness and Kurtosis....234
Some Features of the Normal Distribution....234
Measures of Central Tendency: Arithmetic and Geometric Means, Median, and Mode....235
Measures of Dispersion: Variance, Standard Deviation, CV, and Interquartile Range....235
Robustness in Statistics; the Robust CV....235
"Box-and-Whiskers" Plots of Distributions....236
Calculating and Displaying Histograms....236
Bivariate and Multivariate Distributions and Displays....237
Dot Plots; Correlation and Covariance....237
Linear Regression; Least-Squares Fits....237
Breaking off Undiplomatic Correlations....238
Multivariate Measures of Central Tendency and Dispersion....238
Beyond Dot Plots: Two-Parameter Histograms....238
Bivariate Distributions: Display's The Thing!....238
Displaying by the Numbers....239

5.3 Primary Data: Frequency Distributions (continued)
Economies of Scale ... 240
How Green Were My (Peaks and) Valleys ... 241
Clouds on the Horizon: 3-Dimensional Displays ... 241
5.4 Compensating Without Decompensating ... 242
5.5 Dealing With the Data ... 244
Comparing and Analyzing Univariate Histograms ... 244
The K-S Test, Clonal Excess, and χ^2 Tests ... 245
"Nonparametric" Histogram Comparison ... 245
Cumulative (Overton) Subtraction ... 245
Constant CV Analysis ... 245
Another Approach to Histogram Comparison ... 246
Deconvoluting Single-Parameter Histograms ... 246
Analysis of Two-Parameter Data ... 246
Two-Parameter Gating, Bitmap and Otherwise ... 246
Rectangles and Quadrilaterals: Hardware and Software Gating: ... 246
Ellipses and Beyond: Advantages of Bitmaps ... 246
Storage Requirements for Bitmaps ... 247
Analysis of Two-Parameter Distributions ... 247
See You Around the Quad ... 247
Bivariate Cell Kinetic Analysis ... 247
Bivariate Karyotype Analysis ... 247
Smooth(ing) Operators: When are Filters Cool? ... 248
Bivariate Analysis in Hematology Analyzers ... 248
5.6 Multiparameter Data Analysis ... 248
Multiparameter versus Multivariate Analysis ... 248
Multiparameter Analysis of Leukocyte Types: 1974 ... 248
Automated Differentials via Discriminants ... 249
Interactive Analysis: Finding the Training Set ... 249
Multiparameter Analysis of Leukocyte Types: 2002 ... 250
Procedures for Automated Classification ... 250
Discriminant Functions and How They Work ... 250
Principal Component Analysis ... 252
Cluster Analysis ... 252
Neural Network Analysis ... 252
Genetic Algorithms ... 253
5.7 Analysis of Collected Data: How Much Is Enough / Too Much? ... 253
5.8 Data Analysis Odds and Ends ... 254
Data Storage ... 254
The Flow Cytometry Standard (FCS) File Format ... 254
Magnetic/ Optical Tumors in the Digital Attic ... 255
Linear and Log Scales and Ratios: Proceed with Care! ... 255
Ratios Only Help if Variables are Well Correlated ... 256

6. FLOW SORTING ... 257
6.1 Sort Control (Decision) Logic ... 257
6.2 Preselected Count Circuits and Single Cell Sorting ... 258
6.3 Droplet Sorting, High-Speed and Low ... 258
Droplet Generation ... 259
Drop Charging and Deflection ... 260
Drop Deflection Test Patterns ... 260
Two- and Four-Way Sorts: How Much Voltage? ... 260
How Many Drops Should be Charged? ... 261
Guilty as Charged? ... 261
Determining Droplet Delay Settings ... 262
Fractional Droplet Delays ... 262

6.3 Droplet Sorting (continued)
Transducers and Transducer Drive Signals....263
Improving Droplet Sorting....263
Sorting Large Objects with Droplet Sorters....263
6.4 Fluidic Switching Cell Sorters....264
Sorting Large Objects Using Fluidic Switching....265
Sorting Very Small Objects: Microfluidic Switching....266
6.5 Cell Manipulation By Optical Trapping....266
6.6 Cell Damage Cell Selection ("Cell Zapping")....266
Photodamage Cell Selection....266
Sorting (Zapping) Without Flow (Gasp!)....267
Electrodamage Cell Selection in Flow....267
6.7 Measures of Cell Sorter Performance: Purity, Recovery (Yield), and Efficiency....267
Coincidence Effects on Performance....267
6.8 Other Considerations....268
Doing the Math....268
Speed Limits: The Reynolds Rap....269
Instrument Utilization....269
Monitoring versus Sorting for Cell Preparation....269
Collection Techniques: Life and Death Decisions....269
Dilutions of Grandeur....270
Can Getting Sorted Be Hazardous to Cells' Health?....270
6.9 Biohazard Control and Biosafety in Flow Cytometers and Sorters....271
6.10 Conclusions....271

7. PARAMETERS AND PROBES....273
7.1 Physical Parameters and Their Uses....273
Electrical Parameters....273
DC Impedance (Coulter Volume)....273
AC Impedance (Electrical Opacity); Capacitance....273
Acoustic Measurements of Cells in Flow....274
Optical Parameters: Light Scattering....274
Scattering: The Mueller Matrix Model....274
Forward Light Scattering and Cell Size....275
Forward Scatter and "Viability"....276
Side Scatter and Cytoplasmic Granularity....276
Lymphocyte Gating: Forward Scatter Aside....276
Other Applications of Side Scatter....277
What is the Right Angle for "Right Angle" Scatter?....278
Does Side Scatter = Total Protein?....278
Optimizing Side Scatter: Not as Easy as It Looks....270
Polarized 90° Scatter Reveal Eosinophils and Malaria Pigment-Containing Monocytes....278
Multiple Wavelength Scattering Measurements....279
From Russia with Lobes....279
Optical Parameters: Absorption....281
Absorption Effects on Light Scattering....281
Optical Parameters: Extinction....282
Other Transmitted Light Measurements....282
Interference and Phase Measurements....282
Optical Parameters: Fluorescence....283
Fluorescence Lifetime Measurements....283
Fluorescence Polarization Measurements....283
Energy Transfer Measurements: Something to FRET About....283
Quenching and Energy Transfer....284
Measuring Fluorescence Spectra in Flow....284

Optical Parameters: Fluorescence
Two-Photon Fluorescence Excitation in Flow 284
Bioluminescence detection in Flow? 284
7.2 Intrinsic Cellular Parameters 285
Cell Size 285
Mean Cell Volume: The Cellocrit as Gold Standard 285
Cell Volume, Area, and Diameter 285
Cell Sizing: Slit Scans and Pulse Widths 285
Size Measurements in the Submicron Range 288
Other Size Measurement Techniques 289
Cell Shape and Doublet Discrimination 289
Measurement of Intrinsic Parameters Using Absorption and Extinction Signals 290
Fluorescence Measurement of Intrinsic Parameters 290
Autofluorescence: Pyridine and Flavin Nucleotides 290
Pyridine and Flavin Nucleotides and Redox State 291
Pyridine and Flavin Nucleotides and Cancer 291
Bacterial Autofluorescence Measurements 291
Bacterial Autofluorescence Measurements 291
Porphyrin Fluorescence in Erythroid Cells 292
Other Pigments 292
Chlorophyll and Phycobiliproteins 292
Infrared Spectra and Cancer Diagnosis 293
7.3 Probes, Labels, and [Not] Protocols for Extrinsic Parameter Measurements 293
Probes, Labels, and Dyes 293
Dyes and Quality Control: Gorillas in the NIST 294
The Dyes are Cast: An Overview 295
Mechanisms of Staining by Fluorescent Dyes 298
Environmental Sensitivity 298
Metachromasia 298
Spectral Changes and Ratiometric Measurements 299
Internal Energy Transfer in Probes and Labels 299
"Vital" Staining 299
Staining and "Viability" 299
"Intact" versus "Live" Cells 299
Getting Dyes Into – and Out of – Intact Cells 300
Permeancy and Permeability 300
Vital Dye Toxicity and Photosensitization of Cells 301
Fixation – Why and How 302
Fixation for Biohazard Control 302
Fixation Mechanisms 302
Permeabilization versus Fixation 302
Fixative Effects on Scatter Signals 303
Fixation for Surface Antigen Measurements 303
Fixatives: Coming Out of Aldehyding Places 304
Fixation for Intracellular Antigen Measurements 305
Fixation for DNA Content Determination: Getting DNA (and Antigens) Out of a Tight Fix 305
Catch the Wave: Fixation by the (Cook) Book 305
Fixation Artifacts 305
Red Blood Cell Lysis: The Distilled Essence 306
7.4 Nucleic Acid Dyes and Their Uses 306
DNA Content Measurement 306
Feulgen Staining for DNA Content 306
DNA Staining with Ethidium and Propidium 306
Ethidium & Propidium: Ionic Strength Effects 307
DNA Content: Sample Preparation and Standards 307
Chromomycin A_3, Mithramycin, and Olivomycin 307

Mithramycin Plus Ethidium: Do's and Don'ts....308
DNA Content Measurement (continued)
The Hoechst Dyes (33258, 33342, 34580?)....308
Detecting BrUdR by Hoechst Dye Quenching....308
Hoechst Dyes Have an A-T Base Preference....308
Hoechst Dyes In – And Out Of – Living Cells: The Drug Efflux Pump Discovered....309
Hoechst Dye Staining Mechanisms....309
Hoechst 34580: Violet Time?....310
DAPI (and DIPI): Dyes Known for Precision....310
Determinants of High Precision in DNA Analysis....311
7-Aminoactinomycin D (7-AAD)....311
Acridine Orange....312
Styryl Dyes; LDS-751....312
Cyanine Dyes I: Thiazole Orange, etc.....312
Cyanine Dyes II: TO'TO and YOYO à GoGo....314
Cyanine Dyes III: Alphabet Soup....315
Seeing Red: LD700, Oxazine 750, Rhodamine 800, TO-PRO3, and DRAQ5 as DNA Stains....315
Miscellaneous DNA-Selective Dyes....316
What Do DNA Stains Stain?....316
DNA Ploidy and Aneuploidy: The DNA Index....317
Sample Preparation for DNA Content Analysis....317
DNA Base Composition....317
Chromatin Structure; Identifying Cells in Mitosis....319
Chromatin Structure Identifies Mitotic Cells....320
RNA Content....320
RNA/DNA Staining with Acridine Orange (AO)....320
Cell Cycle Compartments Defined on the Basis of RNA and DNA Content....320
AO: Problems and Some Solutions....321
Pyronin Y, Oxazine 1, and Other Tricyclic Heteroaromatic Dyes as RNA Stains....322
What Does Pyronin Y Stain? Double-Stranded (Ribosomal) RNA and Sometimes Mitochondria....323
Surviving Vital Staining with Pyronin Y....324
Other DNA Dyes Usable with Pyronin Y....324
Tips on Tricyclics (Don't Get Depressed)....325
Tricyclics Gag on Mucopolysaccharides....325
Reticulocyte Counting: Cyanines Beat Tricyclics; RNA in Nucleated Cells: Cyanines Don't....326
Propidium Stains Double-Stranded RNA: What of Other Dyes?....326
7.5 Fluorescent Labels and Protein Dyes....326
Estimating Total and Basic Protein Content of Cells....327
Fluorescein Isothiocyanate (FITC)....327
Sulforhodamine 101 (SR101)....327
Hematoporphyrin (HP) as a Protein Stain....328
Rhodamine 101 (or 640) as a Vital Protein Stain....328
Staining to Demonstrate Basic Protein....328
Covalent Labels for Antibodies and Other Molecules....328
Fluorescein Isothiocyanate (FITC) as a Label....329
Labeling with Lissamine Rhodamine B and Tetramethylrhodamine Isothiocyanate (TRITC)....329
Multicolor Fluorescence I: FITC and TRITC....329
Multicolor Fluorescence II: Rhodamine 101 Dyes....330
Early Problems with Multicolor Fluorescence....331
Phycobiliproteins to the Rescue!....331
Phycoerythrins: R-PE, B-PE and Others....332
Allophycocyanin (APC) and APC-B....332
Phycocyanins....332
Phycobiliprotein Tandem Conjugates: PE-APC, PE-Texas Red, PE-Cy5, PE-Cy5.5, PE-Cy7, etc....333
Allophycocyanin Tandem Conjugates: APC-Cy7 and APC-Cy5.5....333

Phycobiliproteins to the Rescue! (continued)
Mercy Me! PerCP! ... 333
Phycobiliproteins and Tandems: Dirty Little Secrets ... 334
Future Tandems: Heterocycles Built for Two? ... 335
Cyanine Dye Labels: From Cy-Fi to Hi5 for Cy5 ... 336
Blue Notes: AMCA and Cascade Blue ... 337
Hey, BODIPY! ... 337
Alexa Dyes: Some Thoughts on Dyemographics ... 338
Other Organic Fluorescent Labels: A Dye Named Joe, etc. ... 338
Quantum Dots ... 339
Getting Labels Onto Molecules of Interest ... 340
7.6 Improving Signals from Labels: Amplification and Other Techniques ... 340
Limits to Sensitivity: Autofluorescence ... 341
Improving Sensitivity: The New Wave(length) ... 342
Correcting and Quenching Autofluorescence ... 342
Raman Scattering Effects on Sensitivity ... 342
Increasing Sensitivity: Amplification Techniques ... 343
Amplification by Indirect Staining ... 343
Amplification Using Labeled Particles ... 343
Amplification Using Enzymes as Labels: Playing the Hole CARD ... 344
Amplifying the Analyte: The Polymerase Chain Reaction (PCR) ... 344
Amplification Techniques: Pros and Cons; Fluorescent versus Nonfluorescent Labels ... 344
Improving Sensitivity: Time-Resolved Fluorescence ... 345
7.7 Measuring Cell Surface and Intracellular Antigens ... 345
History and Background ... 345
Monoclonal Antibodies for the Uninitiated ... 346
Cell Surface Antigens: Structure versus Function ... 347
Moving Toward Multicolor Immunofluorescence ... 347
Antibody Reagents and Staining Procedures ... 348
Antibody Fragments versus Antibodies as Reagents ... 348
Engineered Antibodies: Phage Display and scFvs ... 348
Molecular Probes' Zenon Antibody Labeling ... 348
Antibody Shelf Life and Quality Control ... 349
Direct Staining Using Monoclonal Antibodies for 2, 3, and More Colors Using 488 nm Excitation. 349
Multicolor Work Using Multiple Lasers; Biotin-Avidin Labeling ... 349
Mixing Colors: Do's and Don'ts ... 349
Cocktails for Five: Multiplex Immunofluorescence ... 350
Cocktail Staining Helps Identify Rare Cells ... 352
Immunofluorescence Staining Procedures ... 352
Automated Sample Preparation ... 353
Fluorescence Measurements: Lurching Toward Quantitation ... 353
Calibration and Controls: Round One ... 353
Quantitative Fluorescence Cytometry: Definitions ... 354
Calibration Particles for QFCM ... 354
Defining a Window of Analysis ... 356
Type IIA versus Type IIIB and IIIC Standards ... 357
Other Aspects of Fluorescence Quantitation ... 358
What is "Positive"? What is "Negative"? ... 358
Making Weakly Fluorescent Beads and Cells: Do Try This Trick at Home! ... 358
Correlating Cytometry and Biochemistry: Studies of Antibody Binding Chemistry ... 359
Correlating Cytometry and Biochemistry: Intracellular Antigen Measurements ... 359
Analyzing Immunofluorescence Data ... 360
Estimating Antigen or Receptor Surface Density ... 360
Quantitative Fluorescence: Problems and Prospects ... 361
7.8 Nucleic Acid Sequence Detection ... 361
Peptide Nucleic Acid (PNA) Probes ... 362

7.9 Probes for Various Cell Constituents 362
Surface Sugars (Lectin Binding Sites 362
Analysis of Total Carbohydrate Content 363
Specific Detection of Cellulose 363
A Probe for Cell Surface Aldehydes 363
Probes for Lipids and Cholesterol 364
Nile Red 364
Filipin 364
Lipid Droplet Detection Using Scatter Signals 364
Probes for Cytoskeletal Organization/Actins 364
7.10 Time as a Parameter: Kinetic Measurements 364
Sample Handling for Kinetic Measurements 365
Time as a Quality Control Parameter 366
Slooowww Flooowww 366
7.11 Labeled Ligand Binding 366
Labeling Strategies 367
Formal Analysis of Ligand binding 367
Labeled Ligands versus Anti-Receptor Antibodies 368
Ligand Binding Detected by Functional Changes 368
Fluorescent Ligand Binding: Some Examples 368
7.12 Functional Parameters I 369
Cell Surface Charge 369
Cell Membrane Characteristics 369
Membrane Integrity versus "Viability": Dye Exclusion Tests 369
Detecting "Dead" Cells in Fixed Samples 369
Membrane Fusion and Turnover; Cell Tracking 371
Cell Proliferation Analyzed Using Tracking Dyes 371
Membrane Organization and Fluidity/Viscosity 374
Lipid Packing Assessed with Merocyanine 540 374
Membrane Fluidity and Microviscosity: Assessment Using Fluorescence Polarization 374
Lipid Peroxidation 375
Membrane Permeability to Dyes and Drugs: The Drug Efflux Pump Revisited 376
Endocytosis of Macromolecules and Particles 377
Enzyme Activity 378
Indicators of Oxidative Metabolism I: Tetrazolium Dye Reduction 379
Indicators of Oxidative Metabolism II: 2,7-Dichlorofluorescin Diacetate (DCFH-DA), etc. 379
Indicators of Oxidative Metabolism III: Hydroethidine (Dihydroethidium) 379
Indicators of Oxidative Metabolism IV: Dihydrorhodamine 123 379
Indicators of Oxidative Metabolism V: Detection of Hypoxic Cells 380
Detection of Caspase Activity 380
Other Enzymes 380
Detection of Enzymes and Products by Antibodies 380
Enzyme Kinetics in Single Cells 380
Sulfhydryl (Thiol) Groups; Glutathione 381
7.13 Functional Probes II: Indicators of Cell Activation 381
Introduction 381
Changes in the Cellular Ionic Environment Following Activation by Ligand Interaction with Cell Surface Receptors 382
"Structuredness of Cytoplasmic Matrix" (SCM) and the Cercek Test for Cancer 383
Optical Probes of Cell Membrane Potential 385
Membrane Potential and Its Physicochemical Bases 385
$\Delta\Psi$ Measurement Using Microelectrodes 386
Single Cell Measurements with Distributional Probes 387
Oxonol Dyes as Membrane Potential Probes 390
Possible Alternatives to Distributional Probes for Flow Cytometry of Membrane Potentials 391
Ratiometric Probes for Membrane Potential 391

Optical Probes of Cell Membrane Potential (continued)
Using Cyanine Dyes for Flow Cytometric $\Delta\Psi$ Estimation, In Case You're Still Interested 392
Cytoplasmic Membrane Potential: Summing Up 394
Mitochondrial Membrane Potential ($\Delta\Psi_m$) 394
Mitochondrial Staining with Rhodamine 123 Is Membrane Potential-Dependent 394
The Search for Better $\Delta\Psi_m$ Probes: Round One 397
$\Delta\Psi_m$, JC-1, and Apoptosis 397
The Search for Better $\Delta\Psi_m$ Probes: Round Two 398
Bacterial Membrane Potentials 400
Ratiometric $\Delta\Psi$ Measurement in Bacteria 401
$\Delta\Psi$ Measurement: Cautions and Conclusions 402
Optical Probes of Intracellular Calcium 402
The Bad Old Days 402
Chlortetracycline as a Probe of "Membrane-Bound" Calcium in Cells 402
Probes for Free Cytoplasmic Calcium: Quin-2 403
Fura-2 and Indo-1: Ratiometric Ca^{++} Indicators 403
Fluo-3 and Other Visible-Excited Ca^{++} Probes 404
Flow Cytometric Probes of Intracellular pH 405
The Hat Trick: Multiparameter Approaches to Ion Flux Measurements in Cell Activation 407
NOsing Around for Nitric Oxide 408
Other Ions in the Fire 408
7.14 Reporter Genes 408
Somebody Cloned My Gal: Enzymes as Reporter Genes 408
Green Fluorescent Protein (GFP) et al 409
Minority Report(er)? 410

8. BUYING FLOW CYTOMETERS 411
8.1 Introduction 411
8.2 History 411
8.3 BD Biosciences 412
Background 412
The BD FACS Vantage SE™ Cell Sorter 413
The BD FACSCalibur™ Analyzer 414
The B-D™ LSR II Analyzer 416
The B-D FACSAria™ Cell Sorter 417
The B-D FACSCount 418
8.4 Beckman Coulter, Inc. 418
Background – and Signal-to-Background 418
The Beckman Coulter EPICS® ALTRA™ Cell Sorter 419
The Beckman Coulter Cytomics™ FC 500 Analyzer 420
The EPICS® XL and XL-MCL Analyzers 422
8.5 DakoCytomation 423
Background 423
The MoFlo® Cell Sorter 423
The CyAn™ Flow Cytometer 424
8.6 Cytopeia 425
The InFlux Cell Sorter 425
8.7 Optoflow AS 426
Background 426
The MICROCYTE® Flow Cytometer 426
8.8 Partec GmbH 427
Background 427
The CyFlow® and CyFlow® ML Flow Cytometers 427
The PAS, PAS II, and PAS III Flow Cytometers 428
PA Ploidy Analyzer and CCA Cell Counter Analyzer 429

8. BUYING FLOW CYTOMETERS (continued)
8.9 Some Other Flow Cytometer Companies....429
Advanced Analytical Technologies, Inc. (AATI)....429
Agilent Technologies, Inc. 429
Apogee Flow Systems Ltd. 430
Bentley Instruments....430
Chemunex SA....430
CytoBuoy b.v. 430
Delta Instruments bv....431
Fluid Imaging Technologies, Inc. 431
FOSS Electric A/S 431
Guava Technologies, Inc. 431
Howard M. Shapiro, M.D., P.C. 431
iCyt – Visionary Bioscience 431
International Remote Imaging Systems....431
Luminex Corporation....431
NPE Systems, Inc. 432
Union Biometrica, Inc. 432
8.10. Hematology Instruments, Etc. 433
8.11 Little Orphan Analyzers (And Big Orphan Sorters)....434
Bio/Physics and Ortho: Cytofluorograf to Cytoron....434
HEKA Elektronik GMBH: The FLUVO II Analyzer 435
The Kratel Partograph 435
The ODAM ATC 3000....435
Also Among the Missing....436
Flow Cytometer Rehabilitation; Used Instruments....436
Following Suit 436
8.12 Third Party Software....437
8.13 The Selling of Flow Cytometers: Hype and Reality 437
8.14. Applying for a Grant for a Cytometer 438

9. BUILDING FLOW CYTOMETERS....441
9.1 Why Buy a Flow Cytometer?....441
9.2 Why Build a Flow Cytometer?....441
9.3 Learning to Build Your Own....442

10. USING FLOW CYTOMETERS: APPLICATIONS, EXTENSIONS, AND ALTERNATIVES 443
10.1 The Daily Grind 443
Keeping the Instrument Running: Diet and Exercise 443
Particulars: Drawing a Bead on Flow Cytometer Alignment, Calibration, and Standardization 444
Alignment Particles: Fearful Asymmetry....445
Reference and Calibration Particles 445
Compensation Standards....446
Cells and Nuclei as Alignment Particles....446
Rose Colored Glasses: Optical Filter Selection 446
Experimental Controls....447
Shake Well Before Using: When Controls Won't Help....447
10.2 Significant Events in the Lives of Cells....448
Taking the Census: Cell Counting....448
A Counting Alternative: Image Analysis 448
The Doubled Helix: Reproduction 448
The Cell Cycle and Cell Growth 448
DNA Content Analysis 448
Mathematical Models for DNA Analysis....449
Clinical Application of DNA Content Analysis....450

DNA Content Analysis(continued)
DNA Content Alternatives: Static Photometry and Scanning Laser Cytometry 451
The Mummy's GC/AT: DNA Content Analysis in Anthropology and Forensic Science 451
Half a Genome is Better Than None: Sperm Sorting 452
The Widening G_0/G_1 re Detecting Mutation 453
Detecting DNA Synthesis: Cell Kinetics 453
Kinetics Before Flow Cytometry: Mitotic Indices, Doubling Times, and Radiolabel Studies 453
Labeling Index versus DNA Content 454
Early Flow Cytometric Approaches to Labeling Using BrUdR and ^{3}H-TdR 455
Detection of Incorporated BrUdR with Hoechst Dyes and Propidium Iodide 455
Detection of BrUdR Incorporation with Anti-BrUdR Antibodies 455
Cytochemical Detection of BrUdR Incorporation Using Difference and Ratio Signals 456
Breaking Up Is Easy To Do: SBIP, a Simpler Way to Detect BrUdR Incorporation into DNA 456
Anti-BrUdR Antibody: Seeing the Light 457
Cytochemical Detection of BrUdR: Still Around 457
Detecting RNA Synthesis Using Bromouridine 458
Generation Gaps: Tracking Dyes and Cell Kinetics 458
Cell-Cycle Related Proteins: Cyclins, Etc. 458
Detecting Mitotic Cells 462
Memento Mori: Detecting Cell Death 462
Necrosis versus Apoptosis 462
Identifying Apoptotic Cells 462
Les Feuilles Mortes (Autumn Leaves) 462
Apoptosis: Getting With the Program 463
ISNT there Light at the End of the TUNEL? 463
Apoptosis: The Case Against Flow Cytometry 463
Die Another Day: Cytometry of Telomeres 464
10.3 Identification of Cells in Mixed Populations 464
Mixed Genotypes versus Mixed Phenotypes 464
No Parameter Identifies Cancer Cells 464
Many Parameters Identify Blood Cells 464
Flow Cytometric Parameters Useful for Blood Cells 464
Specific Gene Products Identify Cell Types 465
Maturation Processes and "Missing Links": The "Ginger Root" Model 465
Practical Multiparameter Gating: Color Wars 467
Finding Rare Cells 469
One Parameter is Not Enough 469
Cocktail Staining Can Help 470
Dirt, Noise, and Rare Event Detection 470
Really, Really Rare Events: Alternatives to Flow 470
10.4 Tricks and Twists: Odd Jobs for Flow Cytometry 471
Single Molecule Detection 471
DNA Sizing, if not Sequencing, in Flow 471
Solid Phase (Bead) Assays Using Flow Cytometry 473
Cocktails for 100: Multiplexed Bead Assays 473
Cells in Gel Microdroplets and on Microspheres 474
Hanging Ten Pseudopodia? 475
10.5 Single Cell Analysis: When Flow Won't Do 475
10.6 Applications of Flow Cytometry 476
Cell Differentiation, *Ab Ovo* and *De Novo* 476
Differentiation in the Nervous System 476
Whole Embryo Sorting 476
Somatic Cell Genetics and Cell Hybridization 477
Reporter Genes Revisited 477
Isolating and Characterizing Hybrid Cells 477
Chromosome Analysis and Sorting and Flow Karyotyping 477

10.6 Applications of Flow Cytometry (continued)

Probing Details of Cellular Structures and Inter- and Intramolecular Interactions 479
Dissection of Structures Using Antibodies, Ligands, and Genetic Methods 479
Intramolecular Interactions 479
Clinical Flow Cytometry: Turf and Surf 480
Hematology 480
Clinical Application: Blood Cell Counting and Sizing 480
Red Blood Cells (Erythrocytes) 481
Clinical Application: Reticulocyte Counts 481
The Reticulocyte Maturity Index (RMI) 482
Erythrocyte Flow Cytometry: Other Clinical Uses 482
White Blood Cells (Leukocytes) 483
Clinical Application: Differential Leukocyte Counting 483
CD Characters: Leukocyte Differentiation Antigens 484
Granulocytes: Basophils 484
Basic Orange 21: The Best Basophil Stain Yet 485
Allergy Tests Using Basophil Degranulation 485
Granulocytes: Eosinophils 486
Granulocytes: Neutrophils 486
(Clinical?) Tests of Neutrophil Function 486
Neutrophil CD64 in Inflammation and Sepsis 487
When I'm Sick - CD64? 487
Platelets and Megakaryocytes 487
Hematopoietic Stem Cells 488
Clinical Application: Monitoring CD34+ Stem Cells According to the ISHAGE Protocol 488
Side Population (SP) Stem Cells: Plastic, Fantastic 489
Immunology 489
Immunologic Applications of Flow Cytometry: Still a Growth Industry 489
HIV Infection – The "Killer Application" 490
Clinical Application: T Cell Subset Analysis 490
T Cell Subsets: Alternative Technologies 491
Clinical Application: Transplantation 493
Detecting Lymphocyte Activation 494
Foundations: From PHA (the Lectin) to PHA (the Pulse Height Analyzer) 495
Functional Probes for Activation 495
DNA, RNA, and Activation Antigens 497
Mitogen Response versus Antigen Response 498
Detecting Activation by CD69 Expression 499
Cytokines: Detecting Activation and More 499
Ins and Outs of Cytokine Staining 500
Tetramer Staining: Talking the Talk; Walking the Walk? 500
Tracking Dyes: Activation and Ontogeny 501
What is "Early" Activation (Trick Question)? 501
Cancer Biology and Clinical Oncology 502
Cancer Diagnosis: Cervical Cytology 503
DNA Content Measurements Yet Again 503
Beyond DNA Content: Antigens, Oncogenes, and Receptors, and Response to Therapy 504
Immunophenotyping in Hematopathology 504
Detecting Minimal Residual Disease 505
Biological Implications of Phenotyping Results 506
Digression: A Slight Case of Cancer 507
Analysis of Sperm 508
Isolating Fetal Cells from the Maternal Circulation for Prenatal Diagnosis 509
The March of Time: Circadian Rhythms, Aging, and Atherosclerosis 510
Clinical Application: Urine Analysis 510
The Animal Kingdom 510

The Animal Kingdom (continued)
Lions and Pumas and Clams, Oh, My! ... 510
Fish Story; FISH Story ... 511
Flow Cytometry: For the Birds? ... 512
Big Stuff, Vegetable, Animal or Mineral ... 512
Flow Cytometry of Plant Cells and Chromosomes ... 512
Measurement of Plant Cell DNA Content ... 513
Plant Chromosome Analysis and Sorting ... 514
Other Flow Cytometric Applications in Plants ... 514
Microbiology, Parasitology and Marine Biology ... 514
Measuring Microbes: Motivation ... 515
Measuring Microbes: Instrument Issues ... 515
Parameters Measured in Microorganisms ... 516
Flow Cytometric "Gram Stains" ... 516
Detection and Sizing: Light Scattering ... 517
Detection and Sizing: Electrical Impedance ... 517
Nucleic Acid (DNA and RNA) Staining ... 517
Total Protein Content: Scatter versus Stains ... 518
Antibodies, Etc.: Labeling Strategies ... 518
Ribosomal RNA-Based Species Identification ... 518
Functional Probes in Bacteria ... 518
Potential, Permeability, "Viability", and Metabolic Activity ... 519
Digression: A Therapeutic Approach Based on Transient Permeabilization ... 522
So Few Molecules; So Little Time ... 522
Applications in Marine Microbiology ... 524
Extensions: Cytometers for Marine Applications ... 527
References: Flow Cytometry and Oceanography ... 527
General Microbiology ... 527
Previously Noted ... 527
Cell Cycles and Cell Division ... 528
Fluorescent Protein Methods in Microbes ... 528
Microbial Communities: Will Flow Work? ... 528
Bad Guys Don't All Wear Black Hats: Microbial Detection/Identification in Health-Related Contexts ... 528
The Basic Questions ... 528
Detection: Intrinsic Parameters are Not Enough ... 529
Detection: Fluorescence Improves Accuracy ... 529
Detection: When the Tough Get Going ... 529
Identification: Too Many Broths... ... 530
Identification: Can Multiplexing Help? ... 531
Environmental and Sanitary Microbiology ... 531
Water That Made Milwaukee (and Sydney) Infamous ... 531
Food Microbiology ... 532
Bioterrorism and Bioopportunism ... 532
Viruses and Other Intracellular Pathogens ... 532
Clinical Microbiology ... 533
Antimicrobial Susceptibility Testing: One Size Does Not Fit All ... 534
Bacteria: Confusion Reigns ... 535
Mycobacteria: Down for the Count ... 535
Antifungal Susceptibility: Flow Does the Job ... 535
Antiviral Susceptibility by Flow Cytometry ... 536
Cytometry in Vaccine Development ... 536
Microbiology Odds and Ends ... 536
Parasitology ... 536
Pharmacology and Toxicology ... 537
Drugs and the Life and Death of Cells ... 538

Pharmacology and Toxicology (continued)
Erythrocyte Micronucleus Assays....538
Toxic Waste and B Cell Proliferation....538
Radiation Dosimetry....538
Food Science....538
Somatic Cell Counts in Milk....538
Brewhaha....539
A Loaf of Bread, A Jug of Wine.......539
Seeing the Blight....539
Major Food Group: Chocolate....539
Biotechniques and Biotechnology....539
Protein and Gene Expression on Cells and Beads....540
Getting Big Molecules into Small Cells....540
Staying Alive, Staying Alive....540
Et Cetera....540
Alternatives: Microfluidic Cytometers, Flow and Static....541
Cytometry Afield....541
The Lymphocytes of the Long Distance Runner....541
War and Peace....541
Blood, Sweat and Tears?....542
Pulp Nonfiction....542
Flow Cytometry On the Rocks....542
To Boldly Go Where No Cytometer Has Gone Before....542

II. SOURCES OF SUPPLY....543
II.1 Resources, Societies, Journals....543
II.2 Optical Supply Houses....543
II.3 Probes and Reagents....544
II.4 Calibration Particles/Cytometry Controls....548
II.5 Flow Cytometers....549
Hematology Instruments....551
II.6 Data Analysis Software/Systems....551
Hardware and Software....551
Commercial Software Sources....552
Noncommercial Software Sources....552
II.7 Cytometer Rehabilitation/Add-ons....553
II.8 Flow Cytometer Parts....553
Flow System Plumbing....553
Photodetectors....554
DC-DC Converter Modules for HV Power Supplies....555
Power Supplies (Low Voltage)....555
Other Electronics....555
II.9 Lasers....555
Laser Trade Publications....555
Laser Manufacturers....555
II.10 Optical Filters....556
Color Glass Filters....556
Interference Filters....557
Neutral Density Filters....557
Polarizing Filters and Optics....557
Tunable Filters....557
II.11 Aids to Troubleshooting Flow Cytometers When All Else Fails....557
II.12 Proficiency Testing....557
II.13 Sex Selection....557
II.14 Alternative Technology....558

12. AFTERWORD 561
12.1 Dotting i's and Crossing t's 561
12.2 Late Breaking News 561
New Book 561
New Protein Stain 561
Caveat on Fluorescent Caspase Inhibitors 561
Polyamide Probes 561
Tearing Down the (Picket) Fences 562
New Instrument: The BD FACSArray™ 563
Science Special Section: Biological Imaging 563
Cytomics in Predictive Medicine: a *Clinical Cytometry* Special Issue and Other Recent Citings and Sightings 563
12.3 Analytical Biology, Such as it Isn't: Is This Any Way to Run a Science? 563
12.4 Colophon 564
12.5 Unfinished Business 565
AIDS and Infectious Disease in the Third World 565
A Center for Microbial Cytometry 565
A Nobel Prize for Herzenberg and Kamentsky? 566
12.6 Flow and the Human Condition 566
There's No Business Like Flow Business 566
12.7 One More Thing 566

TABLES AND FIGURES

TABLES

1-1. Some parameters measurable by cytometry 3

3-1. A brief outline of flow cytometric history (1945-2000) 100

4-1. SI units and prefixes 102
4-2. Emission wavelengths of lasers 139
4-3. Cathode quantum efficiencies of diode and PMT detectors between 300 and 800 nm 165
4-4. Logarithmic Amplifiers: What goes in, what comes out 203
4-5. Characteristics of analog-to-digital converters 206

5-1. Some landmarks of the normal or Gaussian distribution 234
5-2. Equations (1-4) that must be solved to permit 4-color fluorescence compensation 242
5-3. Header and text portion of an FCS2.0 data file 254

6-1. Safe speed limits for sorting based on Reynolds number calculations 269

7-1. Some cellular parameters measurable by cytometry 286
7-2. Fluorescence spectral properties of a selection of reagents usable for common cytometric tasks 297
7-3. Tricyclic heteroaromatic compounds usable for staining DNA and/or RNA 323
7-4. Raman emission from water 343

FIGURES

1-1. Interaction of light with a cell 4
1-2. Transmitted light and dark field images of an unstained suspension of human peripheral blood leuokocytes 7
1-3. Transmitted light microscope images of an unstained smear of human peripheral blood 8
1-4. Schematic of a fluorescence microscope 9
1-5. Scanned images of Feulgen-stained lymphoblastoid cells 15
1-6. One-dimensional scanning of cells deposited in a narrow line 16
1-7. Idealized plot of signal amplitude vs. time 16
1-8. Ideal and "real" DNA content distributions 22
1-9. Single parameter histogram displays from a multichannel pulse height analyzer 24
1-10. Use of a mathematical model to determine fractions of DNA-aneuploid breast cancer cells 25
1-11. Dot plot (cytogram) of Hoechst 33342 and fluorescein fluorescence in CCRF-CEM cells 26
1-12. Gating regions for counting or sorting set electronically, drawn on an oscilloscope display 27
1-13. Histogram of 90° (side) scatter from leukocytes in lysed whole blood 30
1-14. Bivariate distribution of anti-CD3 antibody fluorescence intensity vs. large angle scatter in leukocytes 31
1-15. The bivariate distribution of Figure 1-14 shown as an isometric or "peak-and-valley" plot 32
1-16. The two-parameter histogram of Figures 1-14 and 1-15 displayed as a contour plot 32
1-17. Identification of human peripheral blood T-lymphocytes bearing CD4 and CD8 antigens 34
1-18. Why fluorescence compensation is necessary 37
1-19. How compensation gets data to fit into quadrants 38
1-20. Fluorescence intensities of antibody stained cells and beads bearing known amounts of antibody 49
1-21. Schematic of the optical system of a fluorescence flow cytometer 51
1-22. A typical flow chamber design 56
1-23. FACScan Analyzer (Becton-Dickinson) 58
1-24. MoFlo High Speed Sorter (Cytomation) 58
1-25. Microcyte Cytometer (Optoflow) 58
1-26. Estimated numbers of fluorescence flow cytometers in use worldwide, 1975-92 59

2-1. Growth of the flow cytometry literature, 1987-93 64

3-1. The first working flow cytometer (Gucker particle counter) 74
3-2. Digitized image of a neutrophil polymorphonuclear leukocyte 82
3-3. Refined and prototype versions of Kamentsky's Rapid Cell Spectrophotometer (RCS) 84
3-4. A two-parameter histogram of blood cells analyzed in the RCS 84
3-5. Louis Kamentsky and the Bio/Physics Systems Cytofluorograf 87
3-6. The Technicon Hemalog D Differential Leukocyte Counter 88
3-7. Leonard Herzenberg with B-D's first commercial version of the Fluorescence Activated Cell Sorter (FACS) 88
3-8. A two-parameter display from the Block differential counter showing five leukocyte clusters 89
3-9. The author with Cytomutt and Cerberus 94
3-10. Cell cycle phases defined by DNA content and by DNA/RNA content 97

4-1. Radian and steradian 101
4-2. Light as an electromagnetic wave 104
4-3. Constructive and destructive interference 105
4-4. Circularly polarized light 105
4-5. Reflection and refraction of light at a surface 106
4-6. The Jablonski diagram of electronic energy levels, or states, and transitions 112
4-7. Fluorescence spectrum of fluorescein 113
4-8. Light from a point source at the focal length of a lens is collimated 119
4-9. Rays from a point source can be focused to an image point 119
4-10. Rays from many points of an object add up to make an image 120
4-11. Elements of a typical microscope lens, showing the half angle that defines the acceptance cone and N.A. 120
4-12. Showing the effect of N.A. on light collection 121
4-13. Multiple views of magnification 123

FIGURES (continued)

4-14. Output characteristics of arc, quartz-halogen, and deuterium lamps 125
4-15. Köhler and critical illumination 128
4-16. Optics for arc source epiillumination for fluorescence microscopy or flow cytometry 129
4-17. Use of crossed cylindrical lenses to focus a laser beam to an elliptical spot on the core stream 131
4-18. Energy levels involved in laser action 133
4-19. Schematic of a laser 134
4-20. Laser transverse excitation modes 134
4-21. Measured beam intensity profiles of diode, CO_2, and He-Ne lasers 136
4-22. Intensity profiles of a focused and defocused violet laser diode beam 136
4-23. Sizes, power requirements, and approximate costs of some smaller lasers used for cytometry 145
4-24. Effect of noise compensation circuitry on precision of fluorescence measurements 147
4-25. Looking at the observation point 150
4-26. Maximizing light collection: Not always a good way to do things 151
4-27. A prism monochromator 153
4-28. Light transmission characteristics of bandpass, short pass, and long pass interference filters 154
4-29. Transmission of several wavelength regions through different dichroic configurations 155
4-30. Cube and plate beamsplitters 156
4-31. Total internal reflection 157
4-32. A fiber optical waveguide 157
4-33. Optical arrangements for collection of forward scattered light 159
4-34. Elements of a photomultiplier tube (PMT) 160
4-35. PMT electrode voltage supply circuits: dynode chain and Cockcroft-Walton voltage multiplier 162
4-36. Detectors and housings 163
4-37. Fluid flow in a flow cytometer 167
4-38. Laminar flow profile illustrated by diatoms in the "Flow CAM" imaging flow cytometer 167
4-39. Flow chamber designs 169
4-40. New angles on light collection in flow 171
4-41. Flow chamber designs used with arc source flow cytometers 173
4-42. Minimizing turbulence generated at the sheath inlet to flow chambers 175
4-43. Sheath fluid supply plumbing 175
4-44. The Coulter orifice 183
4-45. Effect of beam geometry on pulse shape 184
4-46. Some circuit elements 185
4-47. A line-powered DC power supply 187
4-48. Basic operational amplifier circuits 190
4-49. A photodetector preamplifier circuit 191
4-50. Waveforms in preamplifier, front end electronics, and peak detector circuits 192
4-51. Schematic diagram of a peak detector 192
4-52. Preamp and peak detector outputs (oscilloscope traces) 193
4-53. Telling two cells from one gets harder as the cells go through closer together 196
4-54. Uncompensated and compensated fluorescence signals from FL- and PE-labeled beads 198
4-55. One side of a two-color compensation circuit 198
4-56. Signals from PE-labeled antibody bound to beads, on linear and 4-decade logarithmic scales 199
4-57. Response curves of different types of log amps as determined according to Parks, Bigos, and Moore 202
4-58. Continuous and sampled signals 205
4-59. Digital pulse processing: "slicing" a slightly noisy Gaussian pulse with a baseline 209
4-60. MESF threshold sensitivity determination using fluorescein-labeled beads 216
4-61. Fluorescence distributions for bead sets measured with progressively lower values of Q 222
4-62. Separation (or lack thereof) of CD4+ lymphocytes and unstained cells at various values of Q and B 223

5-1. Distributions of sums of uniformly distributed random numbers approach the normal distribution 231
5-2. Pascal's triangle 232
5-3. Binomial distributions for $n = 2, 4, 8$, and 16, with $p = q = 0.5$ 232
5-4. Binomial distributions for $n = 16$ and $p = 0.5$, 0.25, and 0.125; they are skewed when $p \neq 0.5$ 233

FIGURES (continued)

5-5. Euclidean distance between two points, with an assist from Pythagoras 234
5-6. "Box-and-whiskers" plots showing medians and interquartile ranges of distributions, after Tukey and Tufte 236
5-7. Histogram display formats 237
5-8. Dot plots of computer-generated data showing various degrees of correlation 237
5-9. Varieties of two-parameter data display (cover figure) 239
5-10. Density plot showing a scale indicating numbers of events 240
5-11. 3-Dimensional "cloud" plots of CD3, CD4, and CD8 antigens on blood lymphocytes and thymocytes 241
5-12. How compensation gets data to not quite fit into quadrants 243
5-13. Two generated near-normal distributions and their cumulative distributions, or integrals 245
5-14. Quadrant statistics 247
5-15. Multiparameter analysis of peripheral blood leukocyte types: partitioning in two-dimensional subspaces 249
5-16. Linear transformation of data to separate clusters, as is done in linear discriminant analysis 251
5-17. Calculation is not always necessary to reduce the dimensionality of data 254
5-18. Linear and log scales revisited 255

6-1. Droplet sorting 259
6-2. A droplet sorter test stream pattern 261
6-3. Mack Fulwyler with his islet sorter 264
6-4. Fluidic sorter designs 264
6-5. A microfluidic flow sorter for bacteria 265

7-1. Forward scatter does not measure particle size 275
7-2. Depolarized 90° scatter signals can be used to identify eosinophil granulocytes 278
7-3. Indicatrices (plots of intensity vs. scattering angle) of particles and cells 280
7-4. Erythrocytes scatter less light at a wavelength at which hemoglobin exhibits strong absorption 281
7-5. Side scatter signals from T2 bacteriophages 288
7-6. The principle of doublet discrimination using pulse height and pulse integral measurements 290
7-7. Fluorescence spectra of some materials implicated in mammalian cell autofluorescence 291
7-8. Zinc protoporphyrin fluorescence in human red cells 292
7-9. Probe fluorescence spectra and source emission wavelengths 296
7-10. A "rogues' gallery" of nucleic acid dyes 301
7-11. DNA content distributions in sperm from a normal ram and a ram bearing a translocation 311
7-12. Structure of symmetric cyanine dyes given the formula "DiYC$_{n,1}$(2m + 1)" by Sims et al 313
7-13. Flow karyotype of human chromosomes stained with Hoechst 33258 and chromomycin A$_3$ 318
7-14. Hoechst/chromomycin fluorescence signatures of bacteria with different DNA base compositions 318
7-15. Flow cytometry of chromatin structure identifies cells in mitosis 320
7-16. DNA and RNA content analysis of mitogen-stimulated lymphocytes 321
7-17. Chemical structures of some reactive labels 327
7-18. Multiplex immunofluorescent labeling to demonstrate multiple cell types in blood 351
7-19. Quantitative determination of CD4 epitopes on peripheral blood lymphocytes and monocytes 356
7-20. Flow cytometric detection of HIV-1 nucleic acids in cells after *in situ* PCR 361
7-21. Plot of cytoplasmic [Ca^{++}] as indicated by indo-1 fluorescence ratio versus time 365
7-22. Time used as a quality control parameter in DNA analysis (after Watson) 366
7-23. Cell proliferation indicated by dilution of fluorescence of the tracking dye PKH26 372
7-24. Cell proliferation indicated by dilution of fluorescence of CFSE-labeled CD4+ lymphocytes 373
7-25. Specific staining of glutathione in cells by monobromobimane (MBB) 381
7-26. Valinomycin-induced changes in fluorescence intensity of cyanine dye-loaded red cell suspensions 387
7-27. Distributions of the fluorescence of DiOC$_6$(3) in CCRF-CEM T-lymphoblasts 388
7-28. Distributions of membrane potential in cells suspended in NaCL, KCl and a mixture of the two 389
7-29. Structures of two membrane potential probes, the cyanine DiOC$_5$(3) and the oxonol DiBAC$_4$(3) 390
7-30. Two-parameter analyses of lectin-stimulated lymphocytes: DNA vs. RNA and membrane potential 396
7-31. Demonstration of apoptotic HL-60 cells with deenergized mitochondria by JC-1 staining 399
7-32. Measurement of membrane potential of *Staphylococcus aureus* using a ratiometric technique 400
7-33. Emission spectra of indo-1 in solutions of increasing free calcium ion concentration 404

FIGURES (continued)

7-34. Emission spectra of fluo-3 in solutions of increasing free Ca^{++} concentration 405
7-35. Estimation of cytoplasmic pH in human lymphocytes from carboxyfluorescein fluorescence ratio....406
7-36. The pH-dependent emission spectra of carboxy SNARF-1 excited at 488 nm....407

8-1. The BD FACSVantage cell sorter....413
8-2. The BD FACSCalibur benchtop cell sorter....415
8-3. The BD LSR multi-beam benchtop analyzer....416
8-4. BD's "Octagon" collection optics....416
8-5. The BD FACSAria cell sorter....417
8-6. The Beckman Coulter EPICS Altra sorter....419
8-7. The Beckman Coulter Cytomics FC 500 analyzer....421
8-8. The Beckman Coulter EPICS XL-MCL analyzer....422
8-9. The CyAn benchtop flow cytometer [DakoCytomation]....425
8-10. Cytopeia's InFlux cell sorter platform....426
8-11. Partec's CyFlow flow cytometer....427
8-12. The Partec PAS cytometer....429

10-1. Using DRAQ5-stained nuclei as alignment particles....446
10-2. "Equal opportunity" and "unequal opportunity" staining of T-cells....447
10-3. Separation of X- and Y- bull sperm....453
10-4. Detection of BrUdR incorporation using anti-BrUdR antibody and the SBIP method....457
10-5. Use of a combination of propidium and TO-PRO-3 to detect bromodeoxyuridine incorporation....458
10-6. DNA content vs. expression of cyclins B and E in exponentially growing MOLT-4 cells....459
10-7. DNA content vs. RNA content and CD71 expression in activated CD4 cells....460
10-8. Identification of mitotic cells by antibody to phosphorylated histone H3....462
10-9. Subsetting of human T-cells into memory classes and measurement of kinases using 11-color fluorescence....468
10-10. Analysis of bacteriophage lambda DNA and fragments from a digest of lambda DNA in a slow flow system....472
10-11. Clusters representing 100 different color-coded beads used with Luminex's system for multiplexed analysis....473
10-12. Growth of an encapsulated Gram-positive marine bacterium in gel microdroplets....474
10-13. Identification of occupied and unoccupied gel microdroplets....475
10-14. Univariate flow karyotype of human chromosomes stained with propidium iodide....477
10-15. Bivariate karyotypes of RPET001 and Daudi human cell lines....478
10-16. Clusters of peripheral blood leukocyte types in two-dimensional displays from a hematology analyzer....483
10-17. Side population (SP) stem cells identified by blue vs, red Hoechst 33342 fluorescence....489
10-18. Time course of events in T-lymphocyte activation and probes for their cytometric detection....494
10-19. Intracellular cytokine staining....500
10-20. ERK1/2 kinase phosphorylation in T-cells exposed to various activation stimuli....501
10-21. Gating scheme for detection of minimal residual disease in chronic lymphocytic leukemia....505
10-22. T-cell subset analysis in lion and puma peripheral lymphocytes....511
10-23. Analysis of clam cells in a hematology analyzer....511
10-24. Determination of nuclear genome size in diploid banana....513
10-25. DNA content of cactus nuclei showing endopolyploidy....513
10-26. Flow karyotype of a translocation line of broad bean....514
10-27. rRNA probes show differences in enteric flora between breast-fed infants and infants fed reconstituted milk....518
10-28. Membrane potential in dormant and resuscitated cultures of *Micrococcus luteus*....519
10-29. Combined rRNA probe and CTC staining of a genetically and metabolically complex cell mixture....520
10-30. Functional states of *Salmonella typhimurium* shown by staining with $DiBAC_4(3)$, ethidium, and propidium....521
10-31. Effects of amoxicillin on [ratiometric] membrane potential and permeability of *Staphylococcus aureus*....521
10-32. Fluorescence profiles of viruses stained with SYBR Green I....523
10-33. Forward scatter, Hoechst 33342, and chlorophyll fluorescence of the marine bacterium *Prochlorococcus*....524
10-34. Side scatter and fluorescence signatures of four viruses shown in Figure 10-32....525
10-35. Side scatter and fluorescence signatures of viruses and bacteria in a water sample from a small Alpine pond....525
10-36. Size and DNA content of bacteria in seawater from Prince William Sound, Alaska....526
10-37. Size and DNA content of *Oligobacterium* RB1 from Resurrection Bay, Alaska....526

FIGURES (continued)

10-38. Flow cytometry *in vivo* 542

12-1. Tearing down the "picket fence" and reuniting the negatives using a BiExponential data transform 562

7. PARAMETERS AND PROBES

We will now begin a detailed discussion of the applications of flow cytometry by considering the **parameters**, i.e., what can be measured, and the **probes**, i.e., the reagents that may be needed necessary to make the measurements.

In Chapter 1 (p. 2), I mentioned that the term **parameter** is used in several different senses in cytometric jargon. It is helpful to differentiate between the **physical parameters**, such as electrical impedance, light scattering and fluorescence, that are detected and quantified by the instrument, and the **cellular parameters**, such as cell size, cytoplasmic granularity, and DNA content, values of which we derive, or hope to derive, from measurements of the physical parameters. I will consider the physical parameters first.

7.1 PHYSICAL PARAMETERS

Electrical Parameters

DC Impedance (Coulter Volume)

Electronic volume measurement by the **Coulter principle**[49,50,51] is perhaps the most common flow cytometric technique for cell size determination; there are many more electronic cell counters in use worldwide than there are optical flow cytometers. The measurement is described on p. 10 and pp. 182-3; in brief, passage of a nonconductive particle, such as a cell, through the saline-filled orifice of a Coulter volume measurement circuit with a constant (DC) current applied across the orifice produces a voltage pulse with an amplitude that should, theoretically, be proportional to the volume of the particle.

Deviations from ideal behavior in Coulter orifice measurements are typically caused by particles passing through the orifice in close proximity to the walls, or through other regions of the orifice in which the electric field is nonuniform; problems may also occur when particles are asymmetric. Observation of a bimodal red blood cell volume distribution motivated Mack Fulwyler to build his first flow sorter, and thus to identify measurement artifacts as the source of the bimodality. The orifice must be longer than it is wide in order to produce a uniform electric field in the central region. The diameter of the orifice must be at least several times the particle diameter to keep the field in the region of a particle relatively uniform, but, if the orifice diameter is much larger than the particle diameter, the change in impedance produced by particles' traverse of the orifice will be small, decreasing signal-to-noise ratio and sensitivity.

Electronic volume measurements are sensitive to changes in the conductivity of cells; thus, cells with intact membranes, which have very low conductivity, will have a larger apparent volume than cells of the same physical size with damaged membranes, which have higher conductivity.

Volume sensing orifices have been and are incorporated into a number of laboratory-built and commercial flow cytometers, including current models from NPE and Partec. Wietzorrek et al[2524] have described a flow cytometer, capable of measuring DC impedance, fluorescence, and light scattering, that also includes provision for video imaging in flow.

Electronic volume measurement using appropriately sized orifices was employed some years ago to detect and size particles as small as bacteria[680] and viruses[681,2525,2526]; a recent report by Saleh and Sohn[2530] describes the use of a microfabricated "Coulter counter on a chip" to detect and size colloidal particles as small as 87 nm in diameter using orifices with lateral dimensions of only a few micrometers. Detailed discussions of the theory and methodology of electronic cell volume measurement appear elsewhere[9,682-5,1151].

AC Impedance (Electrical Opacity); Capacitance

Cells' impedance has resistive and capacitive or dielectric components. When direct current (DC) or low frequency

alternating current (AC) is applied across the orifice, cell impedance is determined primarily by the dielectric properties of the plasma membrane. As higher frequencies are applied, the dielectric properties of the cell interior become more important in determining impedance.

Coulter and Hogg[715] developed apparatus in which both DC resistance and radio frequency (34 MHz) AC impedance were measured, and defined **opacity** as the ratio of AC impedance to DC resistance. Leif et al[716], using the apparatus built by Coulter and Hogg, found that various fractions of human erythrocytes separated on the basis of buoyant density differed in opacity but not in volume; opacity measurements are also said to be capable of discriminating among different types of leukocytes. Hoffman and Britt[717] studied impedance of CHO cells at a lower AC frequency (1 MHz) and found the DC and AC impedance signals to be well correlated, although they did note substantial differences in the ratio of DC and AC signals between cells and plastic spheres.

Bulk physical separation of different cell types, presumably on the basis of dielectric properties, has been done using applied AC fields, and it seems likely that cell types separable in bulk by dielectrophoresis will also be found to be distinguishable on the basis of opacity measurements. If, however, the same underlying structural differences, e.g., in cytoplasmic granularity, underlie differences in cells' internal dielectric properties as are responsible for differences in light scattering behavior, the utility of opacity measurements will be considerably less than the utility of dielectrophoresis.

AC impedance measurements are not, as far as I know, provided for in any commercial fluorescence flow cytometers; however, both DC and AC impedance measurements are used in hematology instruments. Kraai et al[2531] reported that hematopoietic stem cells, normally detected by immunofluorescence measurements of CD34 antigen, appeared in the "immature" region defined by AC and DC impedance measurements in a Sysmex hematology counter.

Sohn et al[2532] measured **capacitance** of SP2/0 mouse myeloma cells in a microfluidic flow system, and reported that the histogram of capacitance values tracked the histogram of DNA content as measured by fluorescence flow cytometry. The CV of the capacitance histogram was much higher than one would expect or accept in a fluorescence measurement, but there is presumably some room for improvement.

Acoustic Measurements of Cells in Flow

Changes in cellular structure change the mechanical and, therefore, the acoustic properties as well as the optical and electrical properties of cells. In order to achieve the same spatial resolution with acoustic measurements as is achieved using visible light, equivalent wavelengths are required; these correspond to acoustic frequencies of several GHz. **Acoustic microscopy** on fixed and living cells has been done using apparatus operating at these high frequencies[718,9]. In 1984, Sweet, Fulwyler, and Herzenberg[720] reported making "zero-resolution" measurements of cells in a flow system at much lower acoustic frequencies (25-150 MHz). Apparently, the gain wasn't worth the pain; they thereafter remained with the stain.

Optical Parameters: Light Scattering

Almost all fluorescence flow cytometers, and many hematology counters, measure light scattering at small and larger angles to the incident beam, which we have come to know as **forward scatter** and **side scatter**. I have already cautioned (p. 5) against acceptance of the oversimplified and erroneous notion that forward scatter intensity is a measure of cell size. The simplified concept of side scatter intensity as an indicator of internal granular structure is somewhat more defensible, but the fact is that light scattering is a complex phenomenon.

Scattering: The Mueller Matrix Model

A general model for dealing with light scattering by particles, accounting for scattering of light of all polarizations at all angles, is based on the **Stokes vector** and the **Mueller matrix**[713,1244]. The Stokes vectors describe incident and scattered light; each has four components representing intensity and the degrees of linear and circular polarization. The Mueller matrix characterizes a scattering particle; it has sixteen elements, each of which is a function of the scattering angle. The Stokes vector for scattered light is the product of the Stokes vector for incident light and the Mueller matrix. In principle, if you know all the elements of the Mueller matrix, you have completely characterized the light scattering behavior of a particle but, in general, you can't compute the sixteen elements of the Mueller matrix simply by knowing the four elements of the Stokes vector for incident light and measuring the four elements of the Stokes vector for light scattered by the particle. However, the number of independent elements in the Mueller matrix is generally less than sixteen because of symmetry.

In the case of spherical particles, the Mueller matrix has four independent elements, which can be calculated as a function of particle radius according to Mie theory. For particles with a plane of symmetry, there are seven independent elements in the Mueller matrix, and you have a shot at finding them by making measurements of the intensity and polarization of scattered light. This, if you will, is the Holy Grail long sought by the knights of Los Alamos' round table, who, beginning in the late 1960's, measured scattering by plastic particles and by cells over a large range of angles, wavelengths, and linear polarizations. This took a lot more hardware than you'll find in the flow cytometers at the general store. The question remains as to whether the benefit, in terms of the information obtained about the biological particles under study, is worth the cost.

Knowing all 16 elements of the Mueller matrix, which tells you everything there is to know about scattering, leaves you with only half the information you'd get from Los Alamos' old 32-angle scatter measurement system, but that's

still a lot of numbers to crunch. Those numbers also pose some problems because many don't relate in straightforward ways to observable morphological, biochemical, or functional parameters of cells. We use forward scatter measurements all the time because they're very reliable for telling us when there's a cell or other particle in our measurement system, and frequently useful for telling us roughly how big the cell is, and/or whether it's dead or alive. We use side scatter measurements all the time because they let us distinguish different cell types, but we're most comfortable when the distinctions made by side scatter measurements correspond to differences we can easily see by looking under a dark field or phase or interference contrast microscope. The failure of fancier scattering measurements to catch on may not lie so much in the difficulty of implementing them as in the difficulty of reconciling them with the rest of our experience. So let's get back to the simpler scattering measurements for a while, and then see what additions might or might not be worthwhile to pursue further.

Forward Light Scattering and Cell Size

Forward scatter measurements have been widely used for estimation of cell size since it was demonstrated by Mullaney et al[110] that the intensity of light scattered at small angles (0.5-2.0°) from an incident laser beam was roughly proportional to particle volume, as predicted by Mie's earlier theoretical work. So-called **forward scatter** or **small-angle scatter** measurements can be useful, provided one remains aware of their limitations. Most of these arise from the fact that many factors other than cell size influence cells' small-angle light scattering, as is attested to by a large body of literature[93,97-8,171,353-63,1244-5].

Forward light scatter signal intensity is strongly affected by the **wavelength** of light used and by the precise **range of angles** over which light is collected, the latter being determined by the focal lengths and numerical apertures of collecting lenses and the size, shape, and position of irises, slits, and obscuration bars in the optical system. Since no two manufacturers of flow cytometers use the same optical design for forward scatter measurements, it is unlikely that exactly the same results will be obtained from measuring the same cells in different instruments.

Among cellular properties other than size that influence forward scatter measurements are differences in **refractive index** between the cells and the suspending medium, cells' internal structure, and the presence within or upon cells of material with strong **absorption** at the illumination wavelength used. If the refractive indices of cells were the same as that of the suspending medium, the cells would not scatter incident light. The difference in index between cells and the medium is maintained, at least in part, by the action of the membrane as a permeability barrier to water and solutes. Cells with damaged membranes, i.e., those cells which are identified as "dead" by uptake of dyes such as trypan blue or ethidium bromide, have a lower refractive index, and thus produce smaller forward scatter signals. This characteristic was originally used in flow cytometric immunofluorescence work to discriminate damaged cells, which tend to stain nonspecifically with fluorescent antibodies, from the intact cells that were of interest to experimenters[354,164]. Such discrimination is less than perfect[165], particularly when the sample contains cells of different types and/or sizes.

The presence of strongly absorbing material in cells tends to decrease the amplitude of forward scatter signals; highly textured surface or internal structures, e.g., the specific granules of blood granulocytes, may have a similar effect. Electronic volume measurement indicates that blood granulocytes have a larger volume (about 350 fl) than lymphocytes (about 200 fl), but granulocytes produce smaller forward scatter signals in some flow cytometers. Thus, one cannot reliably estimate the relative sizes of two cells of different types from small-angle light scatter signals. Not only can't we compare apples and oranges; we can't, strictly speaking, always compare apples and apples, because **theory predicts, and experiments confirm, that, even for uniform particles, forward scatter amplitude will not be a monotonic function of particle size.**

I can't think of a better way to illustrate this than to include pictures from a poster presentation made by Kevin Becker et al at the ISAC XXI Congress in May, 2002[2551], which I have adapted into Figure 7-1.

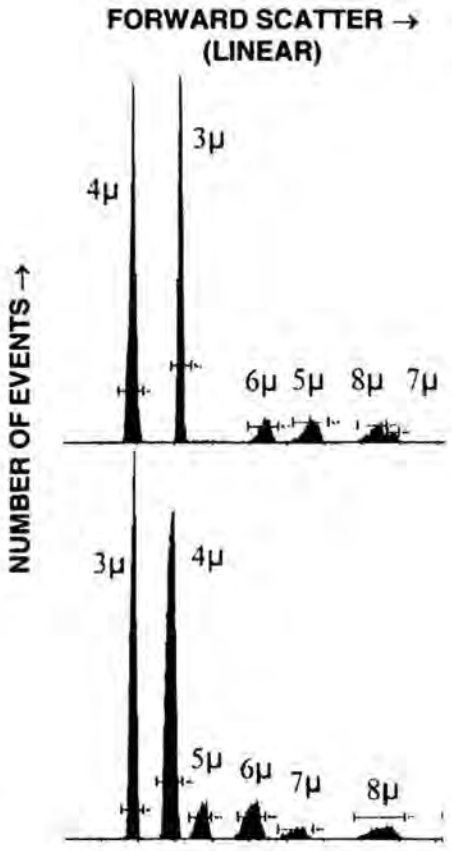


Figure 7-1. Forward scatter does not measure particle size (courtesy of Kevin Becker, Phoenix Flow Systems).

The histograms in Figure 7-1 show forward scatter intensities for polystyrene beads of various diameters, as measured using two popular benchtop flow cytometers. The trace on the top is from a BD Biosciences FACSCalibur, and the one on the bottom is from a Beckman Coulter EPICS XL. Both instruments use low-power, air-cooled 488 nm argon ion laser light sources. The relationship between forward scatter intensity and bead diameter indicated by the top histogram is not monotonic, that is, the signals from bigger beads are not necessarily bigger than the signals from smaller beads. The bottom histogram looks a little more promising, but I can tell you that there is no way to draw a calibration curve that relates forward scatter signal intensity to the first, second, or third power of particle size in any believable way, thus excluding the possibility that the forward scatter signal intensity is proportional to particle diameter, cross-sectional area, or volume. And these are beads; their diameters can be and have been measured accurately by electron microscopy, and their refractive indices are pretty much all the same, so we can't find any way to wiggle out of accepting the fact that forward scatter does not measure size.

This need not engender despair on the part of flow cytometer users. Like many of the other relatively rough measurements made by scientists, forward scatter measurements are good enough for many, and perhaps even most, of the purposes for which they are used. It is ignorance of and/or blind faith in techniques that gets experimenters into trouble.

After the first edition of this book came out, a reviewer of a manuscript cited my statement, printed in boldface on the previous page, as invalidating calculations of cell surface antigen density based upon ratios of fluorescence and forward scatter measurements. The measurements in question were made on cells in different stages of the cell cycle, and DNA content was also measured. In this case, knowing that S and G_2 phase cells are bigger than G_1 phase cells, it was not illogical to treat their forward scatter signals as roughly indicative of area, particularly since nobody has convincingly demonstrated that other parameters, such as refractive index, change drastically during the cell cycle. In other circumstances, e.g., granulocyte stimulation, changes in forward scatter signals may be influenced by changes in granule morphology as well as by swelling due predominantly to water movements, with accompanying changes in refractive index; it is thus hard to determine the extent to which a change in forward scatter signals reflects a change in size. It is always risky to assume that small (say 2 to 5%) differences in forward scatter signals precisely reflect small differences in size.

Forward Scatter and "Viability"

In general, "dead" cells, i.e., cells with sufficient membrane damage to render them permeable to dyes such as propidium, which normally does not enter intact cells, have lower forward scatter signals than live cells. McGann, Walterson, and Hogg[125] measured forward and side scatter and Coulter volume of osmotically stressed and frozen-thawed cells. Osmotic swelling increased volume and decreased scatter signals, while membrane damage from freezing and thawing decreased scatter signals, but not cell volume. Scherer et al[253,4] noted that changes in membrane lipid packing such as those that occur in apoptosis can affect forward scatter signals in the absence of apparent changes in cell volume or refractive index. In general, care is required when drawing conclusions about changes in scatter values. Care may also be required when drawing conclusions about relationships between dye uptake and cell death, but we'll open that can of worms later.

Side Scatter and Cytoplasmic Granularity

The group at Los Alamos set the pace for flow cytometric measurement of laser light scattering at multiple angles, as they had set the pace for forward light scattering measurements. The most elaborate of the instruments built at Los Alamos for this purpose[111] incorporated a sectoral solid state detector that measured 32 different signals, each representing the intensity of light scattered over a different range of angles from the incident beam. A dedicated minicomputer was required for data handling; while this apparatus was used to demonstrate differences in 32-parameter multiangle scatter signatures among different subpopulations in a variety of cell samples, it was difficult to determine whether a few and which few of the 32 scattering angle regions from which measurements were taken might contain the information most useful for cell discrimination[231,570,698].

In 1975, Salzman et al showed[157] that unfixed, unstained blood lymphocytes, monocytes, and granulocytes could be distinguished from one another by using measurements of forward and **orthogonal (90°) scatter** (now almost always called **side scatter**). Most of the information required for this discrimination is obtained from the side scatter signal, which is low for lymphocytes, higher for monocytes, and highest for granulocytes. The granular structures in the cytoplasm of granulocytes obviously present many more opportunities for scattering of incident light than does the more uniform cytoplasm of lymphocytes, and the higher intensity of light scattered at large angles to the incident beam probably represents some combination of multiple reflections and the summation of single scattering events from individual granules.

Whether or not theory can provide a complete explanation for the effect, it is reproducible and useful. After learning of the work at Los Alamos, I convinced my colleagues to incorporate side scatter measurement channels into Block's Cytomat-H differential counter prototypes and Cytomat-R research apparatus[92,3], where they proved useful enough in discriminating lymphocytes from monocytes and granulocytes to render our patented three-dye staining process largely unnecessary (see pp. 253-4).

Lymphocyte Gating: Forward Scatter Aside

When monoclonal antibody reagents became available, in the late 1970's and early 1980's, forward and side scatter

measurements were used to identify lymphocytes and set a gate for immunofluorescence analyses in antibody-stained samples from lysed whole blood or buffy coat, following a procedure established by Hoffman et al[175,176,699]. **Two-angle scatter gating** of lymphocytes eliminated the time-consuming and labor-intensive process of enriching samples for mononuclear cells by centrifugation over a discontinuous density gradient using Ficoll-Hypaque or other separation media; it was also desirable because the separation procedure could lead to differential loss of lymphocyte subpopulations, e.g., the CD8+ (cytotoxic/suppressor) T cells[592-3]. It was not long, however, before trouble came to Paradise.

It was first noted that the advantages of two-angle scatter gating might not be realized if windows were improperly set[662,700]. In the mid-1970's, when the technique was first described, there was no better way to establish the extent to which lymphocytes and monocytes might cross-contaminate one another's gates. In 1990, Loken at al[1251] described the technique of **back-gating**, in which a sample stained with anti-CD14 and anti-CD45 antibodies (lymphocytes have high CD45, and monocytes high CD14) is used to allow determination of the fraction of the total lymphocyte population excluded from, and the fraction of other cell types included in, a particular lymphocyte gate. Widespread application of back-gating helped make it feasible for large numbers of laboratories to deal consistently with T cell subset analyses in HIV-infected patients.

While back-gating represented an improvement over simple two-angle scatter gating, it has substantial limitations. Once a scatter gate has been established by back-gating, subsequent analyses do not explicitly identify cells within the gate as lymphocytes or other cell types. If, for example, an experimenter wanted to determine levels of an antigen that was found on activated, but not resting, lymphocytes, and which was also present on other cell types, it would not be possible to know precisely which antigen-bearing cells in the scatter gate were and were not lymphocytes.

As more monoclonal antibodies and labels for them became available, making three-color immunofluorescence measurements feasible for routine clinical use, back-gating has largely been replaced by more specific gating procedures. **T-gating**, which identified T lymphocytes as lying in a gate drawn on a plot of side scatter vs. CD3 antibody immunofluorescence (as in Figures 1-14, 1-15, and 1-16, pp. 31-32) was described by Mandy et al[1027]. While it improved the accuracy with which CD4- and CD8-positive T lymphocytes could be identified, T-gating did not allow an estimate to be made of the size of the total lymphocyte population, which is often of clinical relevance.

Current practice, as described by Nicholson, Jones, and Hubbard[1252] defines a lymphocyte gate on the basis of high CD45 antigen expression and low side scatter, as illustrated in Figure 1-17 (p. 34). T cells in the lymphocyte gate are then identified by the presence of CD3 antigen. A four-color immunofluorescence measurement using antibodies to CD45, CD3, CD4, and CD8 allows $CD3^+4^+8^-$, $CD3^+4^-8^+$, $CD3^-4^+8^-$, and $CD3^-4^-8^+$ populations to be identified in a single tube (Figure 1-19, p. 38). An additional point in favor of more specific gating comes from the knowledge that different lymphocyte subsets are not uniformly distributed within the forward vs. side scatter gate but, rather, tend to have different median values of forward and side scatter[703,1247,1253]. A tightly set scatter gate will, therefore, selectively exclude one or more lymphocyte types.

Other Applications of Side Scatter

Changes in the side scatter signals of neutrophils occur in association with degranulation and membrane ruffling following activation[592,701]; side scatter signal amplitude also decreases on storage of anticoagulated blood samples, making it advisable to do gated immunofluorescence measurements on whole blood within 24 hrs or less following collection of samples.

The combination of forward and side scatter measurements was used, alone or in combination with measurements of lectin binding, autofluorescence, or immunofluorescence, in the earliest successful attempts to enrich **hematopoietic cell populations** by sorting[161,177-9], and to discriminate cell subpopulations in samples from a variety of sites[703-705].

Forward and side scatter signals have also been used to assess **nuclear morphology** of prostate[706] and bladder (J. Coon, personal communication) cancer cells. Papa et al[1254] reported that side scatter signal intensity from nuclei decreases as chromatin is decondensed by lowering ionic strength or by releasing histone H1 at low pH. Zucker et al[1255] and Nusse et al[1256] showed that, when certain preparative steps are employed, **mitotic nuclei** can be discriminated on bivariate displays of DNA content (propidium fluorescence) vs. side scatter.

Scatter signals may be profoundly influenced by inclusions in cells, particularly if these contain material with a refractive index markedly different from that of the cytoplasm. For example, Dubelaar et al[707] found marked differences in forward and side scatter signals between cyanobacteria containing and lacking **gas vacuoles**.

Nordström et al[2535] report that increased side scatter provides a good indication of whether or not insect cells have been infected with recombinant baculoviruses, eliminating the need for and cost of a fluorescent marker.

Extrinsic cellular parameters can be measured with appropriate reagents using side scatter signals. For example, Böhmer and King[708] labeled lymphocytes with **antibodies conjugated to colloidal 40-nm gold particles**; the gold label produced increased side scatter signal amplitudes more than tenfold and did not interfere with fluorescent antibody labeling.

The orthogonal design of most laboratory-built and commercial laser source flow cytometers has made it relatively easy to measure forward scatter, and to utilize the collection optics also used for fluorescence to measure side scatter. It requires at least a little bit of instrument modification to make measurements of light scattered over other angular

ranges, and, while collection at two angles undoubtedly provides a great deal more information than collection at one angle, I am not yet convinced that collection at 32 angles provides an equivalent improvement over collection at two angles. The side scatter parameter has proven useful enough to have been incorporated into almost all commercial designs.

What is the Right Angle for "Right Angle" Scatter?

As the number of immunofluorescence signals measured increases, it may become difficult to make room in the orthogonal detector optical assembly for a scatter measurement detector. Stovel et al[709] coped with this problem by equipping the Stanford cell sorter with an outboard detector for large angle scatter signals, using a 2 mm diameter gradient index ("GRIN") lens coupled to the detector via a fiber optic. This lens collected light scattered at 130° from the beam, and its optical axis was not perpendicular to the direction of fluid flow. The 130° scatter signal was said to provide information equivalent to that in the side scatter signal for discriminating lymphocytes from other leukocytes; in addition, the positioning of the detector greatly reduced orientation artifacts normally found in side scatter signals from erythrocytes.

As was mentioned on p. 159, Steen[1147] noted that scatter signals collected at angles as small as 18° from the beam axis have the characteristics, and reflect the same cellular features, as signals collected orthogonal to the axis. In selecting a collection angle for large angle scatter, we therefore have a great deal of latitude. I have mentioned that Mariella et al collected very good large angle scatter signals by placing a fiber optic in the stream with its axis along the axis of flow[2455-6]; as a rule, however, there are practical reasons for not doing this.

Does Side Scatter = Total Protein?

I and others have observed[8,103,1255] that side scatter measurements correlate pretty well with flow cytometric measurements of **total protein** made using covalently and noncovalently bonded fluorescent dyes such as brilliant sulfaflavine, fluorescein isothiocyanate, sulforhodamine 101, and "LN" (also see Fig. 5-17, p. 254). I will discuss this further in the section on measurement of protein content.

Optimizing Side Scatter: Not as Easy as It Looks

We pretty much take it for granted that we can set up and align a flow cytometer using polystyrene beads with a very narrow size distribution, tweaking the optics to get the largest amplitude and the lowest CV we can in forward scatter and fluorescence measurements. However, as Doornbos et al noted[2512], it may be difficult to play this game with a side scatter channel; plots of forward vs. side scatter often show "Lissajous-like" patterns of wavy lines and loops, with relatively small CVs in forward scatter and large CVs in side scatter. This is explicable by Mie theory (which holds reasonably well for beads, if not for cells), and is due to extreme sensitivity of the side scatter signal to small variations in the size of highly symmetric particles. Such variations are typically found in small subpopulations of beads as a result of imperfections in the production process. The implication of all this for the average user: minimizing the CV of the side scatter distribution of beads doesn't always guarantee optimal alignment of your instrument. If forward scatter and fluorescence look good, and side scatter doesn't, don't futz with side scatter unless you can improve it without losing performance on the other channels.

Polarized 90° Scatter Measurements Reveal Eosinophils and Malaria Pigment-Containing Monocytes

Polarization measurements of orthogonal light scattering were introduced by de Grooth et al[210]. Under normal circumstances, randomly polarized light scattered orthogonal to the incident beam becomes linearly polarized (see pp. 78-82); linearly polarized light scattered at 90° remains polarized. In theory, some portion of the light collected orthogonal to the incident beam represents light scattered several times; the more times, the greater the likelihood that this light will be depolarized. **Eosinophil** granulocytes were found to be distinguishable from neutrophil granulocytes by higher values of depolarized side scatter. An as yet unidentified subpopulation of lymphocytes was also distinguished by higher depolarized scatter signals.

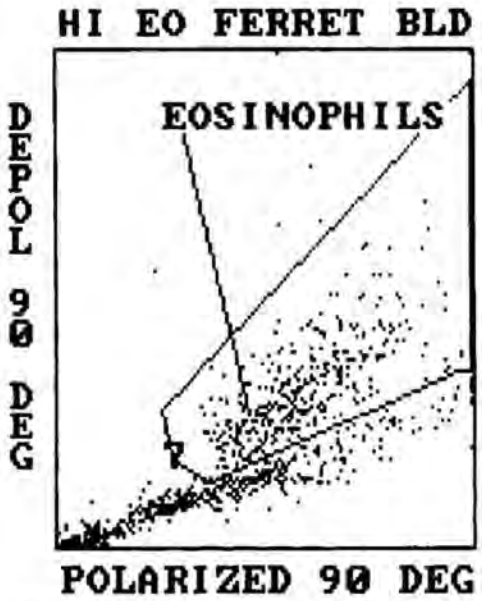


Figure 7-2. Depolarized 90° scatter signals can be used to identify eosinophil granulocytes.

Figure 7-2 shows polarized vs. depolarized 90° scatter values for leukocytes in lysed whole blood from a ferret with a high eosinophil count due to an experimental infection with microfilaria. The eosinophils are clearly separable from the other white cell types; a count of 100 particles sorted from a gate set as shown in the figure revealed 99 eosinophils and one worm.

It is relatively trivial to set up an instrument to make depolarized scatter measurements using inexpensive plastic

polarizing filters (see p. 157). The technique requires no reagents, and represents the easiest way to count and sort eosinophils from a wide range of species (L. Terstappen, personal communication). The sorter manufacturers won't tell you about it, because it is the subject of a patent now held by Abbott and used in that company's Cell-Dyn hematology instruments. The birefringence of eosinophil granules, which is responsible for the cells' higher depolarized scatter signals, was noted decades ago; one could very likely use polarized and depolarized extinction signals to count or sort eosinophils without infringing on anybody's patent.

In 1999, Mendelow et al[2536] reported that a population of cells with relatively low polarized side scatter values and high depolarized side scatter values appeared when the peripheral blood of malaria patients was analyzed in a Cell-Dyn instrument. It was suggested that these cells were monocytes containing the malaria pigment hemozoin, which is known to be birefringent. Nordström et al[2537] subsequently confirmed this by cell sorting.

Many bacteria have birefringent cell walls, which suggests that polarized and depolarized scatter measurements might be useful in discriminating among genera or species. However, depolarized scatter signals, even from eukaryotic cells, are typically of much lower intensity than polarized scatter signals, suggesting that depolarized signals from bacteria could be too weak to permit precise measurements.

Multiple Wavelength Scattering Measurements

Any apparatus that incorporates a lamp instead of a laser as a light source for light scattering measurements will, obviously, measure light scattered over a larger range of wavelengths than will a laser source instrument. Technicon's older blood cell and differential counters[84,85], the Cytomat arc source instrument[88], the apparatus (Skatron Argus, Bio-Rad Bryte, etc.) developed by Lindmo and Steen[100-3], and the old B-D FACS analyzer all fell into this category.

The Technicon Hemalog D apparatus was noteworthy for its utilization of measurements of light scattering at different wavelengths for cell classification. In this system, basophil leukocytes were stained with a blue basic dye, which imparted a blue color to their specific granules. The granules therefore absorbed red light; however, their absorption was not high enough to permit unequivocal discrimination between basophils and other cells on the basis of absorption, especially since the number of granules per cell is highly variable. Satisfactory discrimination was achieved by making separate measurements of the scattering of red and near-infrared light by the cells. Since basophils, which contained the blue dye, absorbed more red light than infrared light, the ratio of red scatter amplitude to near-IR scatter amplitude was lower for the basophils, which could thus be discriminated from other cell types in the two-dimensional measurement space.

While developing the Block differential counter, we measured forward and 90° scatter signals from fixed and unfixed, unstained leukocytes at different laser wavelengths (325 and 441 nm from a helium-cadmium laser, 488 and 515 nm from an argon ion laser, and 633 nm from a helium-neon laser), and were somewhat surprised to find that ratios of scatter intensities at different wavelengths were different for different cell types, to an extent that allowed us to obtain differential counts of lymphocytes, monocytes, neutrophils, and eosinophils in unstained blood samples. Our enthusiasm for further work along these lines was tempered when we found that slight alterations in the geometry of the optical system used for forward scatter measurements could produce large changes in the relative positions of cell clusters. I was thus not surprised to read others' reports[186,1612,1880] that laser light scattering at different wavelengths (351/363, 457, 488, and 515 nm, all from argon lasers) provided information that could discriminate different types of blood cells.

A principal problem with studies of this type lies in the difficulty of making sure that the optical geometry is the same at the different wavelengths used. Even in the case in which UV and visible light are emitted in the same collinear beam by the same argon laser, the beam diameters are apt to be different, and the focusing lens, unless custom made for the purpose, will not have the same focal length at both wavelengths. This makes it hard to determine the extent to which apparent differences in scattering at different wavelengths may be due to small but significant differences in such factors as beam size and collection angle. Others have reported that UV scatter signals, obtained from the B-D FACS using an argon laser source, were less satisfactory than signals at 488 nm for cell discrimination. Using the Block instruments, we usually obtained better discrimination from the UV scatter signals than from signals at 488 nm. This may represent another instance among many in which each of several groups gets its best results when using the methodology with which it is most familiar.

From Russia with Lobes

A few pages back, I said we'd get back to the complex stuff about scatter; by now, you probably think the Mueller matrix has been sent to Siberia. Well, it has, quite literally, and I am happy to report that it is alive and well there, in Valeri Maltsev's lab at the Institute of Chemical Kinetics and Combustion.

Over the years, a few attempts have been made to apply relatively sophisticated multiangle scattering measurements to cell sizing and characterization. Since Mie's theory of scattering, which forms the basis for attempts to measure cell size measurement by forward scatter, uses a model in which particles are spherical and homogeneous, we might reasonably expect that, however bad our results might be with spherical cells, they would get worse when we tried to size asymmetric cells. This presented a problem to people concerned with the most common and most profitable type of cell volume measurements, i.e., the manufacturers of blood cell counters for clinical laboratories, because erythrocytes are normally not spherical. Technicon's H-1 hematology

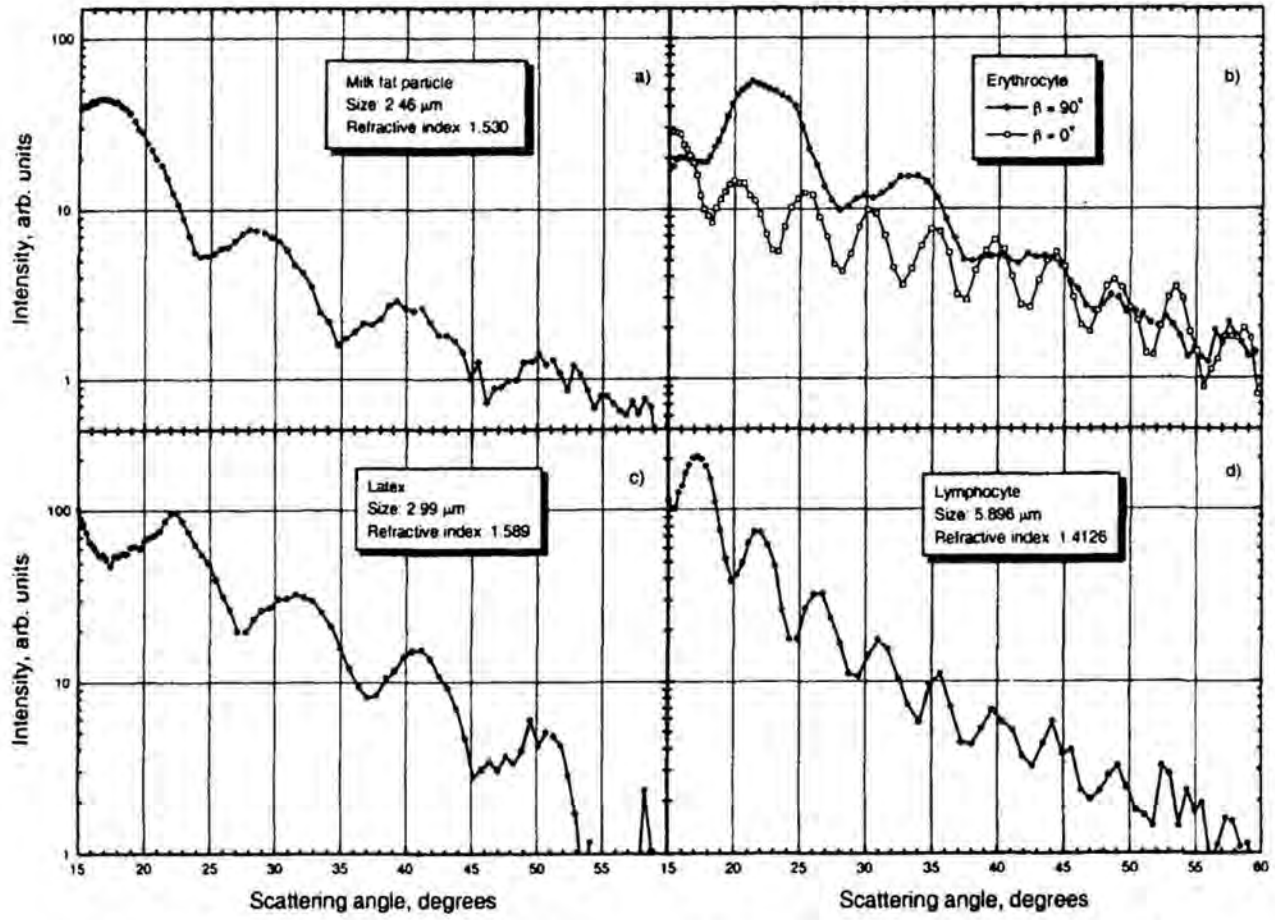


Figure 7-3. Indicatrices (plots of intensity vs. scattering angle) of a milk fat globule, a latex bead, a lymphocyte, and two erythrocytes. From: Shvalov AN et al, Cytometry 37:215-220, 1999 (Reference 2539), © John Wiley & Sons, Inc., used by permission.

instruments, and their successors (Technicon is now Bayer Diagnostics; see Chapter 8), employ a couple of ingenious maneuvers to deal with the problem. The discoid erythrocytes are converted, without changing their volumes, to spheres, using a procedure described by Kim and Ornstein[166]. This eliminates artifacts due to cell asymmetry; however, one still encounters substantial variation in the refractive indices of individual cells due to cell-to-cell differences in hemoglobin concentration. A measurement procedure devised by Tycko et al[684] meets this problem head-on; since the variation of refractive index with hemoglobin concentration is linear, it is possible, by making measurements of light scattered at two angles, to determine hemoglobin concentration and obtain volume from tables calculated using Mie theory. The system can be calibrated in absolute units of volume, using droplets of water-immiscible oils of different refractive indices as standards. This elegant methodology is demonstrably successful for its clinical hematologic purpose; it is unlikely to be adaptable to sizing other cell types.

Maltsev et al have come up with a simpler way of sizing sphered red cells in the course of extensive investigations on multiangle light scattering by cells and beads. They have devised a unique scanning flow cytometer in which particles are illuminated by a laser beam directed along the axis of flow; a fixed spherical mirror is used to collect scattered light. As the particle moves down the flow stream, the scattering angle from which light reaches the mirror changes. Thus, it is possible to derive a plot of intensity vs. scattering angle, known as an **indicatrix**, for each individual particle traversing the system. Indicatrices for a milk fat particle, a latex bead, a lymphocyte, and two (unsphered) differently oriented erythrocytes appear in Figure 7-3.

Indicatrices are uniquely characteristic of particle types; those for beads agree closely with calculations according to Mie theory. The sizes and refractive indices of spherical and near-spherical particles can be determined from their indicatrices, and, in at least some cases, it is possible to specify two or three angles for which light scattering measurements can be used for sizing. However, as Murphy's Law would predict, these angles are different for different cell types.

In cytometry, as in many other fields, there is little new under the sun; Loken, Sweet, and Herzenberg made measurements of multiangle light scattering in a modified FACS in the 1970's[155]; they did not, however, pursue the theoretical side of their investigations far enough to yield practical results. A commercial application of the Maltsev group's

work to hematology is now being pursued, but it still seems unlikely that the high-speed cell sorter manufacturers will be rushing to put indicatrix measurement capability into their products any time soon.

Optical Parameters: Absorption

Since, even in this day and age, a lot of quantitative chemical and biochemical analyses are done with absorption measurements, we might consider why we don't make more use of absorption in cytometry. Absorption measurements are somewhat more demanding than scatter and fluorescence measurements. In any microscope, light scattered at larger angles than can be collected by the microscope objective used cannot readily be distinguished from light absorbed by the specimen; accurate absorption measurements therefore require light collection over a relatively large angle, necessitating use of a lens with a high N.A. It's not that hard to build a flow cytometer with high-N.A. lenses, oriented along the same axis, for illumination and collection, suitable for absorption measurements; this configuration is used in blood cell counters. However, most laser source fluorescence flow cytometers incorporate a high-N.A. collection lens placed at right angles to the illuminating beam, making it impossible to mount a high-N.A. lens along the beam axis, and use low-N.A. optics to form an illuminating beam, which is not effective for absorption measurements.

To maximize precision in absorption measurements, it is also necessary to match the refractive indices of the object under study and the medium in which it is suspended, this maneuver minimizes apparent absorption due to scattering. However, in work with intact cells, it is generally not possible to completely avoid scattering by internal cellular structures, e.g., cytoplasmic granules, even when the indices of sheath, sample, and cell membranes are matched.

The major problem with absorption measurements arises from the fact that, in most cases, cells, even when stained, do not absorb more than a small fraction of the light passing through them. Most of the light reaching the detector is unaffected by interaction with the specimen; it is, therefore, background, and, as Johnnie Cochran might summarize the Wood-Hoffman model discussed on pp. 221-3, "If there's too high a B, you just can't see." Fluctuations in the intensity of illumination therefore have larger effects on absorption measurements than on measurements of scattered light and fluorescence. In the latter, signal intensity is proportional to source intensity; a 1% change in illumination intensity produces a 1% change in a scatter or fluorescence signal. Suppose, however, that an absorption measurement is made of a particle that removes 10% of the light from the incident beam. A 1% increase in illumination intensity occurring while the particle passes through the observation region would result in an apparent light loss of 9% instead of 10%, while a 1% decrease in illumination intensity would result in an apparent light loss of 11%. In this case, a 1% change in illumination intensity produces a 10% change in the amplitude of an absorption signal; the less light the particle removes from the beam, the larger the effect of source intensity fluctuations. The intensity fluctuations of the laser sources most commonly used in fluorescence flow cytometers, while small (a few percent peak-to-peak), are sufficient to make absorption measurements unacceptably imprecise. Because of the problems just discussed, the use of absorption measurements in flow cytometry is somewhat restricted; they are most commonly employed for semiquantitative detection of strongly absorbing substances in apparatus designed for blood cell counting and sizing, employing lamps rather than lasers as light sources.

Absorption Effects on Light Scattering

I noted on p. 279 that the presence of an absorbing (colored) substance in cells may be inferred from differences in intensity of scattering signals at wavelengths at which the material does and does not absorb strongly. A dramatic illustration of this, shown in Figure 7-4, comes from the work of Ost et al[2449], who measured red and violet light scattering by leukocytes and erythrocytes in unstained dilute whole blood.

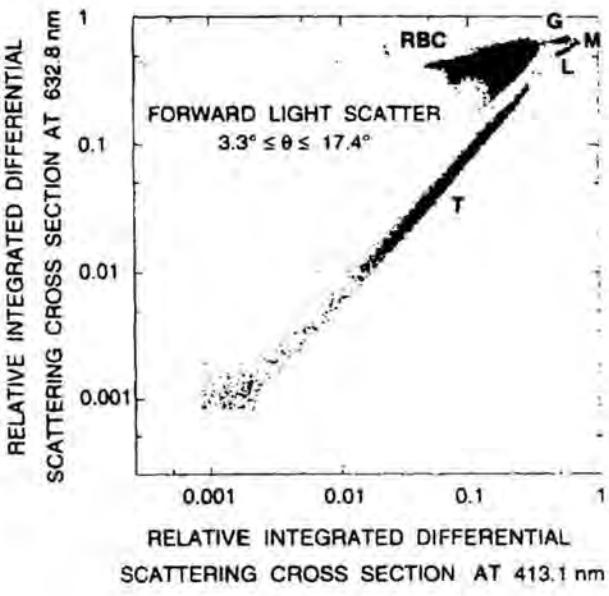


Figure 7-4. Erythrocytes scatter less light at a wavelength at which hemoglobin exhibits strong absorption. G: granulocytes; L: lymphocytes, M: monocytes, RBC: erythrocytes, T: thrombocytes. From: Ost V et al, Cytometry 32:191-197, 1998 (Reference 2449), © John Wiley & Sons, Inc., used by permission.

Erythrocytes contain high concentrations of hemoglobin, which absorbs strongly in the violet spectral region but only weakly in the red spectral region. If more of the photons incident on a cell are absorbed, fewer remain to be scattered. Their relatively low forward scatter intensities at 413.1 nm (violet) allow the erythrocytes (RBC) to be distinguished from leukocytes (G, M, L) and thrombocytes (T) on the two-dimensional dot plot of violet vs. red forward scatter.

Optical Parameters: Extinction

Extinction is a convenient term that describes **light loss** from the incident beam regardless of the mechanism involved. If a detector is placed where the beam stop used for a forward scatter measurement would normally be (see Fig. 1-21, p. 51), the passage of a cell through the measurement system will result in the detector signal decreasing in proportion to the total amount of light absorbed by the cell or scattered out of the field of view of the detector. Axial extinction or light loss signals are relatively easy to measure; photodiodes are typically used for the purpose. Like absorption signals, extinction signals are more sensitive to source noise fluctuations than are scatter and fluorescence signals. Although extinction measurements do not seem to be available in current commercial systems, Ortho's System 30 and System 50 instruments, made between the late 1970's and the late 1980's, featured an extinction measurement; the light source was a very low power (0.8 mW) He-Ne laser with very low RMS noise (0.05%). Steinkamp[659] described noise compensation circuitry that allowed fairly precise light loss measurements to be made using somewhat noisier argon lasers. It is now possible to achieve very low noise levels in diode lasers, which could be economical light sources for extinction measurements should anyone still be interested in doing them.

Returning for the moment to the subject matter of Figure 7-4 (previous page), Ost et al[2449] pointed out that, unlike forward scatter measurements, extinction measurements in the violet beam would not have been able to discriminate erythrocytes from other cell types, because, while the erythrocytes absorb more light and scatter less light than the other cell types, the total light losses from the beam are approximately equal for erythrocytes and other cells. To generalize, extinction measurements are not particularly good for quantifying amounts of stuff in or on cells or particles. So why should anyone still be interested in doing them?

The answer is that extinction measurements are useful for sizing particles; pulse width, rather than pulse height or area, is the critical characteristic. I will say more about this in the discussion of measurement of intrinsic cellular parameters (pp. 285-8).

Other Transmitted Light Measurements

Progress beyond van Leeuwenhoek's level in the microscopy of living, unstained biological materials has largely been made in this century with the development of dark field, polarized light, phase contrast, and interference contrast techniques. From the 1930's on, the newer methods of microscopy were, in their turn, adapted to quantitative measurement. The apparatus originally built[712] for **interferometric dry mass determinations** and **phase-based optical path length measurements** was cumbersome and difficult to use, but did yield accurate results, and was applied to a reasonable range of biological specimens.

Flow cytometry has benefited tremendously from the phenomenal pace of technological growth since the 1960's, which gave us lasers, vastly improved detectors and imaging devices, integrated circuits, microprocessors, and the electronics and computational methods required to store, manage, and process the bewildering mass of data we can generate. We can easily implement the entire range of microscopic measurement techniques with which our predecessors struggled. Turned on by technology, and surrounded by its cornucopia of gadgets, we tend to forget that, even with genetic engineering, we're basically looking at the same animalcules that fascinated van Leeuwenhoek.

By the 1920's, dark field microscopy could be used to visualize viruses and other particles below the resolution limit of transmitted light microscopy, as well as to examine the structural details of unstained cells; the obvious utility of the technique led to the development of the first flow cytometers, designed to detect and count particles based on light scattering, by the 1940's. The range of light scattering measurements available in modern flow cytometers essentially encompasses the subject material of dark field microscopy, and has expanded into polarized light microscopy.

Interference and Phase Measurements

The technology exists for making flow cytometric measurements of **optical path** and **dry mass** corresponding to those done with much greater difficulty by an older generation of **phase** and **interference microscopes**[714]. Again, it's harder to do these measurements than to do our bread-and-butter scatter, extinction, and fluorescence measurements. Work in this direction will probably yield a couple of parameters corresponding to things we can observe, at least some of which may be measurable more easily by other methods, and a whole bunch of data, which nobody will be able to interpret, but which will be just interesting enough to keep another generation of investigators funded. That's science. If we want to learn from history, however, we should note that biological microscopy has been advanced far more by the discovery, use, and refinement of staining methods than by the improvement of techniques for observation of unstained specimens, and that the primary path of development of analytical cytology has, similarly, been in the direction of measurement techniques using reagents, which have enabled us to characterize cells' chemistry and function with amazing sensitivity, specificity, and precision using relatively pedestrian measurement techniques.

There are instances, however, where the increased complexity of the instrumentation needed to make a measurement without using a reagent are offset by the potential disadvantages associated with use of the reagent. A good example is the sorting of sperm for sex selection in animals and humans. This was mentioned briefly on pp. 26 and 178 and will be discussed further in Chapter 10. Of note here is van Munster's work on enrichment of X- and Y-sperm by sorting based on interferometric volume measurement[3541,2].

Optical Parameters: Fluorescence

There is not much to add to what I have said to this point about basic fluorescence measurement in flow cytometry. Observation periods in conventional flow cytometers are on the order of microseconds, while the fluorescence lifetimes (pp. 112-8) of most probes and labels, and of fluorescent constituents of cells, are on the order of a few nanoseconds. This means that hundreds of photons are likely to be emitted from each fluorescent molecule in or on a cell during the cell's traverse of an illuminating beam at a wavelength at or near the molecule's excitation maximum.

While even the most efficient fluorescence collection optics collect no more than about 20% of the total emission from cells, the discussion of Q and B on pp. 221-3 tells us that, during the time a cell spends in the beam, the photocathode of a detector PMT will crank out photoelectron for every few molecules of our most efficient probes, and perhaps one photoelectron for every few hundred molecules of our least efficient probes. Using our conventional measurement technique, once we have determined the spectral bandwidth of a particular detector, we have no way of telling whether the photons reaching it to generate the photoelectron current we measure came from a dye we were trying to measure, from a fluorescent cellular constituent, or from stray excitation light. There are, however, ways of making at least some of those distinctions.

Fluorescence Lifetime Measurements

Pinsky et al[1274] and Steinkamp and Crissman[1275] used **phase-sensitive detection** to measure **fluorescence lifetimes** by flow cytometry. The phase referred to here relates to the electronic signal, not the phase of light waves. The laser used for excitation is modulated at a frequency between 10 and 50 MHz, meaning that the intensity fluctuates with a period of 20 to 100 nsec. The fluorescence emitted by cells also fluctuates at the modulation frequency, but there is a difference in phase between the excitation and emission waveforms, corresponding to the excited state lifetime. It is relatively simple to electronically dissect components of the fluorescence signal having different phase relationships to the excitation waveform, and therefore representing emission from fluorophores with different lifetimes. This enables the separation of signals from molecules with similar emission spectra.

Using the phase-sensitive flow cytometer built at Los Alamos, Steinkamp and his colleagues[2543-7] have demonstrated several possible uses of the fluorescence lifetime measurement, including separating weak signals from fluorescently labeled antibodies and/or gene probes from the autofluorescence background, discriminating signals from two probes with similar emission spectra but different lifetimes, and distinguishing emission signals from a single probe under different binding conditions. Capacity for lifetime measurement has not yet been incorporated into commercial flow cytometers. Lifetime measurements may also be made in imaging systems; van Zandvoort et al[2548] were able to distinguish signals from the dye SYTO-13 bound to DNA and the same dye bound to RNA using this method.

Fluorescence Polarization Measurements

As was noted on p. 114, fluorescence polarization measurements may be used to assess the mobility of fluorescent molecules. The laser sources used in most flow cytometers emit linearly polarized light. If the molecules in a sample excited by such a laser were completely immobile, the fluorescence emission would also be linearly polarized. However, any molecules that changed their orientations while in the excited state would emit in a different plane of polarization. Small molecules in solution are freer to move than are identical molecules bound to macromolecules or macromolecular assemblies; the degree of polarization of fluorescence emission can, therefore, be used to estimate the proportions of free and bound dye. Typical practice involves measurement of fluorescence emission in two planes of polarization, with analog or digital computation used to derive values of **fluorescence polarization** or **fluorescence anisotropy** using the formulae shown on p. 114.

Flow cytometric measurements of polarization, anisotropy, etc. are not difficult, in principle. Since the laser beams used for excitation in most instruments are already linearly polarized, it is only necessary to use polarizing filters, prisms, or beamsplitters ahead of the fluorescence detectors (PMTs) to make the intensity measurements in two planes of polarization[5,406,407-9]. Asbury et al[2439] have provided the most thorough and most current discussion of this subject.

Energy Transfer Measurements: Something to FRET About

Fluorescence Resonance Energy Transfer (FRET), also distinguished as **Förster energy transfer**, was introduced on pp. 44-5 and p. 115. Intramolecular energy transfer is responsible for the relatively large Stokes' shifts (p. 112-3) of phycobiliproteins and tandem conjugates, but the effect has many other interesting applications in cytometry, most notably in determining proximity between and/or colocalization of different molecules in or on cells.

For energy transfer between two (donor and acceptor) chromophores to occur, the absorption spectrum of the acceptor must overlap the emission spectrum of the donor. If the donor and acceptor are sufficiently close, absorption of excitation energy by the donor can result in nonradiative transfer of this excitation energy to the acceptor, with subsequent emission by the acceptor at wavelengths characteristic of the acceptor's emission spectrum.

The smaller the distance between donor and acceptor, the more likely it becomes that resonance energy transfer, rather than emission of fluorescence by the donor, will occur. Förster showed that the probability of energy transfer varies as the inverse sixth power of the distance between the chromophores, and this high-order dependence allows the intensity of energy transfer to be used to provide a sensitive

measure of this distance, or what Stryer and Haugland[315] termed a "spectroscopic ruler."

Energy transfer measurements using single beam excitation at 488 nm can be made using fluorescein, which is optimally excited at this wavelength, as the donor, and tetramethylrhodamine, which has less than 5% of its maximal absorption at 488 nm, as the acceptor. Chan, Arndt-Jovin, and Jovin[314] used flow cytometric measurements of **energy transfer**[23] between fluorescein- and tetramethylrhodamine-labeled concanavalin A to estimate the proximity of receptors for this lectin on the surface of Friend mouse erythroleukemia cells.

The flow cytometric energy transfer measurement technique originally described by Chan et al is applicable to the study of many different types of ligand-receptor interactions; Szöllösi et al[316] reported that flow cytometry offered advantages over conventional steady-state fluorimetry for energy transfer measurements on cell surfaces.

Several groups have used energy transfer measurements to demonstrate associations between cell surface structures[1508-11,2549-50] and to investigate molecular assemblies on beads[2551]. Bene et al used both energy transfer and anisotropy measurements in a study of receptor clustering[2552]. Energy transfer between different lipid membrane labels has also been used to identify and sort cell hybrids[1512].

General principles and methodology have been reviewed by Szöllösi et al[783, 2547] and by Mátyus[1507]; two recent papers discuss the use of phycoerythrin and allophycocyanin as an energy transfer pair for FRET measurements[2553-4].

Quenching and Energy Transfer

Quenching of fluorescence (p. 115) occurs when energy is transferred from a fluorescent donor to a nonfluorescent acceptor. It can occur via the Förster mechanism or other mechanisms. Such quenching can be undesirable; for example, as one labels an antibody molecule with an increasing number of molecules of a fluorescent dye, each additional molecule adds less and less additional fluorescence because of quenching due to intramolecular interactions.

Parenthetically, while it is true that, if we were able to put dozens of molecules of a covalently bound label on an antibody, we would run the risk of changing the reactivity by getting one of the label molecules into the binding region, it is the quenching effect that prevents us from simply putting a lot of fluorescent dye on some other macromolecule and conjugating that to an antibody.

Quenching can be also desirable; when one is trying to distinguish between fluorescent particles in a cell and those bound to the surface, adding a spectrally appropriate cell-impermeant, nonfluorescent dye to the sample will quench the fluorescence of the extracellular, but not of the intracellular particles.

Matko et al[2555] used quenching by a long range electron transfer (LRET) mechanism to study protein clustering at cell surfaces. Packard and Komoriya[2556-7] have synthesized fluorescent indicators of protease activity in which two dye molecules attached to a peptide quench one another by an exciton transfer mechanism rather than a Förster mechanism; cleavage of the peptide by a protease renders the indicator molecule many times more fluorescent.

Measuring Fluorescence Spectra in Flow

Measurement of fluorescence emission spectra in flow was mentioned on pp. 152-3. Since current commercial instruments from BD Biosciences, DakoCytomation, and Partec permit measurement of fluorescence excited by a single laser (usually at 488 nm) in as many as 7 different spectral bands, using only dichroics and filters for spectral separation, one might say that low-resolution spectral measurement capability is now available off the shelf.

Earlier efforts[122,649,1139-40] and more ambitious later projects have used polychromatic detection. Asbury et al[2558] measured spectra of cells and chromosomes in flow using a monochromator that changed the wavelength detected by a PMT during the course of a run; the overall run yielded spectra of DNA dyes in the cells or chromosomes, although only a single wavelength was detected from any individual particle.

Fuller and Sweedler[2559] built a slow-flow system in which a grating dispersed collected fluorescence emission to a CCD, so that different pixel regions on the CCD responded to different wavelengths. This system was used to discriminate and size submicron synthetic lipid vesicles.

Gauci et al[2560] used a dispersing prism and an image-intensified diode array detector to capture fluorescence spectra of individual *Dictyostelium* spores stained with fluorescent antibodies bearing a variety of labels.

Two-Photon Fluorescence Excitation in Flow

It's not easy, and may not be all that's useful, but it's been done[2442]. See pp. 118-9.

Bioluminescence Detection in Flow?

People ask about this on the Purdue Cytometry Mailing List every now and then. Bioluminescence assays generally involve a very long observation time (some of them use photographic film as a detector), because you don't get a very high photon flux from most luminescent probes. It therefore seems unlikely that you'd collect a lot of photons from a cell bearing luminescent material if you ran it through the flow cytometer for a few microseconds with the laser turned off.

Lindqvist et al[1276] reported detection of luminescence from insect cells transfected with luciferase genes and exposed to luciferin; they did, however, use a 488 nm laser to illuminate the cells, and their paper does not make clear whether the measurements would work with the laser turned off.

So the bottom line of this little section (and of every paragraph in it) is that, when you ask me how I feel about the prospect of doing bioluminescence measurements in flow, I will tell you: turned off.

7.2 INTRINSIC CELLULAR PARAMETERS

I have called cellular parameters that can be measured without reagents **intrinsic**, and those that require reagents, or **probes**, for their measurement **extrinsic**. The contents and physical states of chemically defined entities in cells and organelles are **structural** parameters; **functional** parameters include biological properties and activities as well as a few specific chemical entities, such as intracellular pH and [Ca^{++}], which undergo rapid physiologic changes in living cells. The distinction between structural and functional parameters is more arbitrary than the distinction between intrinsic and extrinsic parameters; obviously, structural parameters such as DNA content provide considerable information about cell function. However, the classification I have used seems agreeable to most people's sensibilities.

Depending upon the composition of a cellular sample and upon the experimenter's goals, the same parameter can sometimes be used both to differentiate one cell type from others in a mixed population and to provide information about the cell's biological state. For example, tumor cells with near haploid DNA content are readily distinguished from normal host cells or stroma in the same sample, and can also be classified as being in the G_0/G_1 or in the S phase of the cell cycle, based solely upon a single measurement of DNA content. Note, however, that, in this instance, tumor cell G_2 and M phase and stromal cell G_0/G_1 phase DNA contents will overlap; distinguishing these populations will therefore require multiparameter measurements.

I will turn now to intrinsic cellular parameters, after which I will introduce probes and extrinsic cellular parameters. The list of measurable cellular **parameters** that appeared as Table 1-1 on p. 3 is reproduced as Table 7-1 on the next page for convenience.

Cell Size

From the preceding sections of this chapter, I hope you have concluded that DC impedance (Coulter volume) measurement is a reasonably good physical parameter to use for measuring cell or particle size (volume, in this case), that forward light scattering is an unreasonably bad one, and that extinction might be useful. It would, however, help if we had a "gold standard" for at least some form of size measurement; there is one, but it is not cytometric, or at least not totally cytometric.

Mean Cell Volume: The Cellocrit as Gold Standard

The Coulter orifice itself does not provide an absolute measurement of cell volume; this is best obtained, at least in terms of a mean value for a cell population, by first determining the **cellocrit**. The cellocrit is analogous to the familiar **hematocrit** measurement of clinical hematology, which determines the fraction of total blood volume occupied by red cells. The cellocrit is obtained by centrifuging a suspension containing a known number of cells per unit volume in a tube or capillary with a uniform cross-section along its length, and measuring the heights of the column of packed cells and of the entire column of fluid (i.e., the packed cells plus the supernatant). The cellocrit, expressed as a decimal fraction, is the ratio of the first of these to the second. If the cellocrit is to be reported as a percentage, the value is 100 times this ratio.

For cellocrit measurements to be accurate, the cells must occupy a fairly high fraction of the fluid volume; red cells are present at very high concentrations (about 5,000,000/μL) in blood, and the normal range of hematocrits runs from about 35% to about 50%. The best way to make cellocrit measurements on cells other than red blood cells is to pellet the cells and make the measurement after the pellet is resuspended in a very small volume of fluid. For critical work, isotope-labeled macromolecules can be added to the suspension to allow correction of cellocrit values for the volume of suspending medium trapped in the packed cell column.

In order to derive a measure of mean cell volume from the cellocrit, an accurate count of cells per unit volume must be obtained from another aliquot of the sample used for cellocrit measurements. You should know by now that you won't get an accurate or precise cell count using a microscope and a hemacytometer; the cell count will have to be done by a cytometer of one sort or another. The mean cell volume is then computed by dividing the cellocrit (as a fraction) by the cell count. Measurements of cell volume made in this fashion provide a primary standard for calibration of apparatus that is used for routine optical and/or electronic measurement of cell size.

Cell Volume, Area, and Diameter

Different cell size measurements may be needed for different applications. For example, if one wants to determine the **concentration** of a dye in cells, a value for cell **volume** is needed, while in calculations of **antigen density, surface area** is the desired quantity. The relationships between these are nonlinear; radius or diameter varies as the cube root of volume, cross-sectional area and surface area as the square of radius or diameter or the two-thirds power of volume. Schwartz et al described a simple method of using log amplifiers to derive cell diameter and surface area from electronic volume measurements[152]; ratio circuits have also been used by others for analog computation of receptor or antigen density from volume and presumptive cross-sectional area measurements[311,657-8]. These days, we'd use digital computers.

Cell Sizing: Slit Scans and Pulse Widths

A somewhat more practical general method of cell size measurement, available in some commercial flow cytometers, relies on the principle of **slit-scanning** (see pp. 183-4). The durations or widths of pulses produced at the detectors by particles passing through the illuminating beam will always vary with the size of the particles; particles with larger diameters or cross-sections will produce wider pulses. However, differences in pulse width between particles of different sizes become most apparent when the illuminating beam is

PARAMETER	MEASUREMENT METHOD AND PROBE IF USED
Intrinsic Structural Parameters (no probe)	
Cell Size	Electronic (DC) impedance, extinction, small angle light scattering; image analysis
Cell shape	Pulse shape analysis (flow); image analysis
Cytoplasmic granularity	Large angle light scattering, Electronic (AC) impedance
Birefringence (e.g., of blood eosinophil granules)	Polarized light scattering, absorption
Hemoglobin, photosynthetic pigments, porphyrins	Absorption, fluorescence, multiangle light scattering
Intrinsic Functional Parameter (no probe)	
Redox state	Fluorescence (endogenous pyridine and flavin nucleotides)
Extrinsic Structural Parameters (probe required)	
DNA content	Fluorescence (propidium, DAPI, Hoechst dyes)
DNA base ratio	Fluorescence (A-T and G-C preference dyes, e.g., Hoechst33258 and chromomycin A_3)
Nucleic acid sequence	Fluorescence (labeled oligonucleotides)
Chromatin structure	Fluorescence (fluorochromes after DNA denaturation)
RNA content (single and double-stranded)	Fluorescence (acridine orange, pyronin Y)
Total protein	Fluorescence (covalent- or ionic-bonded acid dyes)
Basic protein	Fluorescence (acid dyes at high pH)
Surface/Intracellular antigens	Fluorescence; scattering (labeled antibodies)
Surface sugars (lectin binding sites)	Fluorescence (labeled lectins)
Lipids	Fluorescence (Nile red)
Extrinsic Functional Parameters (probe required)	
Surface/intracellular receptors	Fluorescence (labeled ligands)
Surface charge	Fluorescence (labeled polyionic molecules)
Membrane integrity (not always a sign of "viability")	Fluorescence (propidium, fluorescein diacetate [FDA]); absorption or scattering (Trypan blue)
Membrane fusion/turnover	Fluorescence (labeled long chain fatty acid derivatives)
Membrane organization (phospholipids, etc.)	Fluorescence (annexin V, merocyanine 540)
Membrane fluidity or microviscosity	Fluorescence polarization (diphenylhexatriene)
Membrane permeability (dye/drug uptake/efflux)	Fluorescence (anthracyclines, rhodamine 123, cyanines)
Endocytosis	Fluorescence (labeled microbeads or bacteria)
Generation number	Fluorescence (lipophilic or covalent-bonded tracking dyes)
Cytoskeletal organization	Fluorescence (NBD-phallacidin)
Enzyme activity	Fluorescence; absorption (fluorogenic/chromogenic substrates)
Oxidative metabolism	Fluorescence (dichlorofluorescein)
Sulfhydryl groups/glutathione	Fluorescence (bimanes)
DNA synthesis	Fluorescence (anti-BrUdR antibodies, labeled nucleotides)
DNA degradation (as in apoptosis)	Fluorescence (labeled nucleotides)
"Structuredness of cytoplasmic matrix"	Fluorescence (fluorescein diacetate [FDA])
Cytoplasmic/mitochondrial membrane potential	Fluorescence (cyanines, rhodamine 123, oxonols)
"Membrane-bound" Ca^{++}	Fluorescence (chlortetracycline)
Cytoplasmic $[Ca^{++}]$	Fluorescence ratio (indo-1), fluorescence (fluo-3)
Intracellular pH	Fluorescence ratio (BCECF, SNARF-1)
Gene expression	Fluorescence (reporter proteins)

Table 7-1. Some cellular parameters measurable by cytometry.

focused to a spot that has at least one axis (that parallel with the flow) no larger than, and, ideally, smaller than, the diameter of the particles to be measured, producing a slit- scan (pp. 50-1).

The major drawback of typical slit-scanning systems lies in their use of a small focal spot size; the smaller the spot to which a laser beam is focused, the more rapidly the beam converges to and diverges from a focus (pp. 137-8). A beam focused to a height of 2 μm maintains that height over a very small distance; one would have to use a core diameter of 4 μm or less to minimize variations in pulse width due to beam divergence. If the beam height is 5 μm, it is possible to work with a more practical core diameter, 20 μm.

Small beam heights also affect the range of angles over which forward scatter can be measured. A classical forward scatter "size" measurement collects light from angles smaller than 2°, using a beam stop to block the axial illuminating beam from reaching the scatter detector. For this to work, the illuminating beam must be diverging at an angle well below 2°, which can generally be arranged when relatively large focal spots are used. When the spot becomes only a few μm high, the illuminating beam diverges at larger angles, and the angle over which the "forward" scatter signals are collected is correspondingly increased, thus increasing the influence on the scatter signal of internal and surface structure relative to cell size. In a slit-scanning flow cytometer in which observation is done in a cuvette, the forward scatter measurement can be done around a vertical blocker bar; since the width of the illuminating beam is much larger than its height, its divergence in the horizontal plane is smaller than its divergence in the vertical plane, and it is possible to make forward scatter measurements at smaller angles than would be possible with a stream-in-air system, in which a horizontal blocker bar must typically be used in forward scatter measurements to prevent light scattered from the stream itself from reaching the scatter detector. My inclination would be to get rid of this problem by getting rid of forward scatter measurements, but, while I will lay out my rationale over the next few paragraphs, I don't expect the manufacturers to jump on this particular bandwagon any time soon.

I have already mentioned that slit-scanning, i.e., using a small beam height, increases the effect of differences in particle diameter on pulse width. However, Hammond et al[1248] have pointed out that one can, at least up to a point, get reasonable size measurements of particles as small as 1 μm in diameter from a beam with a 20 μm height, simply by subtracting an offset corresponding to the signal component due to beam width. They applied this transformation to pulse width signals from endosomes, and displayed the resultant values on an expanded scale, allowing better visualization of differences between signals from these small particles.

Pulse width measurements have been shown to be useful for cell sizing by several groups of investigators[97,98,104,160,168-9,617-9,2561]; extinction and side scatter as well as forward scatter signals may be used. Accuracy and precision may be increased by using a dual-beam system to monitor flow velocities of individual particles and making corrections to raw pulse width values[619]. However, how pulse width is measured is critical. One can measure the width between two points at a constant threshold level on the rising and falling edges of the pulse, which is referred to as **constant-threshold pulse width**. However, this has the effect of decreasing the pulse width value for lower-amplitude pulses. Hammond et al[1248] used the **constant-fraction pulse width** measurement advocated by Leary et al[104], in which the width is measured between points on the leading and trailing edges of the pulse at signal levels equal to a constant fraction of the pulse peak height.

There is a substantial difference between constant-threshold and constant-fraction pulse width for Gaussian pulses of different heights. However, as the rise and fall times of a pulse become shorter, the difference between constant-threshold and constant-fraction measurements decreases. If one has square rather than Gaussian pulses, there should be no practical difference between the two methods of width measurement.

We ordinarily prefer not to get square pulses out of our cytometers, because we are typically interested in the information contained in the area and/or the peak height of pulses as well as in pulse width information. However, if we split off some of the signal, and put it through a logarithmic amplifier and/or a fairly high-gain linear amplifier before going to a pulse width measurement circuit, we end up with a signal that will give us acceptable pulse width measurements using a constant threshold.

For particles at least several μm in diameter, using an extinction signal for pulse sizing makes a lot of sense. I have already (p. 282) mentioned that extinction is not particularly useful for quantifying amounts of cell-associated material, meaning that we won't usually need the peak height or area of an extinction pulse. A cheap diode laser can be made quiet enough to do precise extinction measurements, and we only need a photodiode detector. The drawback is that the background noise level catches up to us pretty quickly when we try to look at submicron particles. We can't readily limit the view of the optics, because we inevitably have a limited N.A. to work with on the axis of the illuminating beam, where we have to make our extinction measurements, due to the presence of a high-N.A. lens in the fluorescence collection system, and we won't get good enough spatial resolution from a low N.A. lens to look at a really small area of the core.

My proposed solution to the problems of on-axis and near on-axis measurements is to do away with them. The orthogonal collection optics in a flow cytometer are typically high-N.A. optics, meaning they have high spatial resolution. If, instead of focusing the beam to a 5 μm height, one uses a more tractable 10 or 20 μm beam height, and places a slit over the side scatter detector, it is possible to collect a side scatter signal from a region of the beam only a few μm high. If, for example, the orthogonal collection optics have 20 ×

magnification, the image of the intersection of a 20 μm beam with the core stream is 400 μm high, and a 40 μm high slit, readily obtainable from optics supply houses, will restrict the region of side scatter detection to 2 μm. I have already noted that it is impractical to use a 2 μm beam height because of problems with rapid beam divergence; the approach of slit-scanning using a real slit eliminates those problems. And, as usual, there's nothing much new in cytometry; Leon Wheeless told me he made width measurements using slits in the 1970's.

If orthogonal scatter is needed as a trigger signal, it is simple enough to use a beamsplitter to divert the full beam height side scatter signal to one PMT and the slit-height side scatter signal for pulse width sizing to another. Log and/or high-gain amplification produce the near-square pulses we need for the quick-and-dirty width measurement. And, best of all, we have a much better signal-to-noise ratio in side scatter measurement than we do in either forward scatter or extinction measurement.

Size Measurements in the Submicron Range

Scatter measurements for sizing, without benefit of pulse width, are actually more respectable when we're dealing with small stuff like bacteria, endosomes, and viruses, than when we're dealing with eukaryotic cells. Among other things, many bacteria are either spherical or ellipsoidal, or close enough so that they behave according to Mie theory. Maltsev's group will at least concede that they can find angles at which bacteria could be properly characterized by scattering in a standard flow cytometer[2540]. Koch, Robertson, and Button[2562-3] have developed a method for estimating bacterial cell volume and mass from forward scatter signals, using Rayleigh and Rayleigh-Gans theory (applicable to smaller particles than Mie theory) as well as Mie theory.

People who work routinely with bacteria and smaller particles tend to use smaller focal spot sizes than people who work with eukaryotes, although the beam divergence problem previously mentioned limits how small one can practically make the focal spot. Decreasing spot size concentrates the energy in the input laser beam in a smaller volume, increasing signal amplitude from particles in the sample. Noise due to light scattering by particulate contaminants in the sample and sheath fluids may not change appreciably, since, although a smaller volume is illuminated, the intensity of illumination increases. Thus, a substantial increase in signal-to-noise can only be achieved if the amount of stray light collected is decreased.

When cells are measured in a stream in air, decreasing spot diameter to less than half stream diameter greatly reduces stray scatter from the stream; changing to a larger stream or capillary further reduces stray scatter, and substituting a square cuvette makes an additional improvement. The increased beam intensity results in more photons being scattered from particles, which decreases variance of measurements due to photon statistics; however, unless a Gaussian beam is at least 5 times the core stream width, the intensity profile will itself will keep the theoretical minimum CV of measurements above 5 percent[685]. When you start with a square cuvette, making the beam smaller helps, up to a point[686] but, in practice, the decreased spot size starts to catch up with you as the increasing beam divergence causes light to spill around the beam stop. Small marine bacteria[686], small beads[687], and large viruses (F. Elliott and H. Shapiro, unpublished) have been detected using forward scatter in laser source systems using flat-sided cuvettes for observation; the practical particle size limit for detection seems to be about 150 nm.

In the submicron size range, scattering from particles is predominantly Rayleigh scattering, varying in intensity, all other things being equal, as the inverse sixth power of particle diameter[94]. While such scattering remains more intense in the forward direction than at 90°, the relative influences of size, internal and surface structure, and particle asymmetry and orientation no longer vary markedly with scattering angle. It may thus be more practical to use a 90° or large angle scattering measurement than a forward scatter measurement for detection and sizing of submicron particles[687], because, when observation is done in a square cuvette or a water-immersed system[94], and field stops are appropriately used in the detection optics, there is much less background noise from large angle scatter measurements than from forward scatter measurements.

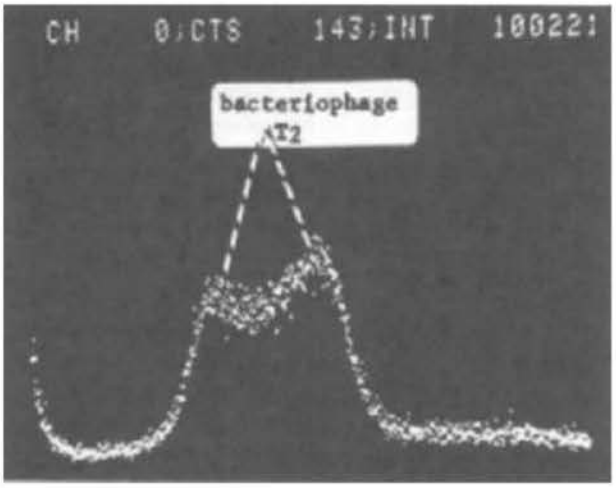


Figure 7-5. Side scatter signals from T2 bacteriophages.

Figure 7-5 shows a distribution of side scatter signals observed from T2 bacteriophages using the water-immersed flow system built at Block[94]; the bimodal distribution, which is well separated from background noise, may reflect the presence of virions with and without DNA. The sample was illuminated by a 100 mW, 488 nm argon laser beam. While the distribution shown is wide, extrapolating backward from the 6th power (Rayleigh) dependence of scattering intensity on particle diameter indicates that the CV of the corresponding diameter measurement should be no more than a few percent. The phages could still be resolved well

above background using the same optics with an air-cooled argon laser source emitting 10 mW at 488 nm; since the limiting noise source in such scatter measurements is stray light, this is not surprising. Steen and Lindmo measured large angle scatter signals from large viruses in their arc source system[688,1246], clearly establishing that, in scattering measurements, problems are generally not solved by throwing more photons at them; Steen (personal communication) has also recently measured scatter signals from viruses in prototype instruments built by **Apogee** (see Chapter 8).

Other Size Measurement Techniques

Terstappen et al[1247] modified the angle of forward scatter collection and used a nonlinear transformation of the side scatter signal to improve resolution of peripheral blood leukocytes. In principle, improving signal-to-noise could further increase the sensitivity of scatter measurements.

Zarrin, Bornhop and Dovichi described an apparatus[689] in which **laser Doppler velocimetry** was used with a square cuvette-based flow cytometer to measure particles as small as 90 nm. In laser Doppler velocimetry, the scatter signal from moving particles is modulated, while the background noise is not; the signal is detected at the modulation frequency, increasing signal-to-noise.

A less radical sizing method was suggested by Gray, Hoffman, and Hansen[167]; samples were prepared in a solution containing a fluorescent compound of high molecular weight, which did not get into the cells. The core diameter was kept constant, resulting in a decrease in the baseline fluorescence signal when a cell passed the observation point. One disadvantage of this approach is that it reduces the number of fluorescence measurements of extrinsic parameters that could be made concomitantly with the cell size measurement. Another is that, when the core size is small, redistribution of dye in the core around cells produces increases in fluorescence over baseline. This "dye exclusion artifact" has recently been further investigated by Steen and Stokke[2564], who note its possible adverse effects on fluorescence measurements under some conditions.

In concluding the discussion of cell size measurements, I should mention an interesting paper by Bator et al[170], who used high speed photography of cells passing through an electronic volume measurement orifice to correlate differences in cell shape with differences in measured volume.

Cell Shape and Doublet Discrimination

The most elegant flow cytometric apparatus for determining cell shapes was, without doubt, the multidimensional high-resolution slit-scanning system developed for cancer cytology studies by Leon Wheeless and his colleagues at the University of Rochester[4,171-4,690], beginning in the 1970's. In this instrument, profiles of cells were obtained in the direction of flow and in two orthogonal directions, using the fluorescence of acridine orange excited by a sharply focused 488 nm laser beam. Rapid digitization allowed several dozen points on each pulse profile to be measured and captured in a dedicated minicomputer system. As I mentioned on p. 212, Wheeless' slit-scanning work represented the first application of digital pulse processing in flow cytometry; while the low resolution of available converters limited the dynamic range of measurements, the large number of points measured per pulse allowed fairly detailed morphologic information to be captured.

Slightly less fancy scanning flow cytometers were built and used for analysis of chromosomes[691-4] and phytoplankton[695], and for two-dimensional imaging of cells in flow[696,1249]. The analytical procedures used in high-resolution slit-scanning and imaging flow cytometers require optical and electronic hardware and software rather different from, and more complex than, that which is used in commercial and most laboratory-built flow cytometers. Progress in electronics has gradually made it easier and more affordable to do multiple point pulse profile processing on both laboratory-built and modified commercial instruments[697,2311,2565], and to incorporate imaging capability into flow systems. Commercial instruments which offer one or both of these features include **Fluid Imaging Technologies'** FlowCAM[2453] (p. 168; also see Chapter 8) and **CytoBuoy b.v.**'s CytoBuoy[2566](see Chapter 8), both designed for aquatic applications, the **Union Biometrica** COPAS systems for large particle sorting (p. 265; also see Chapter 8), and clinical urine analyzers from **International Remote Imaging Systems and Sysmex (Toa)**[2567] (Chapter 8). **Amnis** is developing a flow cytometer with hyperspectral imaging capability[2568]; see Chapter 11 for contact information.

David Galbraith and his colleagues, at the University of Arizona[2473-4] used high-speed digitization to collect multiple point pulse profiles of cells, and found that the skewness and kurtosis (these are higher moments of statistical distributions; see p. 234) of pulses provided useful information for discriminating among cell types.

More information about asymmetric cells than is available in conventional flow cytometers can be derived from making measurements of the same parameter at two different angles; this technique is used in sperm sorting, where the fluorescence of Hoechst 33342 is measured in both forward and orthogonal directions to improve resolution of X- and Y-chromosome bearing cells[651,2322,2569]. Sperm sorting will be discussed further in Chapter 10.

Zucker, Perreault, and Elstein[1250] used a combination of forward scatter and extinction signals to identify sperm of different refractive indices and orientations in an unmodified Ortho flow cytometer; the instrument is no longer available, and current research flow cytometers do not include extinction measurement capability.

However, some information about cell shape and orientation is available even to users of conventional flow cytometers, which have low-resolution slit-scan capability by virtue of using relatively small beam heights. Relationships between extinction pulse widths, peak heights, and integrals, tend to be different for symmetric and asymmetric cells, and for single particles and doublets or multiplets. Some shape in-

formation can also be obtained from the relationship between forward and large angle (orthogonal or 90°) light scatter signals; cells of different shapes will generally cluster in different regions of a two-dimensional distribution of these parameters, although the locations of these clusters may not always be predictable *a priori*.

Wolfgang Göhde, Sr., was one of the first to consider the problem of doublet discrimination. Flow cytometer manufacturers acknowledged his contribution by licensing his patent when they began to promote the use of a combination of pulse height and pulse area as a means of eliminating most doublets from DNA content analyses.

The same amount of fluorescence (i.e., the same value of the pulse integral) will be recorded when a single G_2 or M phase cell passes through the measurement system or when two G_0 or G_1 phase cells pass through in close proximity. However, the height of the fluorescence pulse will, in general, be lower for the doublets than for the singlets; while, in principle, two G_0 or G_1 cells passing through "side by side" should generate a pulse approximately as high as that produced by a single G_2 or M cell, this orientation of doublets is rare because the hydrodynamics of flow favor them being oriented along the axis of flow.

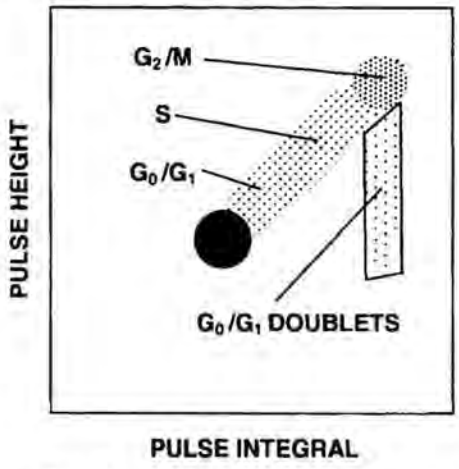


Figure 7-6. The principle of doublet discrimination using pulse height and pulse integral measurements.

Figure 7-6 illustrates the principle of doublet discrimination based on pulse height and integral measurements; the quadrilateral gate shown on the figure would remove most, but not all, G_0/G_1 doublets. Modern DNA histogram analyses procedures employ somewhat more sophisticated methods for doublet and multiplet discrimination, but the pulse height-vs.-pulse integral method is still better than nothing. It might be used more often for immunofluorescence analysis, in which unrecognized doublets may push experimenters to invalid conclusions.

If you go back to high school geometry, and recall that the areas (integrals) of plane figures such as rectangles and triangles are proportional to the product of base (width) times height, you will appreciate that dividing a pulse integral by a pulse height should give a quantity representative of pulse width, meaning that it is possible to obtain pulse width information even in instruments that do not have pulse width measurement circuitry or capability, as long as the beam is small enough so that pulse height and pulse integral do not contain identical information (see pp. 183-4).

Pulse width itself is useful for doublet discrimination[27]; in the context of DNA analysis, G_0/G_1 doublets will have larger pulse widths than single G_2 or M cells. Wersto et al[246] provide a good recent reference on the topic. The **Luminex 100** instrument (see Chapter 8), designed for doing multiplexed ligand binding assays on color coded plastic beads, uses a pulse width measurement obtained by low-resolution digital pulse processing to eliminate doublets from analyses.

Measurement of Intrinsic Parameters Using Absorption or Extinction Signals

Microspectrophotometric absorption measurements of cells on slides can be used for quantitative analysis of substances with weak absorption, e.g., pararosaniline, used in the Feulgen staining procedure, as well as for measurements of substances with high extinction coefficients, e.g. nucleic acids (measured at 260 nm) and hemoglobin (measured in the Soret band around 415 nm). When static specimens are analyzed on slides, it is possible to select mounting and immersion media with refractive indices matched to those of the specimens, thus minimizing artifacts due to light scattering. The spatial resolution and the numerical apertures of illumination and collection optics are typically higher in microspectrophotometers than in flow cytometers, which makes it possible to do better absorption measurements in the former[34,52].

There has been some application of flow cytometers to measurement of nucleic acids and hemoglobin; Kamentsky's original instrument[65,66,77] and the Cytoscreener[76] were both equipped for measurement of nucleic acid absorption at 260 nm, while the Block arc source instrument[88] measured nucleic acid absorption at 260 nm and hemoglobin absorption at 420 nm. The nucleic acid measurements did not appear to be as precise as those obtained by microspectrophotometry; the hemoglobin measurements were adequate for discrimination of erythroid cells from leukocytes and produced estimates of hemoglobin content in reasonable agreement with those obtained by conventional hemoglobinometry.

Stewart, Stewart and Habbersett[125B], using the multiparameter sorter at Los Alamos, demonstrated that dead cells, i.e., cells with membranes permeable to propidium iodide, could be differentiated from other cells in leukocyte suspensions on the basis of lower extinction signals.

Fluorescence Measurements of Intrinsic Parameters

Autofluorescence: Pyridine and Flavin Nucleotides

The **autofluorescence** of most mammalian cells appears to be due primarily to the presence of **pyridine (NAD, NADP) and flavin (FMN, FAD) nucleotides** which, respectively, impart UV-excited blue and blue-excited green

fluorescence to cells[181,183]. Fluorescence spectra of these materials are shown in Figure 7-7.

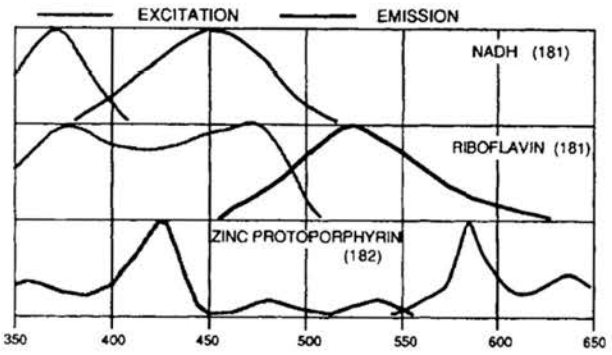


Figure 7-7. Fluorescence spectra of some materials implicated in mammalian cell autofluorescence.

Many investigators have been concerned with autofluorescence solely as a source of interference with measurement of weak fluorescence signals, e.g. fluorescein immunofluorescence. The fluorescence emission from unstained murine lymphocytes, excited at 488 nm and measured through the long pass filter combination used for single parameter measurements of fluorescein immunofluorescence, was originally reported to have an average intensity equal to that which would be measured from 10,000 molecules of antibody-bound fluorescein (reference 184; D. Parks, personal communication). The 10,000 molecule figure was obtained in the days when the FACS measured fluorescence between 520 and about 650 nm, using a long pass color glass filter, and was probably affected by filter fluorescence, Raman scatter, and other factors. Today's instruments use narrower band filters for green fluorescence emission, eliminating the Raman scatter contribution; improved filter design has essentially eliminated filter fluorescence.

Surveys conducted in 1989-90 by Abe Schwartz and his colleagues[1161] found a mean value of 657 fluorescein MESF for lymphocyte autofluorescence; Hoffman and Kuhlmann[2482] reported somewhat lower values, but, even at the level of a few hundred MESF, it is autofluorescence that limits the sensitivity of immunofluorescence measurements using fluorescein-labeled antibodies. Autofluorescence of lymphocytes in the region normally used for phycoerythrin measurement is only 50 MESF.

On the plus side, the high autofluorescence of blood neutrophils[161] and the higher autofluorescence of eosinophils[162] have, in conjunction with forward and side scatter measurements, been used for identification and sorting of these cells. The spectrum of eosinophil autofluorescence is nearly identical to that of riboflavin; Mayeno, Hamann, and Gleich[1259] have shown by chemical analysis of extracts that granule-associated flavin adenine dinucleotide (FAD) accounts for about 85% of eosinophil autofluorescence. In my experience, eosinophil autofluorescence is equivalent to a few thousand fluorescein MESF. However, I have also noted yellow autofluorescence (in the 575 nm spectral region) from eosinophils when using green (532 nm) excitation; I would not expect this to come from flavins (see Figure 7-7). Havenith et al[1260] have sorted alveolar macrophages from dendritic cells based on the high autofluorescence of the former; Njoroge et al[2570] have isolated autofluorescent macrophages from blood cell cultures.

Pyridine and Flavin Nucleotides and Redox State

Pyridine and flavin nucleotide fluorescence vary with the **oxidation-reduction** or **redox state** of cells, and NADH (and NADPH) fluorescence measurements have been used to monitor redox states of cells, tissues, and organs since the technique was described by Britton Chance and Bo Thorell in the late 1950's[185-90]. In 1979, Thorell described flow cytometric measurements of the redox state of liver cells based on NADH fluorescence[191]; by the time of his death in 1982, he had added the capacity to measure endogenous fluorochromes and flavin nucleotides to his apparatus as well[192,193]. Hafeman et al[194] used flow cytometry of NADH fluorescence in blood neutrophils to demonstrate that the respiratory burst induced in these cells by chemotactic stimuli and phorbol esters is an all-or-none event; Van De Winkel and Pipeleers[1261] sorted insulin-containing pancreatic cells based on changes in redox state following exposure to glucose.

Pyridine and Flavin Nucleotides and Cancer

Several groups[1262-5,2571-2] have described characteristic changes of the ratio of pyridine to flavin nucleotide fluorescence in bulk in tissue specimens from tumors and precancerous states and in tumors *in vivo*; this work has not provided a new diagnostic application for flow cytometry but has, instead, led to the development of devices for detection of tissue ischemia[2573] and for endoscopic cancer diagnosis[2574]. **Xillix**, a company in Richmond, British Columbia, Canada <http://www.xillix.com> sells instruments for autofluorescence bronchoscopy and other endoscopic applications.

Bacterial Autofluorescence Measurements

Jim Ho, of the Canadian Defence Research Establishment, has developed instruments that measure UV-excited bacterial autofluorescence and particle size in aerosols; these parameters may help distinguish among species. Like Gucker's original aerosol particle counter (p. 74), Ho's FLAPS (Fluorescence Aerodynamic Particle Sizer)[2575,6] is designed to detect biowarfare agents. A second-generation instrument (J Ho, personal communication; N. Dovichi, personal communication) resulted from collaboration between Jim and Norm Dovichi, then at the University of Alberta and now at the University of Washington. Norm passed through Los Alamos and played with chemical and nonchemical applications of flow cytometry[685,687,689,876] before he put his experience to use in developing the capillary electrophoresis-based gene sequencer[2576-7] and hit the big time. The improved bacterial aerosol analyzer measures fluorescence emission in 16 spectral regions and sizes bacteria by laser Doppler velocimetry[685]; particles are detected and sized

in a red laser beam, and fluorescence is excited by a pulsed tripled YAG laser downstream. Mixed populations are resolved with the aid of principal component analysis (p. 252).

Porphyrin Fluorescence in Erythroid Cells

In the early development of erythroid cells in the bone marrow, **porphyrins** may accumulate in cells in amounts that outstrip the cells' capacity to synthesize **heme** from porphyrin and iron. Heme is nonfluorescent due to the quenching of the intrinsic fluorescence of porphyrin by iron, but both the porphyrin precursors of heme and the **zinc protoporphyrin** formed when iron incorporation is impaired, as occurs in **iron deficiency** and **lead intoxication**, fluoresce[182]. The Stokes shifts for porphyrin fluorescence are large; excitation maxima are in the violet (Soret band) and emission maxima in the orange or red (see Figure 7-7). The fluorescence of red cells in bulk has been used for diagnostic purposes and that of red cell precursors in marrow is detectable in a flow cytometer using excitation from the violet (406-422 nm) lines from a krypton laser (C. Stewart, personal communication). Zinc protoporphyrin has been measured in single cells using image cytometry[1266,7]; I have been able to measure its fluorescence in a flow cytometer using 100 mW excitation at 441 nm from a He-Cd laser (Figure 7-8), but only by taking great pains to reduce stray light and fluorescence from optical components. Using flow or image cytometry to follow the disappearance of fluorescent red cells from the circulation may be helpful in monitoring treatment of lead poisoning, which is a common clinical condition. Violet laser diodes could provide useful, and, ultimately, inexpensive light sources for clinical instruments intended for such measurements.

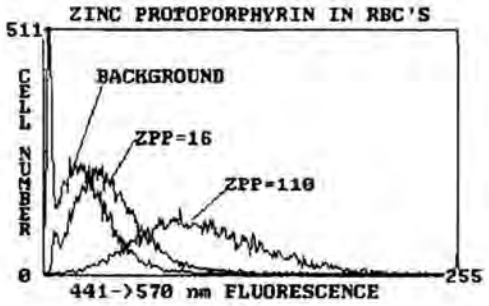


Figure 7-8. Zinc protoporphyrin fluorescence in human red cells; orange fluorescence (>570 nm) was excited with a 100 mW He-Cd laser at 441 nm.

Red cell porphyrin fluorescence is also encountered in **erythropoietic protoporphyria**, a relatively rare hereditary disorder, in which the bones and teeth are colored red by excess porphyrin deposition, and in which the effects of porphyrins on the nervous system lead to bizarre behavior. King George III of England is believed to have been a victim; other sufferers were persecuted as werewolves. Brun, Steen, and Sandberg[1268] have made flow cytometric measurements of porphyrin in patients with this disease, presumably not when the moon was full.

A potential clinical application of porphyrin metabolism in lymphocytes, rather than erythrocytes, is suggested by the fact that activated T cells accumulate substantial amounts of intracellular protoporphyrin IX in the presence of exogenous delta-aminolevulinic acid (ALA)[257,819]. This may allow pathological proliferation of T cells to be at least partially arrested by photodynamic therapy.

Other Pigments

Autofluorescent pigments such as the UV-excited, blue fluorescent **lipofuscins** accumulate within mammalian cells as a function of age. Jongkind et al[195,196] used autofluorescence to sort cells of presumptively different ages for subsequent biochemical analysis. Hunt et al[1269,70] examined the accumulation of **ceroid**, a fluorescent pigment produced by oxidation of lipid/protein complexes, and found in the lipid-laden macrophages, or foam cells, which infiltrate atherosclerotic lesions. They found that a 424 nm bandpass filter was more selective than a 490 nm long pass filter for detection of the UV-excited fluorescence of ceroid in macrophages. Puppels et al[1271] measured **carotenoids** in single cells, but by Raman microspectroscopy rather than fluorescence flow cytometry.

The Jovins, in Göttingen, made flow cytometric measurements of the **fluorescence of aromatic amino acids** in proteins in differentiating cells, using a frequency-doubled argon laser operating in the UV at 257 nm for excitation[199].

Chlorophyll and Phycobiliproteins

Plant photosynthetic pigments, including **chlorophyll**, which contains a magnesium-porphyrin complex, and the **phycobiliproteins** present in algae, have a characteristic autofluorescence that has been studied *in vivo* by Trask et al[197] and Olson et al[198], among others. Chlorophyll itself has absorption regions in the ultraviolet and violet (below about 450 nm) and the far red (about 680 nm), and emits in the near infrared. Since most of the light penetrating past the surface layers of the ocean is in the blue and green regions of the spectrum, most algae contain relatively large amounts of **phycoerythrin**, **phycocyanin**, and **allophycocyanin**, which absorb blue-green, yellow-orange, and red light, respectively, and which, in concert, allow nonradiative transfer of incident light energy to chlorophyll. The phycobiliproteins have, to say the least, been exploited as fluorescent labeling reagents[114] and will be discussed further in this context.

Since different algal species contain different amounts of the various pigments, and since the spectra of the same types of phycobiliproteins (e.g., phycoerythrin) from different species may also differ, it is possible to use multistation flow cytometric measurements of fluorescence excited at different wavelengths to classify and count phytoplankton populations[711]. This has been pursued as an approach to environmental monitoring.

Flow cytometry and flow cytometric measurements of intrinsic pigment fluorescence in phytoplankton and marine bacteria have become widely used in oceanography[1051-2]; among other things, this led to the discovery of extremely abundant, but previously overlooked, chlorophyll-bearing marine bacteria[1272].

Xu, Auger, and Govindjee[1273] used a flow cytometer to measure chlorophyll fluorescence in isolated spinach thylakoids. The cytometer does measure the variable (light-dependent) component of fluorescence, although the high excitation intensity may perturb measurements under some circumstances.

Infrared Spectra and Cancer Diagnosis

Benedetti et al[1277-82] and Wong and Rigas and their collaborators[1283-8], using **Fourier transform infrared (FT-IR) spectroscopy**, described differences between normal cells and cells from leukemias and several solid tumor types. Differences were most consistently found in the nucleic acid phosphate stretch bands at 1080 cm^{-1} and in a protein band at 1540 cm^{-1}. Most of these studies involved bulk measurements, although leukemic cells have been examined by FT-IR microscopy[1281-2].

This work, like the work on pyridine and flavin nucleotide fluorescence mentioned previously, raises an important question. Since, in many cases, e.g., analyses of cervical specimens, actual malignant cells represent a very small fraction of the cells present in an abnormal specimen, the measured differences between specimens are more likely to reflect some alteration or premalignant state in a large fraction of the cells in a specimen than to represent signals from the malignant cells themselves. It is not clear that flow cytometry can contribute to the resolution of this issue.

7.3 PROBES, LABELS, AND [NOT] PROTOCOLS FOR EXTRINSIC PARAMETER MEASUREMENTS

As I said way back in Chapter 1, most of the measurements of extrinsic parameters done in most flow cytometers use fluorescent reagents. The discussion that follows will deal primarily with fluorescent staining and fluorescence measurements, covering other staining techniques when they are applicable in conventional flow cytometers or should be considered as part of an alternative approach to flow cytometry.

I have to introduce some ground rules here, for a number of reasons. There are a lot of probes now; some of them are dyes, and some of them are natural products, and big ones at that, e.g., the fluorescent proteins and the phycobiliproteins. I know a lot about some probes and not much about others, so I will only cover probes with which I have been fairly intimately involved in much detail.

If you need more details, there are two excellent sources. For the classicists, there is the new 10th Edition of *Conn's Biological Stains*, edited by Richard Horobin and John Kiernan[2580]. *Conn's* went 25 years (1977-2002) between the 9th and 10th Editions, so I don't feel too bad about the 8-year (1995-2003) gestation period for this 4th Edition of *Practical Flow Cytometry*.

But I digress. If you want the last word on fluorescent probes, their structure, their spectra, their uses, thousands of references, and (on the web), price and delivery information, you want to look at the 9th Edition of Molecular Probes' *Handbook of Fluorescent Probes and Research Products*[2332], edited by Dick Haugland. There's not much point in duplicating what's in there, especially since you can get the book for nothing (at least if you hurry), or pull up a regularly updated version online at <http://www.probes.com>.

As to protocols, *Practical Flow Cytometry* has always been more of a "why-to" book than a "how-to" book in terms of its discussions of which probes and parameters may be most useful for which applications. I cover how the probes work, just as I cover how the instruments work, but, in the majority of cases, I can't and don't provide the protocols, i.e., detailed information on the exact concentrations of reagents, compositions of buffers, incubation times and temperatures, etc., that you need to make the probes work in your lab with your instrument and your samples.

Although you can't just run out to The Heme Depot and get such information, there are sources. I mentioned several on pp. 62-5. I would turn first to *Current Protocols in Cytometry*[2389], which is available in looseleaf and/or CD-ROM versions, both frequently updated. When a significant methodological advance in flow or image cytometry is reported in the literature, it's a good bet that the editors of *Current Protocols* will hound one or more of the authors into producing a writeup of the procedure including all of the technical details that were omitted from the "Materials and Methods" section of the journal article. The various volumes of *Methods in Cell Biology* devoted to cytometry[1034,2385-8] may also be helpful.

Most people who publish good new methodology are anxious to proselytize; you can usually get experimental details from them via snail mail or e-mail, or from their lab or personal web sites. The Purdue Cytometry Mailing list is also a good place to go for help; you'll get more and better answers from the experts if your inquiries about procedures indicate that you've done your homework.

At this point, having told you what I don't do, I'll get back to what I do do before I get into deep...never mind.

Probes, Labels, and Dyes

I introduced a distinction between probes and labels on pp. 42-3, and I will now say a bit more about that subject. We use reagents to measure extrinsic cellular parameters because there aren't ways, or because we haven't found the ways, to estimate or measure all of the attributes of cells in which we might be interested.

There is a hierarchy of specificity, or of selectivity, of reagents, and we can appreciate it by considering the history of staining, some of which is covered in *Conn's*[2580], and some of which is in older books[24,32-3,1085]. If we look at stains classically used for blood cells, which date back to Paul Ehrlich's work

in the 1880's[33], we find they are mixtures of an acid dye (typically eosin), which binds to basic elements within cells, meaning mostly proteins, and a basic dye(s) (typically one or more of the azure dyes, all thiazines), which bind(s) to acidic elements, notably nucleic acids, but also sulfonated glycosaminoglycans. We don't expect eosin to bind to acidic elements or azure dyes to bind to basic elements, but that's as specific as those dyes get. However, we can legitimately call those dyes **probes**, even if they are probes of some relatively nonspecific characteristics or constituents of cells.

At the other end of the hierarchy, we have antibodies and gene probes, large, or relatively large, molecules themselves, which, respectively, are exquisitely specific for macromolecular structure and sequence, at least when used under appropriate conditions. They, too, are probes, but, in order to detect them using an optical flow cytometer, we have to attach a **label**. Until the 1980's, almost all the labels we had were relatively low molecular weight dyes; since then, it has become increasingly likely that the label used for an antibody will be a macromolecule, specifically, a phycobiliprotein, which may also have small dye molecules covalently attached to it to modify its spectral characteristics.

Some of the dye probes we use are sensitive to changes in their chemical environment, and would be useless if they weren't. Measurements of intracellular pH are usually done using dyes that change their spectral characteristics as pH changes. That's an essential characteristic for a probe, but an undesirable one for a label, which we would like to be able to attach to a specific probe molecule without altering either the spectral characteristics of the label or the specificity of the probe, and which we would like to behave (i.e., fluoresce) pretty much the same way regardless of the environment in which it finds itself. Well, that's not the way the world works; just to cite one example, fluorescein, one of the all-time favorite fluorescent labels, is environmentally sensitive; its fluorescence increases with pH, enough so that derivatives of fluorescein are routinely used as pH probes.

I will start getting down to the specifics by discussing dyes and staining mechanisms in general, and the preparative techniques, such as **fixation** and **permeabilization**, which may be needed to get dyes into cells, and then cover the reagents used to measure the parameters in Table 7-1, starting with nucleic acid dyes and with labels.

Dyes and Quality Control: Gorillas in the NIST

In previous editions of this book, I said that if there were a **Shapiro's Third Law of Flow Cytometry**, it would probably be this:

Shapiro's Third Law of Flow Cytometry:
What's in the Bottle
Isn't Necessarily
What's on the Label!

This was particularly apt to be true for older bottles containing less common dyes; the Biological Stain Commission, which was set up to provide some degree of quality control over stains used routinely in research and clinical laboratories, has never gotten very far into the business of certifying fluorescent dyes, and even certified lots of dye may contain impurities. The problem of dye purity is hardly a new one in histochemistry and cytochemistry; Scott's piece on "Lies, damned lies – and biological stains"[721] and related correspondence[722] and Horobin's review[723] provide some historical background.

Spectroscopy does not provide much assistance when you're trying to find out whether your reagents are pure. You can only compare spectra of your lot with published spectra when you're working with relatively well-known stains; when what you've got definitely isn't the stain you wanted, the spectrum is likely to tell you, but, when what you've got is 45% what you wanted and 55% other junk, or when you're working up new compounds, spectra won't necessarily help.

A widely applicable, and perhaps the most useful, method for determining dye purity is **thin layer chromatography**[724], which can quickly tell you when you've got a mixture of compounds in the bottle. Most of the companies that specialize in dyes for analytical cytology will give you some idea of the purity of their products if you ask. If you're looking for something that isn't in their catalogs, try to find it in laser grade; laser grade dyes are apt to be reasonably clean. I know a lot of people who are happy that they didn't publish results that were obtainable only from a single bottle of dye, and a few who are unhappy that they did. I include myself in the former category.

When measuring fluorescence spectra of dyes, it is a good idea to make sure that the photodetector in your instrument will respond over the spectral range of emissions you intend to measure. Ideally, the fluorescence spectrum should be corrected for variations with wavelength in source emission intensity and detector response. Most spectrofluorometers use photomultiplier tubes with minimal response above 600 nm and negligible response above 650 nm; no amount of electronic "correction" can produce an accurate spectrum at longer wavelengths from such detectors. The Hamamatsu R928 and R1477 will respond to wavelengths as long as 800 nm; beyond that, you need an R3896 or a gallium arsenide tube s uch as an R636. It doesn't matter if the source and excitation monochromator in the instrument will provide excitation and select emission out to 900 nm if the tube won't respond past 650. When in doubt, look at the PMT.

In recent years, the manufacturers and distributors of dyes used in flow cytometry seem to have taken it upon themselves to supply high-quality products. You still need to be careful if you play the kinds of games I play, i.e., buying laser dyes, drugs, and other interesting chemical structures and trying to find out whether they are of any use in flow cytometry.

Since the last edition of this book emerged, several organizations, including the Centers for Disease Control, Food

and Drug Administration, Health Canada, National Institutes of Health, and NCCLS have pursued the standardization of fluorescent reagents. The 800-pound gorilla of standardization, at least in the U.S., is the National Institute of Standards and Technology (NIST) (formerly the National Bureau of Standards), which has been recruited into producing some standardized fluorescent reference materials, starting with a certified fluorescein solution and expected to progress to fluorescein-labeled beads and to solutions and beads containing other fluorescent materials. Several publications have already emerged from NIST's collaborative efforts[2581-4].

The Dyes are Cast: An Overview

The spectral characteristics of a representative sample of fluorescent dyes, probes, and labels, and the excitation wavelengths available from various light sources, are shown in Figure 7-9, on the next page. Although there are thousands of compounds in Molecular Probes' catalog (the indispensable *Handbook*[2332]), and there are at least a few labels that are available conjugated to hundreds of different monoclonal antibodies, I'd guess that at least three-quarters of the samples run through flow cytometers contain at least one of the dyes/probes/labels shown in the figure.

A few selected parameters and applicable fluorescent probes are found in Table 7-2, on the page opposite the spectral chart. I've narrowed down the range of light sources in the chart to include four excitation wavelength ranges likely to be found in fluorescence flow cytometers, i.e., blue-green (488 nm), red (633-640 nm), UV (325-365 nm), and violet (395-415 nm). Probe emission maxima are indicated next to probe names.

Consideration of Figure 7-9 and Table 7-2 makes apparent the rationale for the use of multiple, spatially separated fluorescence excitation beams in multiparameter flow cytometry. Even when one can choose from a number of probes to select those with desired spectral characteristics, the use of several separated beams generally facilitates resolution of fluorescence signals from multiple probes. When a choice of probes is not available, multistation flow cytometry may provide the only means of making correlated measurements of two or more parameters of interest.

I've been beating this drum for over twenty years now; as I write this, I am looking at an article[8] called "Multistation multiparameter flow cytometry: A critical review and rationale," which I published in *Cytometry* (3:227-43) in January 1983. That article, which was adapted from a grant application (not funded the first time around), turned out to be the foundation for *Practical Flow Cytometry* and for this chapter. It included spectra of six nucleic acid dyes, five labels (no phycobiliproteins), six cyanine dyes (used as membrane potential probes; the reactive Cy2, Cy3, Cy5, etc. not having been developed at the time), and chlorotetracycline, a marginally useful probe of membrane-bound calcium. There were no usable diode lasers then, and He-Ne lasers only came in red, but, more to the point, there were no more than a few dozen multibeam flow cytometers in operation, and I'd guess that most of them used argon and krypton or dye lasers to excite fluorescein- and Texas red-labeled monoclonal antibodies. Today, it's hard not to do multiparameter flow cytometry, and getting harder not to do multistation multiparameter flow cytometry; we've got better hardware, better software, and, to get back to the topic immediately at hand, more and better reagents.

The first nineteen spectra shown in Figure 7-9 are those of labels, almost all widely used and readily available conjugated to antibodies and/or nucleic acid probes. The next twelve spectra are of nucleic acid dyes, including all five dyes (ethidium, Hoechst 33342, DAPI, mithramycin, and acridine orange) shown in my 1983 version of the figure. Then come four spectra of fluorescent reporter proteins, none of which had been described (although the original GFP had) when the last edition of this book was written. And, wrapping up, there are spectra of indo-1, a reliable and widely used calcium probe, in the presence and absence of calcium ions. To get 37 spectra onto one page, I had to change my spectrum display format slightly, but it is still essentially a streamlined version of the "box-and whiskers" plot shown in Figure 5-6 (p. 236).

The list of light sources in Figure 7-9 now includes Nd:YAG and semiconductor (diode) lasers as well as argon and krypton ion lasers, He-Cd and He-Ne lasers, and the HG arc lamp. I have drawn long vertical lines corresponding to the popular 488 and 633-635 nm excitation wavelengths through the spectra to facilitate orientation. If you look carefully, you'll notice that phycoerythrin and its tandem conjugates are excited much more efficiently by green light (doubled Nd:YAG lasers at 532 nm, green He-Ne lasers at 543 nm, or the Hg arc line at 546 nm) than by 488 nm light from an argon or semiconductor laser. However, since the use of a green source in place of a 488 nm source precludes excitation of fluorescein and its derivatives, and the use of a green source with a 488 nm source potentially puts stray green light into the fluorescein detector, green sources have not been widely used to date. That may change.

Table 7-2 differs from its predecessors in the article[8] and in previous editions of this book in two respects. They covered many more excitation wavelengths, and they listed dyes that had been used once or twice and weren't widely available. This time around, it made more sense to me to concentrate on materials that were widely used and widely available; there are, for example, UV-excited pH probes, but I didn't list them because they are relatively hard to find and not extensively described. Note that only one of the labels in Figure 7-9 did not make it into Table 7-2; the label is Texas red, which is not particularly well excited by 488 nm or red light, although I have heard claims that it can be excited in the UV and/or violet.

You won't find quantum efficiencies or relative fluorescence intensities of the dyes and labels in either Figure 7-9 or Table 7-2; those details will be covered in subsequent discussions of the individual materials. For now, we'll move on to a consideration of staining mechanisms.

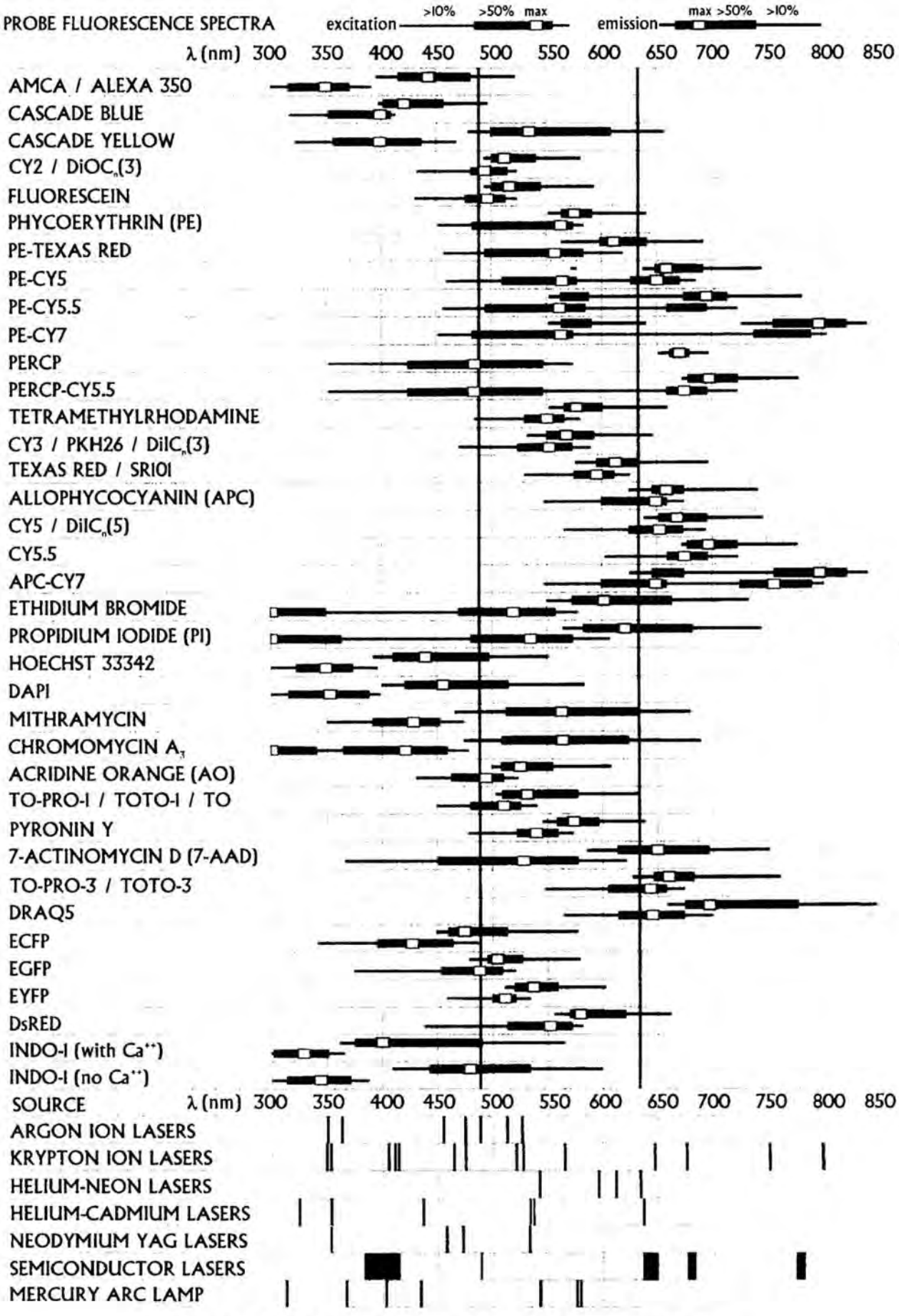


Figure 7-9. Probe fluorescence spectra and source emission wavelengths.

EXCITATION:	UV (325-355 nm)	VIOLET (395-415 nm)	BLUE-GREEN (488 nm)	RED (633-640 nm)
FLUORESCENT LABELS	AMCA, Alexa 350 (440)	Cascade Blue (420) Cascade Yellow (520)	Fluorescein, Cy2 (520) Cy3 (565) PE (575) PE-Texas Red (610) PE-Cy5 (660) PerCP (670) PerCP-Cy5.5, PE-Cy5.5 (700) PE-Cy7 (780)	APC, Cy5 (660) APC-Cy5.5, Cy5.5 (700) APC-Cy7 (780)
DNA-SELECTIVE DYES	Hoechst dyes (440) DAPI (455)	Hoechst Dyes (440), DAPI (455) Chromomycin, Mithramycin (560) ?7-AAD (660)	AO (520) 7-AAD (660) DRAQ5 (700)	DRAQ5 (700)
NONSELECTIVE DNA/NUCLEIC ACID DYES			TO-PRO-1, etc. (530) Pyronin Y (575) Ethidium (600) Propidium (615) AO (650)	TO-PRO-3, etc. (660)
REPORTER PROTEINS		ECFP (470)	EGFP (510) EYFP (535) dsRED (575)	
ENZYME SUBSTRATE-FLUOROPHORES	7-amino-4-chloro-methylcoumarin (470) ELF 97 (530)	3-cyano-7-hydroxycoumarin (450)	Fluorescein, rhodamine 110 (520) resorufin (585)	
MEMBRANE POTENTIAL PROBES			$DiBAC_4(3)$, $DiOC_5(3)$, JC-1, Rhodamine 123 (520) JC-1 (585) $DiOC_5(3)$ (610)	$DiIC_5(5)$ (660)
pH PROBES			BCECF (520) Carboxy SNARF-1 (580) BCECF (620) Carboxy SNARF-1 (640)	
Ca^{++} PROBES	indo-1 (405) Indo-1 (480)		fluo-3 (520) Fura Red (660)	

Table 7-2. Fluorescence spectral properties of a selection of reagents usable for common cytometric tasks. Emission maxima are indicated next to names of probes; probes for which two maxima are listed may be usable for ratiometric measurements.

Mechanisms of Staining by Fluorescent Dyes

The selective staining of different cellular constituents by fluorescent dyes is largely accounted for by two mechanisms.

The first of these is involved in staining by fluorescent and nonfluorescent dyes, and involves the development of contrast due to **differences in concentration** of dye from one region of the cell to another, which result from differences in the affinities of various cellular constituents for the dye. Thus, basic dyes are bound in relatively high concentrations to acidic materials such as nucleic acids and glycosaminoglycans, while dyes with high lipid solubility stain membranes and fat droplets, and so on.

The second mechanism of **fluorochroming** involves an increase in the quantum efficiency of a fluorescent dye when it is bound to a particular substance or in a particular environment (e.g., nonpolar vs. polar). The binding of the Hoechst dyes and DAPI to the outer groove of the DNA molecule results in approximately a hundredfold increase in fluorescence, as does the intercalative binding of ethidium and propidium; cyanine dyes such as thiazole orange (TO in Figure 7-9) and TO-PRO-1 increase fluorescence several thousandfold on intercalative binding to nucleic acid. However, acridine orange (AO), which also intercalates into DNA, exhibits slightly lower quantum efficiency when bound than when free in solution, i.e., the fluorescence is slightly quenched; thus, the bright nuclear staining produced by this dye must result almost exclusively from increased concentration of the dye in the nucleus. Fluorescent nuclear staining with AO or with dyes such as neutral red or safranin, which also decrease quantum efficiency on binding to DNA, improves on microscopic observation as the cell is left illuminated for a few seconds; the free dye, which initially produces high background fluorescence, is bleached more rapidly than the DNA-bound dye. It is hard to observe fluorescence from thiazole orange-stained nuclei under the microscope; there is little or no background fluorescence, and the dye in nuclei bleaches rapidly.

Binding of acid dyes to proteins usually is not associated with an increase in quantum efficiency, and background fluorescence from free dye tends to be relatively high as a result. For this reason, many investigators prefer to use **reactive derivatives of dyes**, e.g., fluorescein isothiocyanate (FITC), for protein staining. After incubation with FITC leaves some fluorescein covalently bound to protein, the unreacted dye is removed by washing, resulting in very low background fluorescence.

Even "specific" stains such as the Hoechst dyes and ethidium may bind nonspecifically to some materials in cells, particularly when the dye and/or the interfering material are present at high concentrations. **Nonspecific staining** may also occur when environmental factors such as salt concentration or pH are outside the range in which specific staining has been reported.

Environmental Sensitivity

Environmentally sensitive dyes are not dyes that recycle their garbage, but, rather, dyes that exhibit changes in quantum efficiency and/or spectral shifts upon binding to macromolecules or ions, changing ionization state, or moving from polar environments, i.e., ionic solutions such as the cytosol, to nonpolar environments, such as membrane lipid bilayers.

Environmental sensitivity is desirable, if not absolutely essential, for DNA stains, for example. You want the dye to fluoresce when bound to DNA and not otherwise. Environmental sensitivity is, in general, undesirable in dyes that you want to use to label antibodies or other ligands. Fluorescein, as I mentioned previously, is sensitive to the pH of its environment; as the pH drops, so does the quantum efficiency. As a result, if you have the same amount of fluorescein antibody bound to a tube of cells at pH 6.5 and to another tube of cells at pH 7, it will appear that there is more antibody bound to the cells at higher pH. Propidium fluorescence varies with salt concentration[227]; if you use a water sheath with a saline sample, you may find that your peak locations are unstable and/or your CVs are high.

Metachromasia

The term **metachromasia** is used to describe pronounced changes in color and/or fluorescence emission (and absorption) wavelength that occur when dyes such as toluidine blue or acridine orange bind to RNA or glycosaminoglycans. While the precise mechanisms of metachromasia have been debated since Paul Ehrlich coined the term[205,206], it is accepted that the effect results from interactions between dye molecules themselves, typically involving the formation of dimers, oligomers, or polymers, in which π orbitals of individual molecules interact one another with a resultant shift in the positions of electronic energy levels, rather than from effects of the environment or other molecular species on the electronic structure of the dye molecules.

The altered spectrum of the **metachromatic** molecular complex is contrasted with the normal **orthochromatic** spectrum of the dye in conditions under which complex formation does not occur. When acridine orange is used for differential staining of DNA and RNA (introduced on pp. 96-7 and discussed further on pp. 312 and 320-2), individual molecules of dye intercalated into the double helix of native DNA are normally far enough from one another to prevent complex formation, and therefore retain their orthochromatic green fluorescence. Dye molecules bound to denatured DNA or single-stranded RNA are free to form metachromatic aggregates.

A metachromatic shift of absorption, excitation or emission maxima to longer wavelengths is described as a **bathochromic shift**, or **red shift**; a shift to shorter wavelengths is described as a **hypsochromic shift**, or **blue shift**. If the absorptivity (i.e., the molar extinction coefficient) of the material increases, it is said to undergo a **hyperchromic shift**; a

decrease in absorptivity is described as a **hypochromic shift**. In fluorescence metachromasia, it is relatively common for the excitation spectrum to shift to shorter wavelengths (hypsochromic shift) while the emission spectrum shifts to longer wavelengths (bathochromic shift). This is what happens in the case of acridine orange; the excitation maximum of the metachromatic red (>650 nm) fluorescence is near 460 nm, while the excitation maximum of the orthochromatic green (520 nm) fluorescence is near 490 nm .

In general, more careful control of dye (and cell) concentrations and staining conditions is needed to get reliable and reproducible metachromatic staining than might be necessary otherwise. Staining of DNA and RNA with acridine orange, for example, can be tricky; stabler staining patterns may be obtained by continuous addition of stain to the running sample[734].

Many dyes change their fluorescence spectra to some extent with changes in the polarity of the solvent; small changes are usually not described as metachromatic, although the underlying mechanism may be the same.

Spectral Changes and Ratiometric Measurements

In order to make ratiometric measurements of cytoplasmic [Ca^{++}] (introduced on p. 47) or pH, we need there to be substantial spectral shifts in the probes used. As can be seen from Figure 7-9, the excitation and emission spectra of indo-1 change substantially when Ca^{++} ions are bound to the probe, allowing the ratio of UV-excited 405 nm and 480 nm emission intensities to be used as an indicator of cytoplasmic [Ca^{++}]. Similarly, ratiometric pH measurement typically depends on differences in excitation and/or emission spectra of different protonation states of the same dye.

Ratiometric measurement of membrane potentials, which will be discussed further on, is more complex; a method described from my lab by Novo et al[2357] takes advantage of what is likely to be metachromasia resulting from formation of dye aggregates at high concentrations, but some other techniques may depend more on environmental sensitivity of probes.

Internal Energy Transfer in Probes and Labels

The phycobiliproteins, which nature has designed for efficient intramolecular energy transfer, and their tandem conjugates, representing early attempts to improve on nature in this regard, remind us that energy transfer may be intimately involved in determining the spectral characteristics of fluorescent reagents. Both phycobiliproteins and tandem conjugates are used almost exclusively as labels; we would prefer that their fluorescence not exhibit pronounced environmental sensitivity, and, in general, it does not.

Newer synthetic probes may use changes in intramolecular energy transfer characteristics to advantage; I have already mentioned probes for protease activity in which fluorescence of a fluorophore quenched by energy transfer in the intact probe molecule is markedly increased when the distance between fluorophore and quencher is changed by enzyme action on the probe[2556-7]. Some other examples will be discussed in subsequent sections.

"Vital" Staining

The availability of flow sorters stimulated interest in the development and application of stains that could permit viable cells with selected characteristics to be isolated for biochemical analysis or for further short- or long-term observation in culture. The stains used for such studies should, ideally, neither perturb the parameters measured nor compromise the viability of the cells being observed. Many of the probes now in use fall short of this ideal; this does not necessarily preclude their use but does require additional caution on the part of experimenters. In essence, we are now forced to reexamine the phenomenon of **vital staining**.

Staining and "Viability"

Dyes that can enter and stain living cells have long been described as **vital stains** even though most such dyes known to classical cytology are also known to be toxic to cells at the concentrations used for so-called vital staining. The semantic problems get worse as we go along; there is considerable disagreement about the definition of "viability" as it applies at the cellular level. People concerned with growing cells in culture generally take **clonogenicity** or **reproductive viability** as a criterion; this has two notable disadvantages. First, the definition of viability in terms of reproductive capacity excludes fully functional differentiated cells such as nerve and muscle cells, blood granulocytes, etc., and preservation of some specific cell function therefore seems to be a more suitable criterion of viability for such cells. Second, while reproduction of cells in culture provides unequivocal evidence of viability, failure to reproduce may be due to deficiencies in the medium and/or the experimenter rather than to cell damage.

If reproductive capacity is too stringent a criterion of viability, it is clear that some other criteria are not stringent enough, e.g. the capacity of the cell to exclude dyes such as trypan blue, eosin, and ethidium bromide. Cells that have been so damaged as to be incapable of performing their typical differentiated functions, e.g., chemotaxis and phagocytosis in the case of granulocytes, may still be classified as "viable" by a **dye exclusion test**.

"Intact" versus "Live" Cells

I find it convenient to use the term **intact cells** to describe cells that have not been treated with fixatives or lysing agents, and that do not show obvious morphologic damage or functional impairment. This avoids the issue of reproductive viability, but does preserve most of the distinction between cells in which studies of functional parameters are and are not appropriate. Among the extrinsic parameters listed in Table 7-1, membrane-bound and cytoplasmic [Ca^{++}], membrane integrity and permeability, endocytosis, membrane fluidity, structuredness of cytoplasmic matrix, membrane potential and pH are meaningful only as characteristics of

intact cells. The validity of studies of responses of these parameters to biologic stimuli is best established by the inclusion of controls that demonstrate known responses to standard stimuli, e.g., changes in calcium distribution in cells treated with calcium ionophores.

Getting Dyes Into – and Out of – Intact Cells

In order to stain constituents not located on the surfaces of intact cells, a dye must be capable of crossing the cell membrane, either by **diffusion** or by some form of **active transport** or **carrier-mediated transport** (endocytosis can be considered as falling in the latter category). Most dyes that have been described as vital stains are small molecules that are relatively lipid soluble and are either positively charged or electrically neutral at physiologic pH. High lipid solubility favors partitioning of dyes from aqueous media into the lipid bilayer phase of the cell membrane and into membranous or lipid-containing intracellular structures. Positively charged dye molecules are attracted to negatively charged cell constituents such as glycosaminoglycans and nucleic acids; in addition, in living cells, positively charged molecules are concentrated from the medium into the cytosol and from the cytosol into mitochondria because there are interior-negative electrical potential gradients across both the cytoplasmic and the mitochondrial membranes.

Active and carrier-mediated transport both giveth and taketh away; there are a number of efflux mechanisms that may be active in cells. Perhaps the most notable is the glycoprotein efflux pump responsible for multiple drug resistance, which efficiently clears a wide variety of molecules from cells. Microorganisms exhibit an even broader range of transport mechanisms than do mammalian cells, making it risky to assume that dyes will interact in the same ways with prokaryotes and eukaryotes.

The cytoplasmic membranes of bacterial, fungal, and plant cells are surrounded by **cell walls**, which may offer barriers to dye entry not encountered in animal cells, which lack cell walls. Of particular note is the **outer membrane** found in Gram-negative bacteria, which, in its native state, prevents most lipophilic materials from entering the organisms[20,78,9].

Permeancy and Permeability

Cytometry has picked up words from the lexicon of histology and histochemistry that describe the propensities of dyes and other chemicals for entering cells and the propensities of cells for taking up dyes and other chemicals. To repeat what I said when I introduced this topic on p. 43, materials that can readily cross the intact cytoplasmic membranes of cells are said to be **membrane-permeant**, or, more simply, **permeant**; materials that are excluded by intact cytoplasmic membranes are described as **membrane-impermeant**, or just **impermeant**. In order to stain living cells, i.e., to act as a **vital stain**, a dye must be permeant.

Cells that can take up a dye or other chemical are said to be **permeable** to the material; cells that cannot take up a material are said to be **impermeable** to it. The terms "permeability" and "impermeability" are used to characterize cell membranes in particular as well as cells in general.

A look at the structures of some nucleic acid dyes, shown in Figure 7-10, on the next page, may provide some help in understanding permeancy and impermeancy. Organic compounds bearing at least two positive charges, exemplified by fluorescent nucleic acid binding dyes such as DAPI, propidium iodide (PI) and TO-PRO-1, are impermeant.

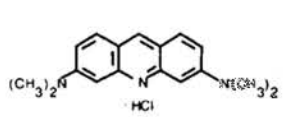
Ethidium bromide (EB), not shown in the figure, shares the heterocyclic ring structure of PI, but carries only a single, delocalized positive charge; the ring nitrogen bears an ethyl (C_2H_5) group instead of the n-propyltrialkyl quaternary ammonium group (the "pro" in propidium) found on the ring nitrogen in PI.

Both dyes form complexes with DNA and RNA, and are toxic to cells once taken up. However, EB normally enters cells, albeit slowly, and is known to be pumped out of at least some bacteria[2585], while PI is normally excluded by its additional charge. Although EB is often used in lieu of PI for dye exclusion tests, it should not be because it is not truly impermeant. One can generalize from this; one should not assume that a dye is impermeant without determining whether or not it is being transported out of cells.

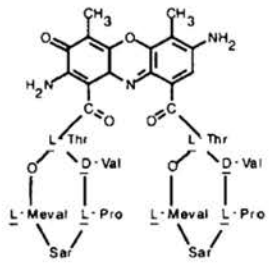
TO-PRO-1, a dye developed by Molecular Probes, has a delocalized positive charge on the heterocyclic ring structure and a propyltrialkyl (quaternary) ammonium on one ring nitrogen; it is, as was noted on the previous page, impermeant. Its parent compound, thiazole orange, has two N-methyl groups and lacks the quaternary ammonium substituent; it carries a single delocalized positive charge and is highly permeant. Thiazole orange was originally synthesized by Lee et al[769] at B-D as a stain for blood reticulocytes, making it highly desirable that it be permeant. Molecular Probes has produced a number of variants of the molecule, both permeant (the SYTO dyes) and impermeant (TO-PRO-1 and its homologues and some of the SYTOX dyes). The fluorescent properties of all of these dyes, which enhance fluorescence as much as several thousand times on binding to DNA or RNA, derive from the heterocyclic ring structure; the permeancy properties derive from the nature of various ring substituents, which have only minor influence on the fluorescence spectrum. Appropriate modification of ring substituents can influence not only whether or not a dye is permeant, but how rapidly it will enter, or leave, cells.

You might want to take some guesses as to the permeancy or impermeancy of the other dyes shown in Figure 7-10; the answers will appear in the subsequent discussion of nucleic acid stains.

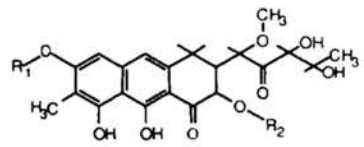
There are two basic strategies for introducing impermeant dye molecules into living cells. The first, **permeabilization**, basically involves making holes in the membrane. This can be done physically, as in microinjection or membrane permeabilization by electrical breakdown (electroporation) or mechanical manipulation. Alternatively, membranes can be permeabilized by treatment with **fixatives**, or with



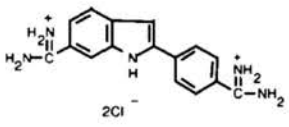
ACRIDINE ORANGE



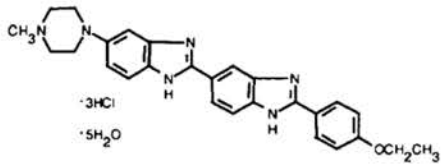
7-AMINOACTINOMYCIN D



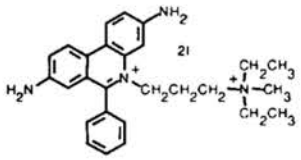
CHROMOMYCIN



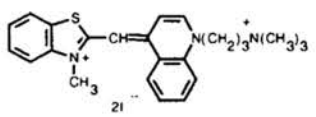
DAPI



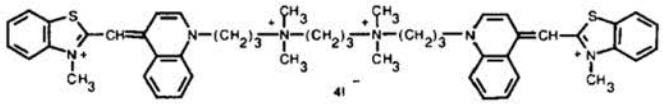
HOECHST 33342



PROPIDIUM IODIDE



TO-PRO-1



TOTO-1

Figure 7-10. A "rogues' gallery" of nucleic acid dyes. The chromomycin structure shown is the chromomycin nucleus; chromomycin A_3, mithramycin, and olivomycin each have different oligosaccharides as R1 and R2. Ethidium is similar to propidium, but with a ring N-ethyl group; thiazole orange (TO) is similar to TO-PRO-1, but has N-methyl groups on both rings. All structures except chromomycin were provided by Molecular Probes, Inc.

milder chemical agents such as lysolecithin. In either case, one can expect that solutes other than dye molecules will pass from cell to medium and *vice versa* during the time in which the membrane is permeable to dye. This in itself can produce alterations in cell physiology[207]; e.g., membrane potential drops to zero for a time. It then falls to the investigator to show that permeabilization didn't perturb the cells sufficiently to cast doubt on the validity of results obtained after staining and cytometry. I have been permeabilized by a 15 gauge hypodermic needle without ill effects; I would not expect to survive permeabilization by a 12 gauge shotgun.

The second strategy for getting dyes across membranes of living cells involves chemical modification of the dye molecules themselves. Acid dyes such as fluorescein do not cross cell membranes, but their electroneutral esters do. Diacetylfluorescein, which will forever be improperly called fluorescein diacetate (FDA), also called is uncharged and lipid soluble, and thus permeant; once inside the cell, ester molecules are readily and rapidly hydrolyzed to free fluorescein by nonspecific esterases, which are present in almost all cells. This effect serves as the basis for a test of cell "viability," or, more accurately, of **membrane integrity**; the ester is not fluorescent, while the free fluorescein anion, which is retained by intact cells, renders them highly fluorescent.

If one makes chromogenic or fluorogenic esters that require less ubiquitous enzymes than nonspecific esterases for hydrolysis, the accumulation of color or fluorescence in intact cells can be used to provide an indication of the presence and relative activity of various enzymes in those cells. Chemical modifications other than esterification, e.g., oxidation or reduction, may also be made to render dye molecules capable of crossing the cell membrane, and may also introduce a requirement for intracellular enzyme action to restore the staining characteristics of the unmodified molecule.

Vital Dye Toxicity and Photosensitization of Cells

It is important to remember that a permeant "vital" stain may eventually damage or kill cells; in this context, as in others, it is wise to establish that measurement conditions do not themselves perturb what one is attempting to measure.

Deleterious effects on cells other than those due to direct chemical toxicity of dyes may occur due to **photosensitization** when stained cells are exposed to high-intensity laser light. Many fluorescent dyes sensitize cells to photodynamic damage, although dyes that bind to DNA, such as the Hoechst dyes and the acridines, are probably best known in this regard. The probability of damage to cells stained with such dyes increases with the laser power used for analysis as well as with dye concentration.

When analyzing possible toxicity due to photosensitizing dyes, one should also bear in mind that a few hours' exposure of stained cells to fluorescent lighting in the laboratory

may produce photodynamic damage equal to or greater than that resulting from a few microseconds in a low-power laser beam. To verify that cells are indeed being damaged by the dye and/or the laser, it is usually necessary to compare treated cells with cells kept in the dark.

Fixation – Why and How

Permeabilization can be, but is not always, accomplished in the context of **fixation** of cells. Most staining procedures in histology and histopathology, and many histochemical and cytochemical procedures, were originally developed using fixed specimens. The term "fixation" itself reminds us that one of the several original purposes of fixation was to make cells and tissues physically rigid enough to survive embedding and sectioning. Fixation was also necessary to make cells permeable to dye, thus allowing optimal staining, and to preserve specimens by inhibition of autolysis and microbial action. Baker[32] provides an excellent discussion of fixation mechanisms and of the classical fixatives; among these, **ethanol** and **formaldehyde** (and **paraformaldehyde**) are widely used for flow cytometry. More modern work on fixatives and mechanisms, with emphasis on the actions and use of **glutaraldehyde**, was summarized by Hopwood[208] and in a volume edited by Stoward[209]; Hopwood[125] provides a somewhat more recent large review.

Fixation is not an option when an experimenter's primary objective is to sort and retrieve living cells. However, when the objective is the demonstration and/or quantification of chemical constituents in cells, and there is no need for the cells to be kept alive during or after the process, it makes sense to work with fixed cells.

Fixation for Biohazard Control

Until the HIV epidemic emerged in the 1980's, most people who made flow cytometric measurements of unfixed cells preferred to work with unfixed material, which was at least perceived as being freer of cell aggregates, debris, etc., and exhibiting less autofluorescence than fixed specimens. While, statistically speaking, experimenters were far more likely to be exposed to such pathogens as the hepatitis B virus than to HIV, the perceived threat from the latter agent was what changed behavior, inside and outside the laboratory. Fixation with the objective of killing HIV and other viruses that may be present in specimens has now become routine in most flow cytometry involving cells or body fluids of human origin, and appropriate precautions against infection are widely, if not universally, observed when unfixed specimens must be analyzed.

The effects of fixatives on the infectivity of cells carrying HIV were examined by Cory, Rapp, and Ohlsson-Wilhelm[1303], who found that 30 min exposure to 0.5% paraformaldehyde, 1.85% formaldehyde, absolute methanol, or 1:1 methanol-acetone reduced infectivity by more than 99.99%.

Ericson et al[1304] studied the effects of commercial proprietary red cell lysing and fixing solutions on the HTLV-1 retrovirus. Coulter ImmunoPrep/QPrep and Immuno-lyse (Coulter Immunology, Hialeah, FL), FACS Lyse (B-D Immunocytometry Systems, San Jose, CA), and GenTrak whole blood lyse and fix solution (GenTrak, Plymouth Meeting, PA) all substantially reduced infectivity of infected cells seeded into blood and cultured after 5 min exposure. Ortho-lyse (Ortho Diagnostic Systems, Raritan, NJ), which had no added fixative, and ammonium chloride lysing solution, with 0.1 or 1.0 % paraformaldehyde added, did not reduce infectivity after 5 min but did after 60 min; other solutions worked better after 60 min than after 5 min.

This is good news and bad news; good news, because most people who do flow cytometry use commercial fixing and lysing solutions containing agents that are known to inactivate at least the two retroviruses studied in the references just cited, and bad news, because the development of new fixation techniques must now entail determining whether or not they inactivate various pathogens, a task for which most experimenters do not have much enthusiasm. If you remain undaunted, read on.

Fixation Mechanisms

Most of the effects of fixatives result from their action on **proteins**, which are denatured, precipitated, and/or **cross-linked** by fixatives at appropriate concentrations. The classification of fixatives as **coagulant** (e.g., acetone, ethanol, and methanol) or **non-coagulant** (e.g., acetic acid and formaldehyde) is based upon visual observation of their effects on solutions of albumin. However, both the coagulant alcohol and the non-coagulant aldehyde fixatives polymerize proteins. While the formation of protein aggregates is generally useful in stabilizing tissue specimens for embedding and sectioning, it is obviously only desirable up to a point when one wants to prepare suspensions of unclumped single cells for flow cytometric analysis. For many applications, it has been found useful to combine fixatives with **detergents**, which improve the speed and uniformity of reagent penetration into cells and tissues[125].

Permeabilization versus Fixation

Since specimens are usually not kept after they have been analyzed by flow cytometry, the preservative action of fixatives is generally unnecessary. In some cases, it may actually be desirable to remove portions of cells, as when flow cytometric measurements of DNA content are made on **isolated nuclei** from which the surrounding cytoplasm and extracellular matrix have been stripped by a combination of mechanical means, enzymes, hypotonic media, and **non-ionic detergents** such as Nonidet P-40 or Triton X-100. In the strictest sense of the term, specimens so treated can be said to consist of "unfixed cells," but they certainly cannot properly be described as "vitally stained." From a practical point of view, it makes sense to consider such cells as fixed; bear in mind, however, that while the cells are dead, accompanying pathogens may well not be.

Cells can be permeabilized without being fixed. Transient permeabilization with lysolecithin or electroporation, or addition of pore-forming peptide antibiotics such as nisin[2586-7], will allow cells to take up normally impermeant dyes such as propidium; at least some such treatments won't even kill the cells, much less fix them. Even the detergent treatment mentioned above, which makes the cells so permeable that everything but the nucleus washes away, doesn't do many of the things we expect fixation to do.

And cells can be fixed without being permeabilized, or at least exposed to fixatives without being permeabilized. The kicker here is that both "permeabilization" and "fixation" are terms covering a multitude of sins. As I wrote a quarter-century ago[93],

> "Though I'm no linguist, I have heard
> that every Eskimo
> Learns sixteen different words describing
> different kinds of snow.
> I find it hard to understand how
> histochemists live
> And work with but a solitary word for fixative."

If we look at an intact cell as a plastic bag, we can envision permeabilization as turning it into a mesh bag. The problem is that it takes a finer mesh bag to hold marbles than to hold golf balls, and a finer mesh bag to hold golf balls than to hold baseballs. The antibiotic gramicidin A forms a 4.7 Å pore in cell membranes[2588]; this makes the membranes of cells exposed to gramicidin A permeable to most inorganic ions, with the result that the transmembrane electrical potential gradient is reduced to zero. However, the cells do not take up propidium. Nisin, which, as mentioned above, does make cells permeable to propidium, forms an 8 Å pore in membranes; bigger impermeant molecules need bigger holes to get through membranes. If you're trying to stain an intracellular antigen with a fluorescein-labeled IgG monoclonal antibody (MW 160,000), you'll probably need a much bigger hole than nisin makes, and, if you're working with a phycoerythrin-labeled monoclonal antibody (MW 400,000), you'll need a bigger hole than that.

If you need to expose large molecules or supramolecular structures in cells to antibodies or gene probes, but you want to keep at least some smaller molecules in or associated with the cells, you'll have to resort to fixation, and, in particular, to fixation with a cross-linking agent, which you will probably need to use in combination with a detergent or other permeabilizing agent. The cross-linking fixative will attach the small stuff you want to bigger stuff, which will keep it from getting through the big holes you made in the membrane.

Fixative Effects on Scatter Signals

The effects of alcohol and aldehyde fixation on proteins result in a marked increase in the **refractive index** of the cytoplasm, which rises from the value of approximately 1.35 observed in living cells to about 1.54. The refractive index of an isotonic saline solution is about 1.335. Since the amount of light scattered by cells is a function of the difference in refractive index between cells and the suspending medium, the amplitudes of light scattering signals are considerably higher for alcohol- or aldehyde-fixed than for unfixed cells. This may improve discrimination between cell types based on light scattering measurements. However, increased scattering may also affect the precision of fluorescence measurements because the effective amplitudes of both the excitation beam and the emitted fluorescence may be altered due to scattering by cytoplasmic structures. Scattering data may be difficult to interpret because various fixatives and postfixation treatments may in themselves change cell sizes, sometimes exerting different effects on different cells or on cells in different states. This topic was discussed in detail by Penttila, McDowell, and Trump[210], who also used flow cytometric measurements of light scattering and extinction to get a clearer description of cell volume changes during cell injury and fixation[211].

Carulli et al[2589] found that 10 minutes' exposure to BD FACS Lysing Solution, which contains a fixative as well as a lysing agent, allowed eosinophils in whole blood samples to be discriminated from other granulocytes on the basis of forward and side scatter signals.

Fixation for Surface Antigen Measurements

While some protein structures and enzyme activities remain unaltered after fixation, it is unwise to assume that the structure that particularly interests you will survive intact. For this reason, it has become common practice to stain cell surface antigens with fluorescent antibodies before fixing the cells to allow fluorescent staining of other constituents, e.g., DNA.

There are several reasons for doing immunofluorescence analyses on fixed cells. One is that appropriate fixation kills pathogens, but there are others. If, for example, you want to do simultaneous analyses of DNA content and surface antigens, using fluorescent antibodies and propidium[330-1], you'll need to fix the cells to permit RNAse treatment and nuclear staining while preserving the antigen-antibody complexes bound to the cell membrane. If you have only occasional access to a flow cytometer, and/or you collect samples over a period of days, you can't have everything stained fresh. And, of course, when you walk into the flow cytometer room with 100 freshly stained samples and the technician tells you the machine is down for two days, fixation is your only salvation.

Before you fix cells, it's a good idea to run them over a Percoll gradient, or do whatever else you like to do, to get rid of dead cells and debris. It's essential to wash the cells several times to get rid of any protein that may be in the medium; otherwise, you will end up with cell clumps at best and fluorescent-labeled aspic at worst.

Years ago, I used a modified version of Raul Braylan's time-honored procedure[331] for ethanol fixation of im-

munofluorescent stained cells. Washed cells, at a concentration of 2 x 10^6/ml or less, in phosphate buffered saline, pH 7.3, at 4 °C, are placed on a vortex mixer, and an equal amount of cold absolute ethanol is added slowly while vortexing. Cells fixed according to this procedure can be kept for at least several days, and often considerably longer, at 4 °C.

A frontal approach to fixation for immunofluorescent staining was taken by Van Ewijk et al[26], who compared immunofluorescence signals from fresh mouse and human lymphoid cells and from similar cells fixed before immunofluorescent staining. Paraformaldehyde, glutaraldehyde, acrolein, and osmium tetroxide at various concentrations were tested as fixatives; staining of Thy-1, T-2090, Lyt-1, Lyt-2, and Th-B antigens on murine and of B1, B2, β_2-microglobulin, HLA-DR, CALLA, OKT-3, and Leu-4 on human cells was quantified by flow cytometry. Fixation with 0.5% paraformaldehyde prior to immunofluorescent staining was found to preserve all mouse and human antigens studied; cells so fixed were stable and could be stored for at least one week prior to immunofluorescent staining without adverse effects.

Fixatives: Coming Out of Aldehyding Places

At present, **formaldehyde** and its supposedly less evil twin, **paraformaldehyde**, are probably the most popular fixative for immunofluorescent stained cells; **ethanol**, glutaraldehyde, and methanol have also been used. One might expect that alcohols would be preferable to aldehydes for fixing cells prior to immunofluorescence measurements, because aldehyde fixatives react with a variety of amines found in cells to produce fluorescent materials. Glutaraldehyde is notably worse than formaldehyde in this regard; on the positive side, this led to widespread use of chicken erythrocytes fixed in glutaraldehyde as low-intensity fluorescent particle "standards"[164] in the early days of immunofluorescence measurements. So-so standards are better than no standards at all.

Formaldehyde itself tends to polymerize in aqueous solution, making it difficult to control the effective concentration of fixative (at some point, the solution should become informaldehyde); methanol is added to many formaldehyde solutions to retard polymerization. Methanol-free formaldehyde is generally regarded as preferable for fixation. Relatively stable, methanol-free formaldehyde solutions are available; however, many people prefer to use paraformaldehyde, which is polymerized formaldehyde, available in solid form, to make up solutions containing a well-controlled concentration of formaldehyde. It is relatively common practice to heat solutions prepared from paraformaldehyde, ostensibly to facilitate depolymerization, to add buffer to prevent the formation of formic acid, and to make up fresh solutions frequently. However, Helander has shown[2590] that depolymerization occurs at room temperature, that only very small amounts of formic acid actually do occur in paraformaldehyde solutions, and that solutions are stable for at least a week. It may take considerably longer than that to dispel the urban legends.

We can certainly put the knock knock on formaldehyde; it's toxic, mutagenic, and potentially carcinogenic. Since detecting the slightest whiff of it in your house is likely to put you on the phone to a trial lawyer, why put up with it in your lab? Bostwick et al[2594] found they could switch to a mixture of 56% ethanol and 20% ethylene glycol and establish a "formalin-free surgical pathology lab." I guess we all have our pet causes.

It may be desirable to use non-aldehyde, cross-linking fixatives such as dimethylsuberimidate[212], 1-Ethyl-3-(3-Dimethylaminopropyl)-Carbodiimide Hydrochloride (EDC)[2592], N-Succinimidyl-3-(2-Pyridyldithio) Propionate (SPDP)[2591], or dimethyl 3,3'dithiobispropionimadate (DTBP)[2593] to minimize fluorescence induced by fixation, although these materials may be more expensive and less stable than more commonly used fixatives. Alternatively, Tagliaferro et al[2595] have described a procedure that uses Schiff base formation with fuchsin to quench fluorescence in glutaraldehyde-fixed material.

Over the years, a fair amount of effort has been devoted to producing stabilized blood cell controls for cytometry, which necessarily involves accomplishing at least some of the goals of fixation. Jani et al[2596] have tested the "TransFix" solution, developed by Barnett et al to prepare one such control[2597], as a fixative and transport medium for blood specimens intended for CD4+ cell counts. They found that counts remained stable in fixed specimens kept for 7 days under simulated tropical conditions expected to be found in resource-poor settings with a high prevalence of HIV infection. TransFix preserves most common surface antigens, and could find a wide range of applications; if it does, it is almost certain that flow cytometer manufacturers and third parties now producing fixing and lysing solutions will work toward producing their own improved products to permit longer specimen storage times under wider ranges of environmental conditions.

There are applications for which existing commercial fixatives are less than ideal; one of them is counting CD34+ stem cells in blood, which are consistently lower in specimens subjected to red cell lysis and fixation than in those subjected to lysis alone[2598]. It has been observed that different commercial fixing and lysing solutions have different effects on the forward and side scatter signals from leukocyte populations and on levels of expression of some antigens[2599,2600]; Macey et al[2600] advocate making immunophenotyping measurements on unfixed, unlysed whole blood using a permeant nuclear stain to identify nucleated cells. This approach can provide a good reference method for analyzing selective cell loss due to lysing reagents and fixatives; more studies in this area are badly needed. Manufacturers' tendency to keep the compositions of their preparative solutions secret does not facilitate evaluation of these products.

Fixation for Intracellular Antigen Measurements

When you're after **intracellular antigens**, with or without surface antigens, the cells have to be fixed before you can finish your immunofluorescent staining. Jacobberger et al[727] and Levitt and King[728] recommended methanol fixation for such purposes; 900 µl of ice-cold or colder 100% methanol are layered over 100 µl phosphate buffered saline (PBS), pH 7.4, containing 10^6 washed cells. Cells so fixed can also be stained with propidium iodide for simultaneous flow cytometry of intracellular immunofluorescence and DNA content. Clevenger, Bauer, and Epstein[1289] fixed cells at 4 °C with 0.5% paraformaldehyde and then permeabilized them with 0.1% Triton X-100 in PBS.

For staining both surface and intracellular antigens, one can either stain the surface antigen and then fix and permeabilize the cells[1290], or fix the cells in such a way that surface antigens are preserved. Other fixatives that have been used include buffered formaldehyde-acetone[1291], periodate-lysine-formaldehyde[1292], and paraformaldehyde followed by methanol, which was found in careful comparative evaluations by Pollice et al[1293] and Schimenti and Jacobberger[1294] to minimize loss of signal from antigens and to provide good DNA staining characteristics in terms of G1 peak location and CV and relative lack of clumps and debris. Schmid, Uittenbogaart, and Giorgi[1295] reported good results with fixation for 1 hr at 4 °C in 0.25% buffered paraformaldehyde followed by permeabilization for 15 min at 37 °C with 0.2% Tween 20; this treatment preserves relationships between leukocyte clusters on displays of forward vs. side scatter. Other permeabilizing agents that have been used for staining nuclear antigens include *n*-octyl-beta-D-glucopyranoside[1296], digitonin[1297], saponin[1298], and lysolecithin[2601].

There is no "one-size-fits-all" solution to the problem of preparing cells for such analyses; Koester and Bolton[2602] offer some guidelines and recommendations. However, there are fixative solutions available from numerous manufacturers that can be used for flow cytometric analysis of a variety of the more widely studied intracellular antigens.

Fixation for DNA Content Determination; Getting DNA (and Antigens) Out of a Tight Fix

DNA content analyses may be done on cells that have been liberated from tissues and tumors by mechanical and/or chemical treatment rough enough to render them permeable, in which case fixation is not necessary to permit staining with impermeant dyes. Fixation remains useful, however, when material needs to be transported before analysis, in which case the fixative serves the classical purpose of preserving the specimen. Howell et al[1299] found the very classical fixative mixture of 20:1 methanol:acetic acid useful in preparing cells from urine and bladder washing for both cytologic examination and DNA content analysis. Rouselle et al[2603] evaluated fixation with a variety of commonly used mixtures and found DNA content distributions with the lowest CVs were obtained using 68% ethanol and 85% methanol.

DNA content analysis may also be done on cells released from paraffin, which may have been fixed before the experimenter was born and which, in hindsight, may have been fixed a little more thoroughly than may be desirable for DNA analysis. Fixation is known to decrease accessibility of DNA stains to DNA, probably as a result of extensive cross-linking of histones to DNA[2604]. Luckily, cross-linking can be reversed; Overton and McCoy[2605] report that resuspending formalin-fixed cells in saline and heating them at 75 °C for at least an hour prior to staining restores the accessibility of the DNA to propidium.

The same general trick may be useful in restoring antigens in fixed tissue to enough of a semblance of their native state to permit or improve immunofluorescent staining. Boenisch[2606] examined **heat-induced antigen retrieval** of a number of tissue antigens using two popular techniques.

Catch the Wave: Fixation by the (Cook) Book

A lot of histologists and pathologists now seem to be using heat, with or without added chemical agents, for fixation. This isn't a completely new idea; in the 1970's, the Block group found that, when warmed to 40 °C, a glutaraldehyde fixative took less than 20 seconds to render red blood cells impervious to lysis by distilled water.

We didn't use a microwave oven back then, but that's what people are doing now. It has been established that the microwaves don't accomplish anything more subtle than heating the specimen, which decreases fixation time when the oven is used in conjunction with a chemical fixative[2607]. And, for those of you who have noticed warm and cold spots in different regions of the same microwaved entree, I will point out that Login et al[2608] have devised methods for calibrating and standardizing microwave ovens for various fixation procedures. I'll have to find out whether they work for day-old Hunan pan-fried noodles.

Microwave fixation does not seem to have been used much for flow cytometry, but a provocative paper by Grutzkau et al[2609] suggests that quantitative flow cytometry to determine optimal conditions for microwave and chemical fixation and for permeabilization could be useful in preparing samples for immunoelectron microscopy, and that microwave fixation might be useful for flow cytometric analysis of intracellular antigens.

Fixation Artifacts

If you are trying to reproduce a staining technique described in the literature, it's a good idea to use the fixation procedure employed by the author(s) of the paper in question. Even then, particularly if you're trying to do quantitative analyses, you may need to find out whether, and to what extent, variations in fixative composition and conditions affect staining. Holtfreter and Cohen[1300] noted that 50% ethanol fixation yielded the same DNA fluorescence from nucleated frog erythrocytes and leukocytes, while higher

concentrations gave bimodal distributions, presumably due to the different density of chromatin in the two cell types. Haynes, Moynihan, and Cohen[1301] found that binding of an anti-human CD25 antibody to paraformaldehyde-fixed frog cells was artifactual, there being no evidence of reactive epitopes on unfixed cells. Jumping to humans, Cahill, Macey, and Newland[1302] reported that formaldehyde fixation of platelets can result in artifactual expression of antigens indicative of activation. The best way to avoid artifacts and other troubles with fixation is, of course, to work with unfixed cells.

Red Blood Cell Lysis: The Distilled Essence

On those occasions when you can get away without fixing, and want to make immunofluorescence measurements of leukocytes from blood or bone marrow without accompanying red cells, you resort to lysing agents, which are often either proprietary mixtures or ammonium chloride solutions (the two are not mutually exclusive). I have always preferred **hypotonic lysis**; I dilute the blood 1:10 with distilled water, wait for a few seconds until it clears, and bring the osmotic strength back to normal with concentrated saline. I was thus pleased to see that Terstappen, Meiners, and Loken[1305], who contributed quite a bit to the analysis of leukocyte antigens, found that hypotonic lysis preserves cellular immunofluorescence and scatter signals, and avoids cell loss encountered with ammonium chloride. This method also requires no washes, something else I favor in my lab, where flow cytometers outnumber people.

7.4 NUCLEIC ACID DYES AND THEIR USES

Fluorescent nucleic acid-binding dyes can used to measure a number of the extrinsic parameters shown in Table 7-1 (p. 286), including **DNA content**, **DNA base ratio**, single- and double-stranded **RNA content**, and also to characterize **chromatin structure** and to detect **DNA synthesis**. A "rogues' gallery" of nucleic acid stains appears in Figure 7-10 (back on p. 301).

DNA Content Measurement

Many, if not most, users of flow cytometers and sorters have at least a passing acquaintance with measurements of the **DNA content** of cells and chromosomes, which can be done rapidly and precisely by flow cytometry using a variety of fluorescent stains. I introduced DNA content measurements and some of the dyes used to make them on pp. 21-26, 43-4, and 96-7.

DNA content measurements were shown to be relevant to tumor pathology and chemotherapy in the late 1960's, and stimulated interest in fluorescence flow cytometry at a time when few, if any, instruments were sensitive enough to make immunofluorescence measurements.

The ideal dye for measurement of DNA content would be **DNA-specific**; that is, it would form a fluorescent complex with DNA, but not with RNA or with other macromolecular species. It would also not exhibit any **base** or **sequence preference**; in other words, the fluorescence from a given number of dye molecules bound to another given number of base pairs' worth of DNA would be the same, regardless of the proportions of A-T and G-C base pairs in the DNA.

Dick Haugland, of Molecular Probes, has taken me to task over the use of the term "DNA-specific" to describe real DNA dyes; he says there aren't any really DNA-specific dyes and suggests **DNA-selective** as a more appropriate adjective. I'll go with that from now on, and recommend you do the same. Some, but not all, of the improvements in DNA content measurement since the 1960's have resulted from the discovery or synthesis and use of dyes with greater DNA selectivity.

Feulgen Staining for DNA Content

By 1969, Van Dilla et al had used a modified **Feulgen procedure** with fluorescent stains (acriflavine and auramine O) and an argon laser source flow cytometer to produce DNA content distributions with a coefficient of variation of 6% for the diploid cell peak[79]. Feulgen staining is highly DNA-selective, but the procedure is also technically intensive, and the search for dyes that might be easier to use began almost immediately.

DNA Staining with Ethidium and Propidium

The first step in this direction was taken in 1969, when Dittrich and Göhde published a relatively sharp DNA content distribution obtained using their arc source flow cytometer to measure the fluorescence of fixed cells stained with **ethidium bromide**[83]. **Propidium iodide**[216] was introduced by Crissman and Steinkamp[217] in 1973 as a substitute for ethidium bromide in procedures for simultaneous quantitative analysis of DNA and protein content, in which fluorescein isothiocyanate (FITC) was used as a covalent stain for protein. Both fluorescein and propidium were excited at 488 nm; the rationale for the use of propidium lay in the fact that its emission maximum is 10-15 nm farther into the red region of the spectrum than that of ethidium, making it easier to separate red and green fluorescence signals from propidium and fluorescein using optical filters. It has generally been noted since that propidium produces fluorescence histograms with somewhat lower coefficients of variation (CVs) than are obtained using ethidium; this, rather than spectral characteristics, probably accounts for the greater popularity of propidium.

Ethidium and propidium form complexes with double-stranded DNA and RNA by intercalating between base pairs[213-5]. An intercalated dye molecule finds itself in a hydrophobic environment that results in a shift of its absorption spectrum and an increase in its fluorescence quantum efficiency. Excitation in the UV (320-360 nm) or blue-green (480-550 nm) spectral regions produces 20 to 30 times as much fluorescence emission from ethidium or propidium molecules bound to nucleic acid as would be emitted by the same number of dye molecules in solution. In addition,

since binding to nucleic acid itself results in a local increase in the concentration of dye molecules, nuclei, chromosomes, and other structures containing double-stranded nucleic acid (DNA or RNA) are brightly stained by ethidium or propidium, provided cells are either fixed or permeabilized to allow the dye to enter.

Since ethidium does not rapidly cross the membranes of intact cells, and is likely to be pumped out when it does, it has widely, but erroneously, been regarded as impermeant, and used in dye exclusion tests; as I mentioned on p. 300, this is not a good idea. Propidium, which, by virtue of its double positive charge (see pp. 299-300) is impermeant, is a suitable alternative. The double charge also gives propidium a higher binding affinity for double-stranded nucleic acid than ethidium; the former dye will displace the latter from cells permeable to both[2610].

Neither ethidium nor propidium is DNA-selective; the dyes were originally used to stain fixed cells, and specimens were treated with RNAse to eliminate artifactual broadening of DNA content distributions that would otherwise result from the fluorescence of dye bound to double-stranded RNA. In 1975, Krishan described a simplified staining method that eliminated the steps of fixation and RNAse treatment; cells were suspended in a solution containing 0.1% sodium citrate and 50 μg/ml propidium iodide[218].

The cells first examined by Krishan were predominantly hematologic in origin; such cells are readily susceptible to lysis in hypotonic media. Substantial amounts of cytoplasm, and of cytoplasmic RNA, are lost as a result of hypotonic treatment, but only in cell types that undergo osmotic lysis. Look et al[221] (also A. T. Look, personal communication) found that the CVs of DNA content histograms obtained from propidium-stained cells were sharpened by the incubation of samples with 0.05 mg/ml ribonuclease (RNAse) for 30 min at room temperature before analysis; these days, almost everybody uses RNAse.

Fried, Perez and Clarkson, who studied hypotonic propidium staining in some detail[219], added 0.1% Triton X-100 to Krishan's propidium/citrate mixture and reported good results in staining cells that had been grown as attached monolayers[220]. The addition of the detergent at this relatively low concentration allows stained samples to be kept at room temperature for at least several days without significant change in the fluorescence histograms.

Neither ethidium nor propidium exhibits a strong base preference; this makes the dyes useful in determination of total DNA content of cells in such applications as plant taxonomy, which will be discussed in Chapter 10.

Ethidium and Propidium: Ionic Strength Effects

The binding affinity of ethidium to DNA is strongly dependent on the **ionic strength** of the solution[215]; fluorescence intensity of a solution of DNA in isotonic saline will be less than that of a solution with the same concentration of DNA and a lower ionic strength. Propidium has similar properties. Martens, van den Engh, and Hagenbeek[227] noted shifting peaks in propidium fluorescence distributions from cell samples in hypotonic solution run in a cell sorter using isotonic saline sheath fluid. This drift can be eliminated by the use of a sheath fluid with the same ionic strength as the sample, i.e., use a distilled water sheath with samples in hypotonic solution, or add salt to taste to the samples if you use a saline sheath in your instrument. This problem has been described to me by many people; the solution is in the solutions.

DNA Content: Sample Preparation and Standards

Because abnormalities in DNA content are commonly found in cancer, and may be relevant to prognosis, applications in clinical oncology motivated much of the work on preparation of tissue samples for DNA content determination.

Four papers[222-5] by Vindeløv and his coworkers summarized their extensive experience in preparation, storage, and analysis of propidium-stained samples; they were also among the first to consider the problem of **standardization of DNA content measurements**. Both **chicken erythrocytes**, with a DNA content of 35% of the human diploid value, and **rainbow trout erythrocytes**, with a DNA content of 80% of the human diploid value, were added to samples[224]. The use of two standards eliminates calibration errors due to **nonlinearity** in the instrument.

Taylor[226] investigated rapid methods for preparation of samples for DNA content analysis from cells grown as monolayers or in suspension, from solid tissues, and solid tumors, using propidium and other stains for DNA. He obtained histograms with good precision using an isotonic saline solution with approximately 1.0% Triton X-100 added. This concentration of detergent lyses cells and solubilizes cytoplasm; it also, unfortunately, tends to lyse nuclei after a few hours. RNAse (1 mg/ml, equivalent to 50-75 Kunitz units/ml) is used with propidium staining to eliminate RNA fluorescence artifacts. Staining according to Taylor generally requires less than 10 min incubation of cells with the staining solution; samples are then filtered through a 50 μm nylon mesh and analyzed.

Singh[2611] reports that passage through a tissue press followed by pipetting yields cleaner suspensions of isolated nuclei for DNA content analysis in less time than does mincing tissue.

Chromomycin A_3, Mithramycin, and Olivomycin

In 1974, before rapid DNA staining techniques employing propidium had been developed, Crissman and Tobey described a rapid DNA staining procedure using the antitumor antibiotic **mithramycin**[228], with argon laser excitation at 457 nm. These authors had used fluorescent Feulgen staining for analysis of drug effects on cell cycle progression[229]; the reduction of sample preparation time to 20 minutes from several hours made it feasible to monitor population kinetics almost continuously during experiments. Cells were stained with mithramycin in a solution containing ethanol, which,

while not fully fixing the cells during the short staining time, did make them permeable to the drug.

The use of mithramycin was prompted by the report that complexes of the drug and DNA were fluorescent, while the drug failed to interact with RNA[230]; thus, no RNAse treatment was required to achieve selective DNA staining. Crissman et al[231] did detailed studies of staining with mithramycin and with the structurally related antibiotics **olivomycin** and **chromomycin A_3**, all of which are highly DNA-selective. They found that optimal staining of cells fixed in ethanol or electron microscopy grade glutaraldehyde was achieved with 50-100 μg/ml dye, with pH in the range 5-9, salt (NaCl) concentration 0.15-1.0 M, and with 15-200 mM added magnesium (Mg^{++}). Magnesium ion is required for formation of the complexes of chromomycin A_3, mithramycin and olivomycin with DNA, which also involve the 2-amino group of guanine[230]; the three dyes have a strong base preference, and act as fluorochromes for **G-C rich regions** of DNA. All are impermeant, at least in terms of short-term staining of intact cells; they would, obviously, be ineffective as antitumor antibiotics if they didn't eventually get in, but this is not the place to delve into pharmacology.

The emission maximum of the olivomycin-DNA complex is at approximately 545 nm, but there is substantial emission between 480 and 500 nm. The chromomycin complex has an emission maximum at about 555 nm, but its emission spectrum does not have the short-wavelength shoulder characteristic of the olivomycin complex. The mithramycin complex spectrum also lacks the shoulder and has an emission maximum at about 575 nm. The excitation maxima of the DNA complexes of all three dyes are at approximately 440 nm[231]. The quantum efficiency of the dye-DNA complex is relatively low; this may limit precision in work with chromosomes or bacteria due to photon statistics.

While chromomycin A_3, mithramycin, and olivomycin can all be excited by the 457 nm argon ion laser line, shorter wavelengths, e.g. the violet lines from a krypton or diode laser, 441 nm from a He-Cd laser or the 436 nm line from a mercury arc lamp, are preferable. The spectral characteristics just mentioned led directly to the development of another popular DNA stain. Until 1974, there was little interaction between American workers, almost all of who were using laser source flow cytometers, and European researchers in the field, who were using arc source instruments[232]. In mid-1974, Barthel Barlogie arrived in Houston, Texas with a Phywe ICP system, with which he began studies of tumor cell DNA content using ethidium bromide, as was then customary. The blue-violet excitation in the ICP seemed better suited to mithramycin than to ethidium, which first prompted a trial of DNA staining with mithramycin (B. Barlogie and H. Shapiro, unpublished), and next motivated the use of a mixture of **mithramycin and ethidium**[233].

Mithramycin Plus Ethidium: Do's and Don'ts

DNA-bound ethidium is not very efficiently excited by blue-violet light; the DNA-mithramycin complex is optimally excited, and energy transfer occurs between mithramycin and ethidium provided the molecules are in close proximity. Thus, in cells stained with the mithramycin-ethidium mixture, ethidium fluorescence comes primarily from ethidium bound to DNA, and broadening of fluorescence distributions due to RNA fluorescence is largely eliminated when violet or blue-violet (400-457 nm) excitation is used. I have run across people who used a mithramycin-ethidium mixture with 488 nm excitation; this makes little or no sense, because excitation of mithramycin at this wavelength is negligible, while excitation of ethidium is quite good. Most of the emitted fluorescence will, therefore, be due to direct emission from the ethidium rather than to energy transfer from mithramycin, and the DNA selectivity gained with blue-violet excitation will be lost.

Interest in chromomycin and mithramycin DNA staining, with or without ethidium, may increase as violet diode lasers, emitting near 405 nm, find their way into more commercial flow cytometers (see Chapter 8); excitation of these dyes at 405 nm is about 80% of maximum.

The Hoechst Dyes (33258, 33342, 34580?)

A series of highly DNA-selective, UV-excited, blue fluorescent bisbenzimidazole dyes, originally synthesized by Loewe[234] for Hoechst as antiprotozoal drugs, and designated as **Hoechst 33258, 33342, 33378**, and **33662**, were introduced to the flow cytometry community in 1974 by Latt[235,8], although they were not widely applied until somewhat later.

Detecting BrUdR by Hoechst Dye Quenching

The original motivation for studies of the Hoechst dyes lay in the fact that complexes of the dyes with DNA containing **bromodeoxyuridine** (variously abbreviated as BrdUrd, BUdr, BrUdR, etc.) were quenched, i.e., less fluorescent than complexes of the dyes with unsubstituted DNA. The fluorescence difference was sufficient to allow detection of **DNA synthesis** and of sister chromatid exchanges in cells incubated with BrUdR. Flow cytometric methods were subsequently developed that allow detection of BrUdR incorporation by Hoechst dye fluorescence quenching without the use of anti-BrUdR antibodies; these will be discussed further in the section on DNA synthesis.

Hoechst Dyes Have an A-T Base Preference

The Hoechst dyes act as DNA-selective fluorochromes, binding to sequences of three A-T base pairs in DNA[26,8]; this strong **A-T base preference** accounts for the popularity of Hoechst 33258 in combination with chromomycin A_3 for staining chromosomes and bacteria, which will be discussed further in the section on DNA base composition. The Hoechst dyes bind in the minor groove of the DNA helix rather than by intercalation. Their affinity for DNA is sufficiently strong that they will displace bound molecules of a variety of intercalating dyes[26,12].

Hoechst 33342 as a Vital DNA Stain

Additional interest in Hoechst 33342 was aroused when Arndt-Jovin and Jovin showed in 1977 that at least some living cells could be stained with this dye, sorted on the basis of DNA content, and subsequently grown in culture[239]. At the time, this finding represented a source of frustration to most of the (lucky few) investigators who had cell sorters, since the argon lasers supplied with most sorters could not emit the UV lines necessary to excite the Hoechst dyes.

Fluorescence histograms in early publications on **vital staining with Hoechst 33342**[239-42] showed broad peaks (CV of 6% or more), which were commonly attributed to cell-to-cell differences in dye uptake. Conventional wisdom held that it was necessary to use at least 100 mW of laser power in the UV to excite Hoechst 33342 to produce acceptable histograms. It is now almost certain that the poor precision of the measurements was due to a combination of noise in the light sources and uneven illumination resulting from the laser beam being focused to too small a spot in the apparatus used by earlier authors. It now seems clear that, at UV power levels of 100 mW or more, dye saturation occurs, eliminating the effects of uneven illumination and reducing CVs.

In 1981, I reported that low-power UV excitation from a mercury arc or 10 mW from an argon or krypton laser could be used, with appropriate optics, to produce Hoechst 33342 fluorescence histograms with low CVs from vitally stained cells[1,5]. I and others[643] have since observed that 1-10 mW at 325 nm from a He-Cd laser provides more than adequate excitation for cells stained with Hoechst dyes in a flow cytometer with a properly designed optical system. In fact, the precision of DNA measurements I have made using air-cooled He-Cd lasers has been better than the precision of measurements I made using large, water-cooled argon and krypton lasers from several manufacturers.

While there are a few reports in the literature[243-6] that suggested that other dyes could be used for flow cytometric determination of DNA content in living cells, Hoechst 33342 is the only compound that has been extensively used for the purpose. It is clear that some cells can survive and have survived staining with the dye, passage through a UV laser beam, sorting, and washing with retention of reproductive integrity, and that other cells, under similar conditions, have failed to survive[239,42,247-55]. Exposure to high laser power levels (over 100 mW) appears to decrease survival[256]. It seems likely that the different toxicity of the dye to different cell types is related to differences in uptake and/or retention.

Hoechst Dyes In – And Out Of – Living Cells: The Drug Efflux Pump Discovered

Stoichiometric vital staining of DNA by Hoechst 33342 generally requires exposure of cells to 5-10 μM dye for at least 30 min. Lower concentrations (1-2 μM) and/or shorter incubation periods can be used to demonstrate differences between cell types in rates of dye uptake and/or efflux. This technique was originally used by Lalande and Miller[248-9], and was later adopted by Loken[241,250] and by me and my coworkers[257] to differentiate resting T lymphocytes (low uptake) from resting B cells and activated T cells (high uptake). Staining differences among lymphoid cell populations are more pronounced in the mouse than in the rat or man (makes you wonder, doesn't it).

The demonstration in 1981 by Lalande, Ling, and Miller[253] that the staining intensity of living cells exposed to Hoechst 33342 is determined by the operation of an **efflux pump** brought flow cytometry to bear on what has since become an active and important area of application, i.e., the study of drug transport and distribution in cells and of transport-related mechanisms of drug resistance. Work along these lines has also provided valuable new insights into the nature of vital staining.

Krishan[729] was one of the first to investigate mechanisms of Hoechst 33342 uptake and retention. He found that some live cells, e.g., cultured leukemic cells resistant to adriamycin, stained poorly, if at all, with Hoechst 33342 because the operation of the energy dependent pump produced rapid efflux of the dye; isolated nuclei from these cells, as expected, stained normally. When the pump was blocked by phenothiazines (e.g., 15 μM trifluoperazine added to mouse splenocytes incubated with 10 μM Hoechst 33342 for 60 min at 37 C) or Ca^{++} channel blockers (e.g., verapamil), Hoechst 33342 produced stoichiometric staining of live cells.

Baines and Visser[2613] reported in 1983 that, when mouse bone marrow was vitally stained with Hoechst 33342 and sorted on the basis of fluorescence intensity, stem cells were found in the lowest-fluorescence fraction. Others[1568,2614-5] have since noted that both Hoechst 33342 and rhodamine 123 fluorescence are low in primitive hematopoietic stem cells. Goodell et al have defined a **side population (SP)** of cells, in which primitive stem cells are found, on the basis of relatively low UV-excited blue and red fluorescence after Hoechst 33342 staining[2616]. The low Hoechst 33342 and rhodamine 123 fluorescence in stem cells result from the activity of one or more efflux pumps; the effects of pumps on staining with Hoechst dyes will be considered further in the discussions on membrane permeability and drug resistance and on stem cells in this chapter and in Chapter 10.

Hoechst Dye Staining Mechanisms

When the Hoechst dyes are used to stain fixed or permeabilized cells for DNA content analysis (see Taylor[226] for one such staining protocol), lower dye concentrations (3 μM or less) than are used for vital stoichiometric staining are mandatory to avoid **nonspecific fluorescence**.

Additional insight into the binding and staining mechanisms of the Hoechst dyes came following the report of Watson et al[730] that the ratios of Hoechst 33342 fluorescences in the 515-560 nm (green) and 390-440 nm (violet) bands were different for different subclasses of chicken thymocytes vitally stained with 5 μM dye. The green fluorescence in one cell type increased over a 2 hour incubation

period; a second cell type reached an equilibrium fluorescence intensity in a few minutes.

Steen and Stokke[731], using an arc source flow cytometer with a grating monochromator fitted to the detector, measured emission spectra of fixed rat thymocytes stained with varying concentrations of Hoechst 33258, and found the emission shifted toward the green at increasing dye concentrations. Stokke and Steen[732] characterized two binding modes of the dye; at low dye/phosphate ratios, high-affinity binding with high quantum yield blue fluorescence is predominant; as dye concentration increases, there is lower affinity binding to secondary sites, with quenching, emission shifting toward the green, and DNA precipitation. Changes in Hoechst dye emission may help probe nuclear **chromatin structure** in different cell types, provided that differences in uptake and/or efflux patterns can be controlled.

Ellwart and Dormer[1310] exploited the spectral shift of Hoechst 33342 as a measure of **cell viability**, or membrane integrity. Live cells exposed to relatively low dye concentrations in the presence of propidium exclude propidium, but retain small amounts of the Hoechst dye, and shorter wavelength emission predominates. Cells that have completely lost membrane integrity take up propidium. Cells in transition exclude propidium, but accumulate higher concentrations of Hoechst 33342, and fluorescence emission shifts to longer wavelengths.

Stokke et al[1311] found that the fluorescence of Hoechst 33258 in fixed erythroid precursor cells was less than that in myeloid cells in the same sample; the fluorescence of the dye in nuclei from erythroid cells was the same as that in myeloid cells. This effect may be due to quenching and/or reabsorption of fluorescence by hemoglobin in the erythroid cells; it is not observed with dyes such as mithramycin.

Vinogradov and Rosanov[1312] have synthesized analogs of the Hoechst dyes lacking the piperazine ring found in the compounds made by Loewe; their DNA-binding selectivity and A-T preference reportedly exceed those of Hoechst 33258.

Hoechst 34580: Violet Time?

As you will find on perusal of Chapter 8, violet diode lasers are rapidly finding their way into commercial flow cytometers. While we normally think of the Hoechst dyes (and DAPI, discussed next) as "UV-excited," these dyes have some excitation cross section left (12% of maximum excitation for DAPI, 3% for Hoechst 33342) even at the 405 nm nominal emission wavelength of violet diodes[2444]. When the Hoechst dyes or DAPI are used to stain mammalian cell nuclei, one can usually expect to find millions of dye molecules in a cell. Under these circumstances, the variances of fluorescence distributions are not greatly broadened by photoelectron statistics when efficient collection optics and PMTs are used, even when only a few mW of excitation power at 405 nm are available.

Hoechst 34580 becomes interesting in this context because, when bound to DNA this dye exhibits an excitation maximum near 380 nm, about 30 nm longer than the absorption maxima of the other Hoechst dyes and 20 nm longer than that of DAPI. Its excitation is 15% of maximum at 405 nm, and 50% of maximum at 395 nm, a wavelength now available from selected violet diodes. With Nancy Perlmutter, I found that Hoechst 34580 was permeant, yielding a DNA histogram with a CV less than 5% from intact Jurkat cells excited by a 4 mW, 397 nm diode laser[2444]. However, the dye appeared to be unstable in solution; we were unable to obtain good histograms from either intact cells or isolated nuclei from day-old solutions. The dye is now available from Molecular Probes, and probably worth some further investigation; I'll get to it when I finish writing.

DAPI (and DIPI): Dyes Known for Precision

A highly DNA-selective, impermeant dye with properties similar to those of the Hoechst dyes, **4'-6-diamidino-2-phenylindole**, or **DAPI**, was introduced for flow cytometry of DNA content by Stöhr et al[258]. The dye had been previously used for visualization of virus and *Mycoplasma* infection of cultured cells[259]; its high DNA specificity and intense fluorescence have allowed visualization of single DAPI-stained virus particles under the fluorescence microscope[260]. Taylor[226] and others[261] have described nuclear isolation protocols for use with DAPI staining.

DAPI, like the Hoechst dyes, has a strong **A-T base preference**. Many people, myself included, believe that DAPI yields DNA histograms with CVs lower than are obtained using other dyes (I have noted some dramatic differences when analyzing cells removed from paraffin-embedded material). While well-controlled studies on whole cells or nuclei seem to be lacking, Otto and Tsou[733] did compare DAPI, the related compound DIPI, and Hoechst 33258 and 33342 as stains for flow karyotyping of chromosomes from CHO cells, using an ICP with arc lamp UV excitation at 366 nm. They found 5 μM to be the optimal concentration of DAPI for staining chromosomes. DIPI staining was very slightly brighter (103%) than DAPI; the Hoechst dyes were only 86% as bright. However, DAPI produced histograms with the lowest CVs (2.2% vs. 2.7% for DIPI, 2.8% for Hoechst 33258, 2.9% for Hoechst 33342).

Figure 7-11, on the facing page, illustrates the most dramatic example of high-precision DNA analysis of which I am aware. Lewalski, Otto, Kranert, and Wassmuth[1313], using a Partec PAS-II flow cytometer, analyzed enzymatically decondensed, DAPI-stained spermatozoa to confirm the suspected production of unbalanced spermatozoa in heterozygous rams carrying a 1; 20 chromosomal translocation. In the top panel, X- and Y-chromosome-bearing spermatozoa from a cytogenetically normal ram appear as two distinct peaks; the difference in DNA fluorescence intensity between the gonosomes averaged 4.8%. In the bottom panel, sperm samples from a heterozygous 1; 20 translocation carrier yield a histograms with five major and two minor (arrows) peaks, attributed to spermatozoa with a normal, balanced, and unbalanced chromosomal status, with CVs of 0.5-0.6%. Be-

cause the translocated chromosomal segment represents 2.4% of the total DNA content, as determined from the flow cytometric data, histograms with five instead of the expected six peaks are observed.

Darzynkiewicz and his colleagues[738,9] have found that staining with DAPI is less affected by the state of chromatin condensation than is staining with other DNA stains; this most probably accounts for the lower CVs generally observed with the dye.

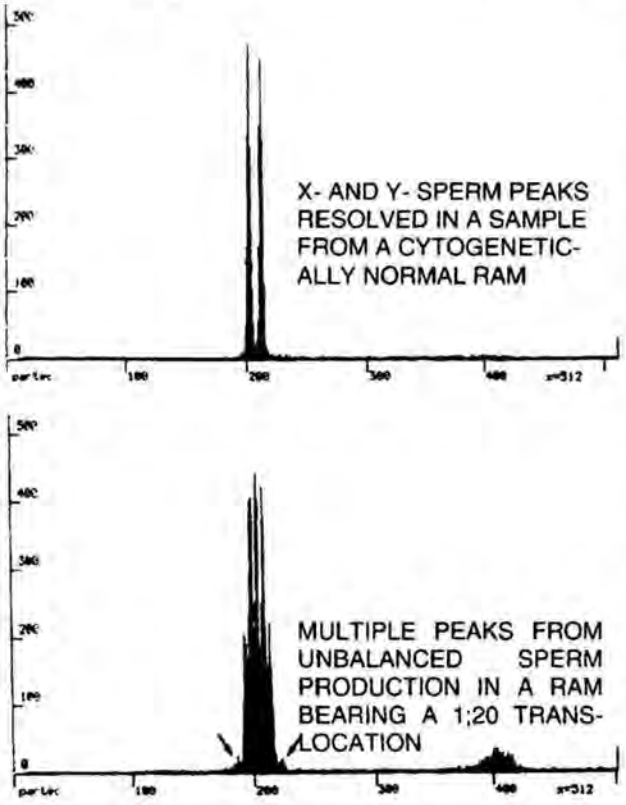


Figure 7-11. DNA content distributions in sperm from a normal ram and a ram bearing a 1;20 chromosomal translocation, stained with DAPI and analyzed on a Partec arc source flow cytometer; peak CV's are 0.5-0.8%. From H. Lewalski et al, Cytogenetics and Cell Genetics 64:286, 1993[313]. The figure was kindly provided by Dr. Lewalski and is reprinted with the permission of S. Karger, publishers.

Determinants of High Precision in DNA Analysis

Because DNA content is so well regulated in most cells, measurements of DNA content are more likely than measurements of any other cellular parameter to result in fluorescence distributions with extremely low CVs. Even at that, the distributions shown in Figure 7-11 are remarkable. The level of precision represented in them is not readily achievable in laser source flow cytometers, for several reasons. Most benchtop laser source instruments use air-cooled argon ion lasers emitting 15-25 mW at 488 nm as light sources; the RMS optical noise level of such lasers is usually specified as 1%, and, since the power output is not sufficient to saturate the dyes used for DNA measurement, the CV of a fluorescence distribution obtained with such an instrument cannot be less than the RMS noise level of the source.

If the laser power were increased to the level needed for photon saturation, and/or the light source noise were reduced to a small fraction of its normal value, there might still be problems associated with the nature of the dyes available for DNA content analysis using 488 nm excitation. Propidium is the most common of these; it is not highly DNA-selective, and the RNAse treatment customarily used to minimize contributions to the fluorescence signal from dye bound to double-stranded RNA may not completely eliminate interfering fluorescence. We can therefore attribute some of the high precision achieved in DNA content measurement with DAPI, and, to a slightly lesser extent, with the Hoechst dyes, to the relatively high DNA-selectivity of the dyes, and to their relative insensitivity (notably that of DAPI) to the differences in chromatin condensation. However, that still isn't the whole story.

I should not need to mention that fluorescence CVs in the range of 1% are unlikely to be achieved in any flow cytometer in which the optics are even slightly misaligned, or in which there are any significant sources of turbulence in the fluidics. For purposes of the present discussion, however, we can assume that the optics and fluidics of whatever cytometer we use can be put into optimal operating condition.

At the end of the day, it is the optical design of the instrument, more than anything else, which makes it possible to achieve extremely low CVs in fluorescence measurement. Most instruments that can do it use arc lamp sources, and have relatively high-N.A. illumination optics, as well as relatively high-N.A. collection optics. As I mentioned on the previous page, photoelectron statistics are not a significant problem in measurements of the DNA content of eukaryotic cells; the relatively low UV power output of the arc lamp is more than adequate for excitation of DAPI or the Hoechst dyes. The high-N.A. (epi)illumination insures that excitation light reaches the cell from a substantially wider range of angles than would be the case in a typical laser source system. This minimizes effects of cellular asymmetry and orientation on illumination and light collection, resulting in lower fluorescence CVs[96]. We will revisit this issue in the discussion of sperm sorting in Chapter 10.

7-Aminoactinomycin D (7-AAD)

7-AAD, a fluorescent analog of the antitumor antibiotic actinomycin D, was synthesized for possible application to chromosome banding by Modest and Sen Gupta[1314], and was investigated as a cytometric DNA stain by Gill et al[1315] and, more recently, by Zelenin et al[739]. The complex of this dye with DNA has an absorption maximum at about 550 nm and an emission maximum at about 660 nm. 7-AAD is impermeant and highly DNA-selective, exhibiting a G-C base preference.

The quantum efficiency of 7-AAD is low, as was interest in the dye until Rabinovitch et al[736] demonstrated that, because of its long emission wavelength, the dye could be used in combination with fluorescein- and phycoerythrin-labeled antibodies for simultaneous flow cytometry of DNA content and two-color immunofluorescence using only a single 488 nm excitation beam. The DNA content distributions obtained using 7-AAD in this way have been disappointingly broad[736], probably because binding of the rather large dye molecule to DNA is affected by chromatin structure to a greater extent than is the case with other DNA stains. Stokke and Steen[740] utilized this property of 7-AAD for discrimination of different leukocyte types based on differences in chromatin structure.

Schmid et al[1316] have used 7-AAD to discriminate dead cells, i.e., cells that have lost membrane integrity, in unfixed samples stained with fluorescein- and phycoerythrin-labeled antibodies. Unlike propidium, which has also been used, 7-AAD emission is at a sufficiently long wavelength to minimize interference with phycoerythrin fluorescence. Schmid, Uittenbogaart, and Giorgi[1317] have also reported that 7-AAD uptake into cells can be used to demonstrate apoptosis in thymocytes also stained with fluorescein- and phycoerythrin-labeled antibodies.

Acridine Orange

Under carefully controlled conditions, the blue-excited green fluorescence of **acridine orange (AO)** molecules intercalated into DNA can be used to provide accurate and precise estimates of cellular DNA content. The techniques described by Darzynkiewicz and his coworkers[262-3], which were mentioned on pp. 44 and 96-7, and will be discussed more fully in the sections on probes of chromatin structure and RNA content, involve detergent treatment to permeabilize cells, acid denaturation to convert RNA to the single-stranded configuration, which forms a red (metachromatic) fluorescent complex with the dye, and careful adjustment of cell and dye concentrations to prevent formation of metachromatic fluorescent dye aggregates in association with DNA.

Many people who have tried to use acridine orange have been frustrated by the sensitivity of staining to very slight changes in operational parameters of the flow cytometer. A paper by Pennings et al[734] showed that DNA/RNA staining with acridine orange could be improved by using a roller pump and manifold to introduce dye and cells continuously into the flow cytometer sample stream, which stabilized the equilibria between free dye, dye intercalated into DNA, and dye complexed with RNA.

Styryl Dyes; LDS-751

Compounds containing a quinolinium, benzothiazole, or other heterocyclic ring system, linked to a substituted aminostyryl group, have been known as fluorescent nuclear stains since 1932, when von Jancso[1318] described staining of intraerythrocytic parasites by styrylquinolin. Perhaps because this brief paper is not widely known, Wang and Jolley[1319], then at Abbott Laboratories, received a patent on staining with styryl dyes in 1985.

In 1988, Terstappen and Loken and their colleagues[1320-1] described cell staining by the laser dye **LDS-751**, which predominantly stains DNA, can be excited effectively at 488 nm, and emits above 640 nm. LDS-751 enters intact cells, but stains cells with damaged membranes more intensely, and can therefore be used to discriminate these two classes of cells, even in fixed samples[1320]. It can also be used in combination with another nucleic acid stain and fluorescent antibodies to perform extended leukocyte differentials, platelet, and reticulocyte counts on unlysed, unfixed whole blood[1321]. LDS-751 was said to be the same dye as the laser dye Styryl-8; this is apparently not the case, at least for the LDS-751 sold by Molecular Probes.[2532].

I have had good luck staining mammalian cell nuclei with LDS-751, but have not succeeded in getting it to stain bacteria, which I find somewhat surprising. I also note a recent report by Snyder and Small[2517], to the effect that cultured murine fibroblasts and monocytes stained with two different samples of Molecular Probes' LDS-751 and examined by confocal microscopy showed membrane potential-dependent mitochondrial staining but no nuclear staining.

Latt et al[470] described fluorescent staining of DNA by three compounds supplied by Eastman Kodak, designated EK4, LL585, and VL772. VL772 forms fluorescent complexes with both DNA and RNA; the DNA complex has an absorption maximum at 510 nm and an emission maximum at about 565 nm. LL585 was said to be DNA-specific; the complex of this dye with DNA has an absorption maximum at 569 nm and an emission maximum at about 600 nm. Both VL772 and LL585 showed a strong A-T preference. I have looked at these dyes; I found that both VL772 and LL585 formed fluorescent complexes with RNA. Also, the dyes are lipophilic; LL585, in particular, stains mitochondria in intact cells. I didn't get very good DNA histograms even when I stained isolated nuclei, and the background fluorescence was too high to do good measurements of bacteria (and, I would presume, of chromosomes). LL585 is a styryl dye; EK4 and VL772 are cyanines.

Cyanine Dyes I: Thiazole Orange, etc.

Cyanine dyes[460-1], many of which were developed by Eastman Kodak as sensitizers for photographic film, are compounds in which two heterocycles (benzoxazoles, benzothiazoles, etc.) are joined by a conjugated polymethine chain. **Symmetric** cyanine dyes, in which the heterocycles are identical in structure and orientation, are well known as probes of **membrane potential**[460]. Cyanines have, however, been known for some time to act as nuclear stains, a property noted in the parent compound, **cyanine** (1,1′di-*iso*-amyl-4,4′-quinocyanine iodide) in the late 1800's. **Dicyanine A** (diethyl-2,4′-quinocarbocyanine iodide), an **asymmetric** cyanine, was described as an RNA stain in Kodak literature in the mid-1970's. Fluorescent nuclear staining by

diethyloxacyanine, used as an optical brightener for textiles, was illustrated by Paton and Jones[1322] in 1976, and Jacobberger, Horan, and Hare described fluorescent staining of DNA in intraerythrocytic malaria parasites and RNA in blood reticulocytes by **dimethyloxacarbocyanine** (**DiOC$_1$(3)** in the notation of Sims et al[460]; see Figure 7-12 below) in 1983[290] and 1984[768], respectively.

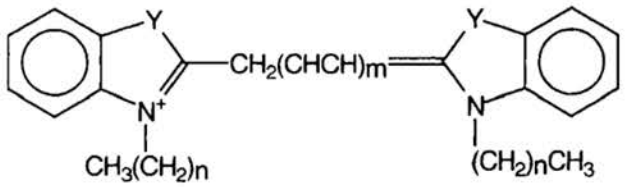


Figure 7-12. Structure of symmetric cyanine dyes given the formula "DiYC$_{n,l}$(2m + l)" by Sims et al[460]. When Y is O or S, the substituent is oxygen or sulfur. When Y is I, the substituent is C(CH$_3$)$_2$. When Y is L or Q, the rings are isoquinolines joined at the 2 or 4 positions, respectively.

In 1983, Sage, O'Connell, and Mercolino[288], then at B-D, developed a reticulocyte analysis technique using **thioflavin T**, a basic thiazole dye mentioned as an RNA stain by Arndt-Jovin[289]. Thioflavin T is a true RNA (and DNA) fluorochrome, increasing its quantum efficiency many times when bound to nucleic acid. The excitation maximum for the dye is at approximately 440 nm, making it usable with an Hg arc lamp source emitting at 436 nm, such as was used in B-D's FACS Analyzer. Thioflavin T can also be excited by He-Cd (441 nm) or argon laser (457, but not 488 nm) sources. Emission is at 490-500 nm.

After B-D introduced the FACScan, a clinically oriented flow cytometer with an excitation wavelength fixed at 488 nm, it became desirable to find a dye with the characteristics of thioflavin T that could be used with that excitation wavelength. Lee, Chien, and Chiu[769,1323] took a frontal approach to this problem, studied the relationship between chemical structure and RNA fluorochrome activity in cyanine dyes, thioflavin, and ethidium, and, in 1987, described **thiazole orange (TO)**, which, chemically, is 1,3′-dimethyl-4,2′-quinothiacyanine, as most suited for reticulocyte analysis. Thiazole orange, when bound to RNA, has an absorption maximum at 509 nm and an emission maximum at 533 nm, and its fluorescence quantum efficiency is increased approximately 3,000 times over that of the free dye. Like thioflavin T, thiazole orange also behaves as a DNA fluorochrome; it and related dyes are useful for reticulocyte counting only because reticulocytes normally contain no DNA. Van Bockstaele and Peetermans[1324] noted in 1989 that 1,3′-diethyl-4,2′-quinothiacyanine iodide, a dye that had been widely available for many years, could be substituted for thiazole orange, which was difficult to get in at least some markets due to patent issues.

Lee and her coworkers at B-D also synthesized 1,3′-dimethyl-4,2′-quinothiacarbocyanine, which they named **thiazole blue**; this dye also behaves as a DNA and RNA fluorochrome and, when bound to nucleic acid, has an excitation maximum at about 640 nm, making it useful with red He-Ne or diode laser sources. As is the case with thiazole orange, the diethyl analog of thiazole blue has been commercially available for some time.

The ring structure of thiazole orange is the same as that of TO-PRO-1 (Figure 7-10, p. 301); the ring structure of thiazole blue has a trimethine bridge instead of a monomethine bridge between the heterocycles, and both thiazole orange and thiazole blue have methyl groups on both ring nitrogens (Molecular Probes' TO-PRO-3 shares the thiazole blue ring structure but has an n-propyltrialkylammonium side chain on the quinoline ring nitrogen, as does TO-PRO-1). Since thiazole orange and thiazole blue cyanine dyes are lipophilic and bear only a single delocalized positive charge; they are permeant (the TO-PRO dyes are impermeant), and are concentrated inside cells (and intracellular organelles) by any inside-negative potential difference across the cytoplasmic and/or organellar membrane. The dyes normally reach even higher concentrations in mitochondria than in the cytosol. Although mitochondrial staining by other cyanine dyes is pronounced, neither thiazole orange nor thiazole blue produces much mitochondrial staining.

This doesn't mean the dyes aren't concentrated in energized mitochondria in intact cells; they virtually have to be, according to chemical principles. However, the dyes aren't all that fluorescent in aqueous solution, and they aren't that much more fluorescent in nonpolar solvents such as butanol. Their fluorescence is enhanced dramatically by intercalation into double-stranded nucleic acid, be it DNA or RNA, and also, somewhat surprisingly, by binding to single stranded nucleic acid.

Symmetric cyanine dyes, such as DiOC$_1$(3), are fluorescent in aqueous solution; their fluorescence is enhanced, typically two- to sixfold, in nonpolar solvents, and enhanced by approximately the same factor when they bind to nucleic acids. The fluorescence both of symmetric dyes and of asymmetric dyes such as thiazole orange and thiazole blue requires that all the ring structures in the dye molecule remain in the same plane, and that the probability of loss of excitation energy due to transfer to other molecules in the environment remain low.

The great degree of fluorescence enhancement noted when thiazole orange or thiazole blue bind to nucleic acid should not be taken as an indication that these dyes have higher quantum efficiencies than the symmetric cyanine dyes; what it does indicate is that thiazole orange and thiazole blue, when not bound to nucleic acid, have very low quantum efficiencies. This is probably so because there is some freedom for one of the rings in the unbound dye to rotate relative to the other; when the rings are not in the same plane, no fluorescence can occur. There may also be more nonradiative loss of excitation from unbound mole-

cules to solvent and other molecules in the environment than there is when the dyes are intercalated into double-stranded nucleic acid.

The high quantum efficiency of bound dye makes thiazole orange and its relatives very difficult dye to use in microscopy; as was discussed on pp. 115-8, high quantum efficiency makes for rapid bleaching. It is relatively hard to do a reticulocyte count with a flow cytometer using acridine orange as the RNA stain, because the RNA-bound dye is quenched and background fluorescence is high. When you look under the microscope, however, the fluorescence of background dye bleaches out quickly and that of the quenched dye-RNA complexes persists, facilitating counting. When you look at thiazole orange-stained cells under a fluorescence microscope, there is very little fluorescence background, but the fluorescence from RNA-bound dye disappears before you have a chance to count the cells. In a flow cytometer, the cell doesn't get a chance to get bleached until it goes through the beam, at which time the detector can capture as much fluorescence as is emitted; thiazole orange works fine. It and its relatives also work fine in other instruments, for example, high-resolution gel scanners for detecting small amounts of DNA following electrophoresis[1325-6].

Cyanine Dyes II: TOTO and YOYO à GoGo

The gel scanning project undertaken by Glazer, Peck, and Mathies[1327] in the 1980's had two goals; the first was optimizing methods for detection of very small amounts of DNA on gels, and the second was developing dyes that could bind so strongly to DNA that dye-labeled fragments could be removed from gels and mixed with unlabeled nucleic acids without dye migrating from the labeled to the unlabeled molecules. The strategy adopted in pursuit of the second goal was the synthesis of homodimeric dyes, the first of which was **ethidium homodimer**. When DNA-ethidium homodimer complex is mixed with a 50-fold excess of unlabeled DNA, about 30% of the dye is retained within the original complex indefinitely.

The quantum efficiency of ethidium increases only 20- to 30-fold on binding to double-stranded nucleic acid; that of thiazole orange, as previously mentioned, increases 3,000-fold. The difference, as just discussed, lies in the lower quantum efficiency of unbound thiazole orange; the use of thiazole orange or a dye with similar fluorescence properties for staining DNA or RNA on gels should, therefore, result in lowered background fluorescence compared to ethidium homodimer.

In order to achieve the high binding affinity of ethidium homodimer and the fluorescence properties of thiazole orange, Rye et al[1328] synthesized compounds named **TOTO-1** and **YOYO-1**, in which two molecules of thiazole orange (TO), in the first case, and oxazole yellow (YO), its quinooxacyanine analog, in the second, were joined by a diazaundecamethylene linker. The binding affinity of these dyes for DNA is sufficiently high so that fragments labeled with TOTO-1 or YOYO-1 and with ethidium can be mixed and separated by electrophoresis. TOTO-1 has the spectral characteristics of thiazole orange; YOYO-1 has those of oxazole yellow (excitation maximum for nucleic acid-bound dye 489 nm; emission maximum 509 nm), and both are over 1,000 times more fluorescent in the nucleic acid-bound than in the free form. As little as 4 picograms of DNA-bound dye can be detected on a gel by the confocal scanner. **TOTO-3**, which combines two thiazole blue chromophores using the same linker as is used in TOTO-1 and YOYO-1, is red-excited. All three dyes and some related dimers are available from Molecular Probes.

Benson, Singh, and Glazer[1328] also synthesized **heterodimeric** DNA-binding dyes designed for energy transfer, including **TOTAB**, a thiazole orange-thiazole blue heterodimer for which the emission maximum of the DNA-bound dye lies at 662 nm. Fluorescence at this wavelength is enhanced 100-fold on binding to double-stranded DNA, while fluorescence of the thiazole orange donor chromophore at 532 nm is quenched by over 90%. The heterodimeric dyes, like the homodimers, are suitable for high-sensitivity detection of nucleic acids on gels[1329]. TOTAB, which, at this writing, is not yet commercially available, could be used for determination of DNA content using 488 nm excitation in cells also stained with fluorescein- and PE-labeled antibodies and, perhaps, PE-Texas Red tandem-labeled antibodies as well. There would, however, also be a catch.

Cyanine Dyes III: Alphabet Soup

Staining fixed cells or permanent cell nuclei for DNA content analysis tends to be a relatively casual procedure; we more or less just throw the dye in and go, without bothering to think that it may take more than a few seconds for dye and cells to come to equilibrium. When van den Engh, Trask, and Gray[1330] actually checked on this point, they found that mouse thymocyte nuclei permeabilized with Triton X-100 and stained with dyes at concentrations normally used for flow cytometry required about 5 min to come to equilibrium with Hoechst 33258, 20 min to equilibrate with propidium, and over an hour to reach equilibrium with chromomycin A_3. These dyes bounce on and off the DNA fairly readily, compared to the dimers just discussed, which stick like glue, and which therefore should take a longer time to equilibrate. I've tried staining permeabilized, RNAse-treated nuclei with TOTO-1 and YOYO-1 (the RNAse is essential because the dyes are not DNA-specific), and found that the DNA histogram peak positions and CVs did not stabilize even after several hours' incubation with the dyes; the monomeric dyes reach equilibrium much faster.

Hirons, Fawcett, and Crissman[1331] described use of TOTO-1 and YOYO-1 for flow cytometric DNA analysis, precipitating a brief stampede in that direction. In my view, however, it is important to separate the desirable spectral characteristics of the dyes from what are likely to be undesirable binding characteristics. Using thiazole orange or its cheaper diethyl analog instead of TOTO-1 to do DNA his-

tograms should, in principle, realize the same advantages while requiring less incubation time.

Richard Haugland, Victoria Singer, Stephen Yue, and others at Molecular Probes have developed additional monomeric and dimeric cyanine DNA and RNA stains with some interesting properties[2332,2618]. The TO-PRO® family of impermeant monomeric dyes contains BO-PRO-1 and -3, JO-PRO-1, LO-PRO-1, PO-PRO-1, and -3, TO-PRO-1, -3, and -5, and YO-PRO-1 and -3, with excitation maxima ranging from 435 to 745 nm and emission maxima ranging from 455 to 770 nm. All TO-PRO series dyes have two positive charges and one intercalating moiety. The TOTO family of impermeant dimeric dyes contains corresponding BOBO, JOJO, LOLO, POPO, TOTO, and YOYO dyes, except that there is no TOTO-5; all TOTO series dyes have four positive charges and are **bis-intercalators**; that is, each has two intercalating moieties, which bind between nearby base pairs of a double-stranded nucleic acid helix, while the linker interacts with the minor groove. The nature of the strong interactions of TO-PRO and TOTO dyes with single-stranded nucleic acids remains less clear.

Molecular Probes' SYTO series of dyes are cell permeant relatives of the TO-PRO dyes. Their permeancy indicates that, like their parent thiazole orange (the TO in TO-PRO, TOTO, and SYTO), they lack the quaternary ammonium groups present in TO-PRO and TOTO dyes. The fact that their structures have not been revealed, at least in the Molecular Probes *Handbook*[2332], suggests that the dyes have extra ring side chains that improve their permeancy, and that the company does not want to make it easy for other people to learn its tricks. Some of the structures may be found in Molecular Probes' patents. The SYTO- dyes stain both DNA and RNA; some of them also stain other cellular structures, e.g., mitochondria.

The SYTOX dyes, are really, really impermeant, suggesting that they bear at least three positive charges (structures have not been published); they are promoted as viability indicators, but SYTOX Orange was found to be an optimal stain for DNA fragment sizing in a slow flow instrument with a green YAG laser source built at Los Alamos[2333-4].

Then there are PicoGreen, designed for quantitative fluorescence assay of double-stranded DNA in solution, and SYBR Green I and II and SYBR Gold, designed for demonstration and quantification of nucleic acids on gels. PicoGreen is reasonably selective for double-stranded DNA, increasing its fluorescence over 1,000 times on binding, while exhibiting a much smaller degree of fluorescence enhancement on binding to double-stranded RNA or to single-stranded nucleic acid. PicoGreen and the SYBR dyes have been used for DNA fragment sizing at Los Alamos[2333] and for detection of viruses in conventional flow cytometers[2336-7].

Base Preference in Cyanine and Styryl Dyes

I have observed (unpublished) that the fluorescence of TOTO-1, YOYO-1, TOTO-3, related monomeric cyanine dyes, and LDS-751 in solutions of a deoxyadenosine/deoxythymidine polymer (polydA-dT) is severalfold higher than the fluorescence of the same dyes in solutions of a deoxyguanosine/deoxycytosine polymer (polydG-dC) at the same dye and polymer concentrations, suggesting that the dyes have an A-T preference. Excitation and emission maxima are slightly different for dye in polydA-dT and in polydG-dC. Stephen Yue of Molecular Probes (personal communication, 1994) has made similar observations. However, it has also been established (R. A. Keller, personal communication, 1994; A. N. Glazer, personal communication, 1994, and references 1144 and 1325-9) that the intensity of TOTO-1, YOYO-1, and TOTAB fluorescence is proportional to the mass of DNA to which the dye is bound, regardless of the base composition of the dye. In this context, at least, the dimeric dyes do not show a base preference; the lack of one is critical for use of dimeric dyes in quantitative analysis of DNA in flow systems, in solution, or on gels.

The issue of base preference of cyanine dyes is further clouded by evidence from my lab (unpublished results and reference 1133), Frey et al[1134], and Hirons, Fawcett and Crissman[1331] that TOTO-1 and YOYO-1, thiazole orange, and thiazole blue produce differential staining of chromosomes with similar DNA content, in much the same way as do dyes with strong base preferences such as Hoechst 33258 and chromomycin A_3. In fact, something approximating the bivariate flow karyotype obtained from chromosomes stained with Hoechst 33258 and chromomycin (see the section on DNA base composition) can be produced by dual beam (UV and visible) excitation of chromosomes stained with TOTO-1 alone[1331]. It would certainly be useful to have a greater variety of dyes available for bivariate chromosome analysis, particularly dyes that could be excited at 488 nm; it is likely, based on studies of the existing cyanine and styryl dyes, that such molecules could be engineered, but there doesn't seem to be enough of a market to get Molecular Probes or other companies to make the effort.

Seeing Red: LD700, Oxazine 750, Rhodamine 800, TO-PRO-3, and DRAQ5 as DNA Stains

In the mid-1980's, while examining a number of dyes suitable for excitation by red (633 nm) helium-neon lasers, Sandra Stephens and I ran across three that stained DNA stoichiometrically[737]. They are LD700, oxazine 750 (OX750), and rhodamine 800 (R800), all developed as laser dyes. The dye-DNA complexes of these three dyes have absorption maxima at 660, 690, and 705 nm and emission maxima at 670, 700, and 715 nm. OX750 appears not to have a base preference; LD700 and R800 have a G-C preference. OX750 and R800 are usable with cheap 670 nm diode lasers.

Red-excited DNA stains aren't all that useful unless you can stain cells simultaneously with them and something else; it would be nice to do DNA/immunofluorescence measurements in a system with a diode laser using R800 and allophycocyanin or Cy5. However, at the concentrations (~25 μM) at which OX750 and R800 have to be used to produce

good staining, they quench the fluorescence of allophycocyanin considerably.

Any of the TO-PRO or SYTOX dyes, and at least some of the SYTO and SYBR series and PicoGreen, should be usable for DNA content analysis in permeabilized or fixed cells treated with RNAse. It has been shown that TO-PRO-3 works well in this context when used with red excitation[2619]; this dye can also be used in combination with propidium in systems with only a single 488 nm laser, as energy transfer from propidium, which excites well at 488 nm, to TO-PRO-3, which does not, is fairly efficient[2620-1].

I mentioned **DRAQ5**[2338-9] on p. 44; this is a permeant anthraquinone dye which, when bound to DNA, has an excitation maximum near 650 nm and an emission maximum near 700 nm. DRAQ5 appears to be reasonably DNA-selective, and the combination of DNA selectivity and permeancy allows it to be used to produce reasonably good DNA content histograms when it is used as a vital stain, making it the only dye other than Hoechst 33342 usable for that purpose.

The fluorescence of DRAQ5 is not significantly increased when the dye is bound to DNA, and some manipulation of the relative concentrations of dye and cells may be necessary to obtain the best quality DNA content measurements. On the plus side, it is possible to excite the dye at 488 nm. DRAQ5 is available from **Biostatus, Limited.** This company also sells the somewhat less permeant DRAQ5NO[2622], also developed by Paul Smith's group, and said to be useful in discriminating cells in various stages of apoptosis, as APOPTRAK™.

Miscellaneous DNA-Selective Dyes

The diamidines **M&B 938**[2623] and **hydroxystilbamidine**[2332,2624] are structurally similar to DAPI; they are UV-excited, impermeant, and relatively highly DNA-selective, with an A-T base preference. M&B 938 was investigated as a drug by Rhône-Poulenc Rorer, now part of Aventis. Hydroxystilbamidine, now available from Molecular Probes, has been used as a viability indicator[2624]; since complexes of the dye with DNA exhibit an excitation maximum at 390 nm[2332], it should be better excited by violet diode lasers than DAPI or the Hoechst dyes.

3-amino-6-methoxy-9-(2-hydroxyethylamine) acridine (AMHA) is maximally excited at 375 and emits maximally at 510 nm; it is permeant and somewhat DNA-selective, probably with an A-T base preference. It is not commercially available

What Do DNA Stains Stain?

DNA content measurements demand high precision because DNA content is so nearly constant for substantial numbers of cells in a sample and because minute variations in DNA content may have considerable biologic significance.

All of the DNA stains just discussed can be used, on appropriately prepared samples and in properly aligned instruments, to give precise estimates of the total DNA content of cells that accurately reflect DNA content differences between different cells and cell types from the same organism, e.g., sperm cells, which are haploid, and somatic cells, which are predominantly diploid, or tumor cells and accompanying normal stromal cells, which may have different modal values of DNA content. This is really quite remarkable in light of the fact that different dyes bind in different fashions and, in some cases, to different chemical components of DNA molecules.

A little more care is required when attempts are made to determine the actual **mass of DNA**[1332,3], or **genome size**[1334-6], in cells from different species. Dyes with different base preferences will give different results in cells with different base compositions; in analyzing cells from 80 species of Tetrapoda, Vinogradov and Borkin[1335] found that ratios of DNA content values determined with different dyes were as high as 1.8 for this reason.

Darzynkiewicz and his colleagues[738-9] examined the accessibility to different dyes of DNA in nuclei under various conditions. During chemically induced differentiation of Friend erythroleukemia cells, and during spermatogenesis, chromatin condenses, and nuclear staining intensity with some DNA stains decreases; accessibility of DNA to different dyes is increased to different extents by acid extraction of nuclear histones. The increase in accessibility is lowest (45%) for DAPI, highest (1200%) for 7-AAD.

It seems logical that the dye least affected by chromatin structure, i.e., DAPI, would give the DNA histograms with the lowest CVs, since the effects of slight cell-to-cell differences in chromatin structure would be minimized, and DAPI indeed seems to produce the lowest CVs (Fig. 7-11, p 311). By contrast, it is hard to get even fair stoichiometric staining with 7-AAD, which has been shown to produce differential staining of different types of leukocytes based on chromatin structure differences[740].

If DAPI is the dye that gives best CVs, mithramycin may be the most DNA-selective dye; DAPI and the Hoechst dyes, while DNA-selective in mammalian cells, may stain other materials in plants and bacteria, often showing some spectral shift when they do.

Rundquist[1357] studied binding of DAPI and 7-AAD to fibroblast nuclei, and found that DAPI binding, but not 7-AAD binding, was increased following detergent treatment. 7-AAD binding was decreased by fixation with formaldehyde, but not with ethanol, following detergent extraction. Removal of basic protein with HCl resulted in an increase of about 100% in both DAPI and 7-AAD binding. Scatchard analysis suggested the existence of at least two classes of binding sites for both dyes; Bertuzzi et al[1358], analyzing propidium binding to fixed lymphocyte nuclei, also found evidence for two classes of binding sites with different affinities.

Beisker and Eisert[1359] used fluorescence depolarization of ethidium and propidium to study denaturation of DNA *in*

situ by acridine orange, which transfers energy nonradiatively to both of the former.

DNA Ploidy and Aneuploidy: The DNA Index

When DNA staining is stoichiometric, we tend to refer interchangeably to cells DNA content and **ploidy**, a practice that was discouraged by the Society for Analytical Cytology's Committee on Nomenclature[741]. It was recommended that measurements of DNA content in abnormal or putatively abnormal "test" cells be made in conjunction with measurements of DNA content in normal diploid "reference" cells from the same individual, and that differences in DNA content from normal be expressed in terms of the **DNA index**, which is the ratio of the mean or modal channel numbers of G_0/G_1 peaks in the distributions from the test and reference cells. The term **DNA aneuploidy** can be used to describe a sample containing a stem line with abnormal DNA content; **aneuploidy** without the qualifier is a term reserved for describing samples with abnormal karyotypes.

Comparisons between karyotype and DNA content as measured by flow cytometry have been done in human tumors and tumor-derived cell lines by Tribukait et al[742], Petersen and Friedrich[743], and Bigner et al[744]. In general, there is good agreement between measured DNA content and chromosome number; discrepancies tend to occur in cases with very high (hypertriploid or more) chromosome numbers, and these tend to have higher DNA content than would be expected from chromosome number. It has been suggested that some abnormal chromosomes may contain increased amounts of DNA.

Sample Preparation for DNA Content Analysis

The "garbage in, garbage out" aspect of flow cytometry affects DNA content measurements in several ways. One typically wants to measure nuclear DNA content in a good representative sample of a cell population. This is easiest when the cell population is a homogeneous line growing in suspension culture. Even when a minimal complicating factor, such as the cells growing attached to a dish, is thrown in, the potential for differential loss during preparation arises. When the sample is from real tissue, or a real tumor, it is necessary to make sure the cells, or nuclei, that are measured come from the part of the specimen that is of interest, and that the method used to prepare a single cell suspension does not selectively destroy some cell types[745]. Debris interferes with measurements; if a piece of tissue is minced too well, or if a paraffin block is cut too thin[746-7], the real cells may get lost in the debris.

It is customary, and acceptable, to use mathematical models[1307-9] to determine fractions of cells in different cell cycle phases and to reduce the contributions of clumps and debris to a DNA histogram (Figure 1-10, pp. 25-6); it is unacceptable, although far from unheard of, to use mathematical models to attempt to derive the fraction of cells in S phase from a histogram with barely recognizable peaks. We will get back to this issue when we talk about applications of DNA content analysis in Chapter 10.

DNA Base Composition

The base-paired structure of double-stranded DNA places constraints on the base composition of properly assembled molecules; the number of adenine residues must be the same as the number of thymine residues, and the number of guanine residues must be the same as the number of cytosine residues. The ratio of **A + T (adenine + thymine)** to **G + C (guanine + cytosine)** is not similarly constrained. In human cells, this ratio happens to be close to one; in bacteria, the G + C content of DNA varies from less than 25% to more than 85%[264]. Less dramatic variations in DNA base composition are observable in human chromosomes.

If a fluorescent dye binds with different affinities to A-T and to G-C pairs (or sequences) in DNA, dye molecules will be concentrated in regions of the DNA molecule containing the bases for which the dye has higher affinity. On the other hand, if binding to A-T and binding to G-C pairs or sequences have different effects on the fluorescence yield of a dye, even if the same amount of dye is bound to A-T and to G-C, there will be differences in the amounts of fluorescence emitted by A-T and G-C bound dye. Both of these mechanisms have been observed in the interactions of fluorescent dyes with DNA[230,265-8].

The first practical application of differential fluorescent staining of DNA came in the late 1960's with the development of **chromosome banding techniques** by Caspersson et al[269-72]. Before this, it was often impossible to obtain accurate karyotypes by visual observation; attempts at automation of karyotyping by analysis of microscope images had reached a dead end because size and shape were the only parameters that were measured. Using quinacrine and other dyes, it became possible to produce banding patterns along chromosomes that facilitated discrimination between chromosomes of similar sizes and shapes. Studies of the mechanisms involved in producing banding led to the development of improved staining techniques that have been applied to flow cytometry as well as to microscopy and image analysis of chromosomes.

Quinacrine binds with similar affinities to A-T and G-C; however, the fluorescence of DNA-quinacrine complexes increases with A + T content[265,273]. Hoechst 33258, which binds preferentially to A-T[268], does not produce a banding pattern when it is used as a single dye to stain chromosomes. However, when a G-C binding molecule such as actinomycin D, which can serve as an acceptor for nonradiative energy transfer, is added in combination with the Hoechst dye, a banding pattern similar to that obtained with quinacrine appears. The fluorescence of Hoechst dye bound to A-T in close proximity to actinomycin bound to G-C is quenched due to energy transfer; the fluorescence of Hoechst dye in regions containing relatively long sequences of A-T pairs is not quenched[274]. The fluorescence of DNA stains is also

affected by interactions between DNA and chromosomal proteins[2,5].

Since differential staining of chromosomes by combinations of fluorescent dyes typically involves energy transfer from molecules of one dye to molecules of the other, dyes that work well in combination almost always have excitation maxima in different spectral regions, because for energy transfer to occur, the absorption spectrum of the acceptor species must overlap the emission spectrum of the donor species. The difference in spectral characteristics makes it necessary to use a flow cytometer with two excitation beams at different wavelengths to fully characterize specimens stained with pairs of DNA fluorochromes.

The combination of Hoechst 33258 and chromomycin A_3, developed for chromosome analysis by the Livermore group[276], provides a good example of a dye pair. Separated UV (351/364 nm) and blue (458 nm) beams from argon lasers are used to excite the blue fluorescence of the A-T bound Hoechst dye and the yellow fluorescence of the G-C bound chromomycin. Figure 7-13 gives an example of the results obtained from dual laser flow cytometric analysis of chromosomes stained with the combination of dyes.

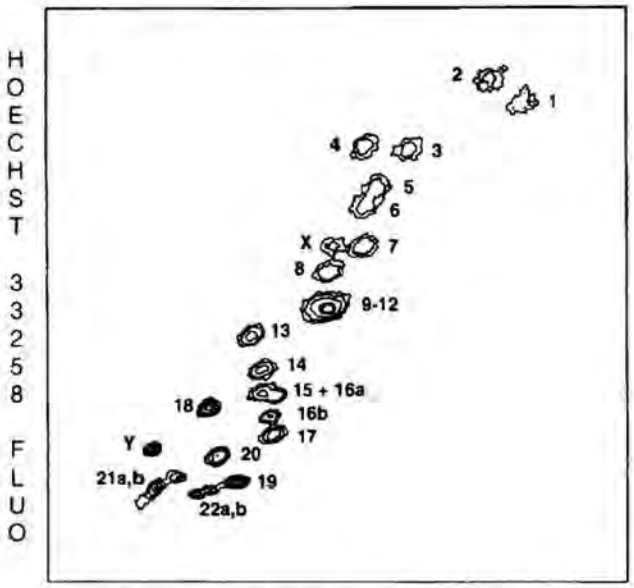


Figure 7-13. Flow karyotype of human chromosomes stained with Hoechst 33258 and chromomycin A_3. Provided by Ger van den Engh.

If the dyes had no base preference, the ratio of chromomycin fluorescence to Hoechst fluorescence would be the same for all chromosomes, and all of the data points would cluster along a straight line at 45° to the x and y axes, making it difficult to resolve chromosomes (e.g., 14-17) with similar DNA content. The differential staining gives greatly improved resolution in the two-dimensional space, because ratios of chromomycin fluorescence (G + C) to Hoechst fluorescence (A + T) do vary substantially among chromosomes of similar DNA content. This is true for humans; it is not for some other species.

Van Dilla et al[279] used the combination of Hoechst 33258 and chromomycin A_3 to differentiate bacterial species with different fractions of G + C; the principle is illustrated in Figure 7-14. The ratios of chromomycin fluorescence to Hoechst dye fluorescence for *Staphylococcus aureus*, *Escherichia coli*, and *Pseudomonas aeruginosa* reflect the marked differences in base composition (% G + C approximately 31, 50, and 67, respectively) among the three species. It is easy to separate the species, either by partitioning the two-dimensional space defined by the chromomycin and Hoechst dye fluorescence intensities, or by partitioning a histogram of fluorescence ratios.

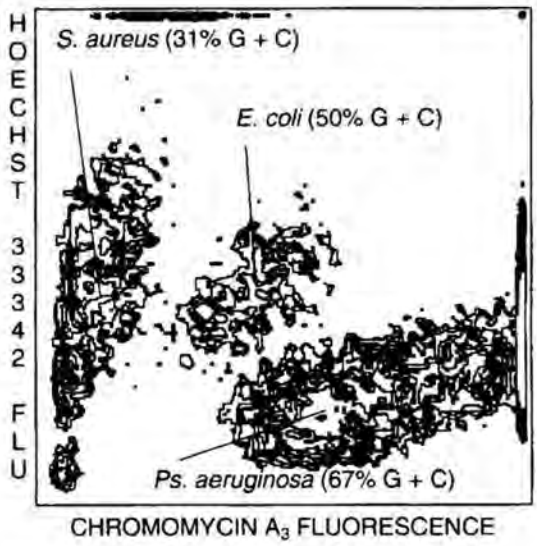


Figure 7-14. Hoechst/chromomycin fluorescence signatures of bacterial species with different DNA base compositions.

Sanders et al[340] found a linear relationship (r = 0.99) between the log of the ratio of chromomycin A3 to Hoechst 33258 fluorescence and the log of % G + C over the range of 28-67% G + C; two cell populations could be identified in mixtures of two species that differed in base composition by as little as 4% G + C. This is a good example of the utility of a ratio as a single parameter in cases in which there are large variances in the absolute intensities of the two signals from which the ratio is derived; note that the clusters are markedly elongated, indicating that the ratio of chromomycin fluorescence to Hoechst dye fluorescence remains nearly constant for each of the bacterial species. In another paper, Sanders et al[341] used changes in base composition to detect bacteriophage infection of *E. coli*.

It has been suggested that Hoechst/chromomycin staining could be useful in clinical laboratories for identification of bacteria in urine specimens. This might be so, provided the clinical instrument did not require the two 12-watt argon lasers used as light sources by van Dilla et al. In previous

editions, I suggested that 5-10 mW at 325 nm and 20-40 mW at 441 nm from air-cooled He-Cd lasers might be adequate, when used with efficient optics, for flow cytometry of bacteria and chromosomes. I have already mentioned (p. 142; references 1133-5 and 1242) that He-Cd lasers have been used for bivariate analysis of chromosomes stained with Hoechst dyes and chromomycin. As for bacteria, Figure 7-14 was obtained using an instrument with a single He-Cd laser emitting 325 and 441 nm beams. Although the simpler instrumentation makes flow cytometry of bacterial base composition easier to do, the time required for fixation and staining and the relative lack of specificity of base composition for identification of bacterial species remain major obstacles to clinical use of the procedure.

In the past, I have used DAPI, which is A-T specific, in combination with olivomycin, which is G-C specific, to stain ethanol-fixed bacteria, choosing this dye pair because the absorption maxima of DAPI and olivomycin are closer to the 325 and 441 nm excitation wavelengths available from He-Cd lasers than are the absorption maxima of Hoechst 33258 and chromomycin A_3, which were used by Van Dilla et al[279]. I have also used mithramycin in place of chromomycin. When stained with DAPI/olivomycin or DAPI/mithramycin, *S. aureus*, *E. coli*, and *Ps. aeruginosa* are well resolved in a dual-beam flow cytometer with He-Cd laser excitation; however, the Hoechst dyes appear to give somewhat better separation than DAPI. Differences in Hoechst dye and DAPI staining of chromosomes have also been noted; Bernheim and Miglierina[1342] find that chromosomes 1 and Y stain more brightly with DAPI than with Hoechst 33258, presumably on the basis of different heterochromatin content.

As I mentioned on p. 315, dyes such as TOTO-1, YOYO-1, thiazole orange, and styryl-8, all excitable at 488 nm, appear to exhibit some sensitivity to base composition when used to stain chromosomes[1153-4,1331]. Since flow cytometers with 488 nm sources outnumber those with UV sources, many more laboratories would be able to do bivariate chromosome analysis and sorting if dye combinations were found that could be excited by a single 488 nm beam. Further work on cyanine and styryl dyes may provide the right dyes, at least for chromosome analysis; since these dyes also stain RNA, and since it is relatively difficult to get rid of RNA in bacteria, it may be harder to find alternatives to DAPI or Hoechst dyes and the chromomycins for determination of bacterial base composition. Structure-activity studies to improve the DNA specificity of cyanine and styryl dyes might help here.

Chromatin Structure; Identifying Cells in Mitosis

Differences in the staining and structure of nuclear chromatin in different cell types from the same organism were described by microscopists during the 1800's, well before the nature and roles of nucleic acids and nucleoproteins were understood. Such differences in chromatin structure are routinely used by hematologists and pathologists as aids in the identification and characterization of normal and abnormal cells, and it seems obvious that objective, quantitative, reproducible flow cytometric measures of chromatin structure should provide information of equivalent value.

The general approach to flow cytometry of chromatin structure is antithetical to the approach used in DNA content analysis. For determination of cellular DNA content with maximum accuracy and precision, it is necessary for the DNA in all cells examined to be equally accessible to the fluorochrome used, a condition best achieved by removal of most of the histones and other proteins that might interfere with staining[738]. For analyses of chromatin structure, it is essential that the conformation of nuclear material either be maintained or be modified in a predictable way.

The most extensive work on flow cytometry of chromatin structure is without doubt that done by Darzynkiewicz and his colleagues[262,1343-4]. They have employed a technique of **partial denaturation of DNA by acid or heat** treatment to demonstrate differences between different cell types and between cells in different phases of the cell cycle. Fixed cells are treated with RNAse to remove RNA, leaving DNA as the only nucleic acid present. Cells are then subjected to conditions that partially denature DNA, e.g., exposure to pH 1.5 for 30 seconds, and are then stained with **acridine orange (AO)**. The denatured DNA assumes a single-stranded conformation, and forms a polymeric complex with AO, shifting the absorption maximum of the dye to shorter wavelengths and the emission maximum to longer wavelengths, i.e., from the green (530 nm) spectral region to the red (>600 nm). AO monomers bind by intercalation to the remaining native helical DNA, retaining their normal absorption and fluorescence characteristics. When the stained cells are measured in a flow cytometer with blue or blue-green excitation (e.g., at 488 nm), the green fluorescence (515-575 nm) provides an estimate of the amount of DNA remaining in the native configuration, while the red fluorescence (600-700 nm) gives an estimate of the amount of denatured DNA.

Stokke and Steen[740] characterized the chromatin structure dependence of **7-aminoactinomycin D** binding to leukocytes. The level of 7-AAD binding is related to transcriptional activity, as indicated by DNA susceptibility to DNAse 1 digestion and by RNA synthesis. Stokke, Holte and Steen[1345] analyzed stimulated lymphocytes, and found that cells in G_1 bound almost twice as much 7-AAD as cells in G_0; dye binding increased almost linearly during the G_0 to G_1 transition, and correlated with expression of the early activation antigen 4F2 (now CD98). In diploid cells from non-Hodgkin's lymphomas, G_0/G_1 cell size, as measured by light scattering, was strongly correlated with 7-AAD binding. Using a dual-beam (UV and 488 nm) instrument, Stokke et al[1346] were able to identify G_0, G_1, S, and G_2 phase cells on a bivariate display of Hoechst dye vs. 7-AAD fluorescence and to discriminate live from dead cells; the mixture of Hoechst dye and 7-AAD can also be combined with fluo-

rescein- and phycoerythrin-labeled antibodies for measurements of two cellular antigens.

Although it seems likely that some of the differences in chromatin structure between different cells could produce different patterns of staining by combinations of DNA fluorochromes, there is very little on this topic in the literature. Cowden and Curtis[280] compared staining of mouse thymocytes (condensed chromatin) and hepatocytes (more loosely organized chromatin) by various dyes, and noted different fluorescence intensities in the two types of nuclei when mithramycin and 7-aminoactinomycin D, among other dyes, were applied following RNAse treatment. Crissman (H. Crissman, personal communication, also reference 1347) has examined the use of combinations of DNA stains in combination with three-beam illumination to demonstrate differences in chromatin conformation by differences in DNA accessibility to different dyes; unfortunately, very few people have access to the three-beam flow cytometers needed to do this kind of work.

Chromatin Structure Identifies Mitotic Cells

The AO/acid denaturation technique provides more information about cells' progress through the cell cycle than can be obtained from DNA content measurements alone; it is particularly useful for discriminating **mitotic (M) cells** from cells in the G_2 phase, which have the same (4C) DNA content. As shown in Figure 7-15, cells in M phase (the identification of clusters was confirmed by flow cytometry of cultures in metaphase arrest) show a much higher red fluorescence, i.e., their DNA is less resistant to denaturation.

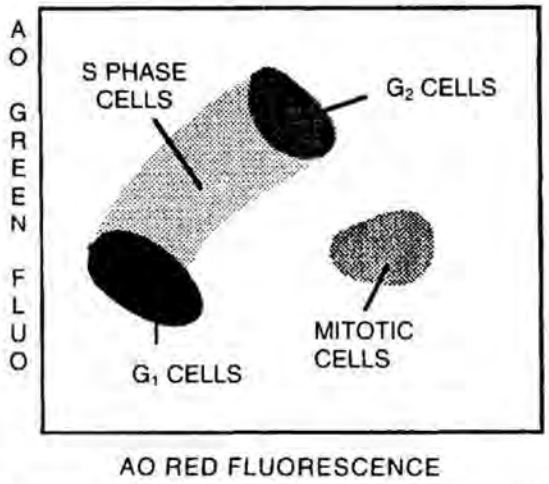


Figure 7-15. Flow cytometry of chromatin structure: AO staining patterns of an exponentially growing culture of Friend mouse erythroleukemia cells following partial DNA denaturation by acid (after Darzynkiewicz et al[262]).

Larsen et al[748] have developed an alternative procedure for **mitotic cell discrimination**; they report that, if nuclei isolated using nonionic detergents are fixed with formaldehyde, their fluorescence intensity following staining with ethidium, mithramycin, or propidium is quenched relative to unfixed isolated nuclei. Quenching is significantly less in the case of mitotic cells, causing these to form a separate cluster in a two-dimensional forward scatter vs. fluorescence measurement space.

It was previously mentioned (p. 277) that changes in **side scatter** of nuclei may reflect changes in chromatin structure[1254] and can be used to identify mitotic cells[1255-7]. Mitotic cells can also be identified by demonstration of certain nuclear antigens; this will be discussed further in subsequent sections.

RNA Content

The presence of relatively large amounts of **RNA** in growing cells was demonstrated many years ago. RNA is largely responsible for the **cytoplasmic basophilia**, or tendency of cytoplasm to stain intensely with basic dyes, which characterizes most immature and some leukemic blood cells. Histochemical demonstration and differentiation of RNA and DNA is largely based on the work of Brachet[40], who showed that a mixture of the basic dyes **methyl green** and **pyronin Y** stained nuclear DNA green and cytoplasmic RNA red. Pyronin Y, like methylene blue, is a basic, tricyclic heteroaromatic dye; both are homologues of **acridine orange**, which is employed in the best known flow cytometric technique for RNA content measurement, that described by Darzynkiewicz et al[262-3] and discussed on pp. 44 and 96-7. In this procedure, AO is used to stain both RNA and DNA, with results illustrated in Figures 3-10 (p. 97) and 7-16 (p. 321).

RNA/DNA Staining with Acridine Orange (AO)

In order to achieve good quantitation of DNA and RNA[1548-9], cells are first permeabilized with Triton X-100, and then stained with AO at a relatively low pH in the presence of EDTA. Under these conditions, DNA remains intact, i.e., in its native, double-stranded, helical form, while virtually all of the RNA present is converted to the single-stranded form. The low pH preserves the cytoplasm, which would otherwise be solubilized by the Triton X-100.

The AO concentration, which is critical, is adjusted so that DNA-bound dye is exclusively in the monomeric, intercalatively bound form, which fluoresces green. The AO bound to RNA is present in the form of a complex of RNA and dye polymers, and exhibits metachromatic red fluorescence. When the proper staining conditions are maintained, DNA content distributions estimated from AO green fluorescence show high precision (CVs less than 3%), while AO red fluorescence comes almost entirely from RNA, as shown by the loss of over 85% of red fluorescence following RNAse treatment.

Cell Cycle Compartments Defined on the Basis of RNA and DNA Content

Darzynkiewicz et al have used RNA and DNA content to define cell cycle compartments[262] on the basis of analysis

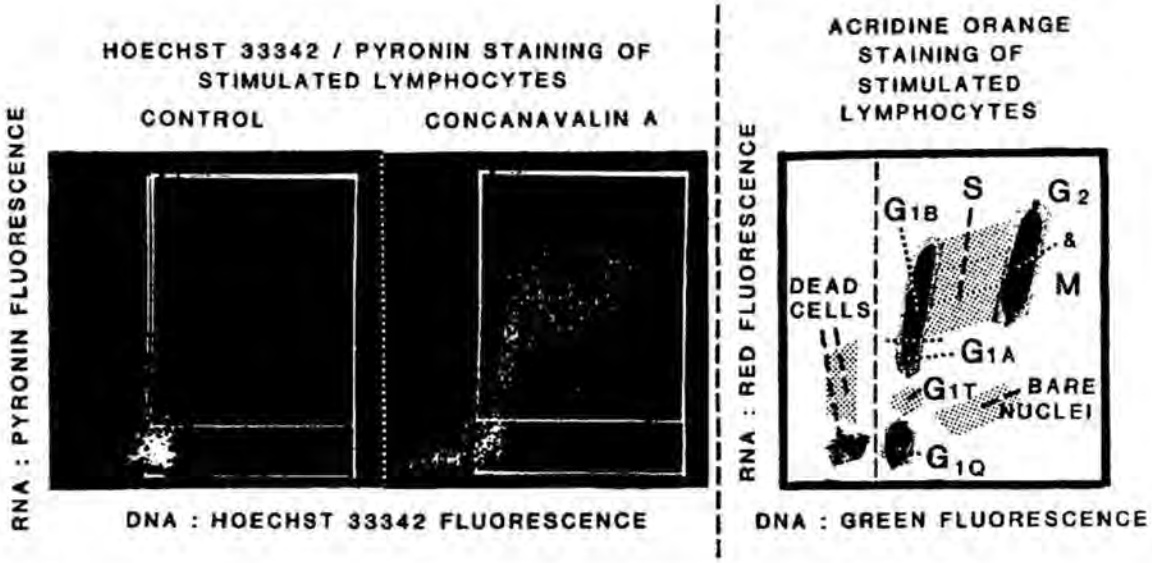


Figure 7-16. DNA and RNA content analysis of mitogen-stimulated lymphocytes. Left: typical results using the combination of Hoechst 33342 and pyronin Y described by the author[103]. Right: Typical results with acridine orange as described by Darzynkiewicz et al[242], showing cell cycle compartments defined on the basis of DNA and RNA content.

of such systems as mitogen-stimulated lymphocytes and leukemic cells undergoing chemical-induced partial differentiation *in vitro*. Typical DNA/RNA staining patterns of stimulated and unstimulated lymphocytes are shown in Figure 7-16, which also shows that other stains for DNA and RNA, in addition to AO, can be used to demonstrate the same cell cycle compartments.

The **quiescent state**, described as G_0 or G_{1Q}, in which cells such as peripheral blood lymphocytes normally remain, is characterized by a "diploid" (2C) DNA content and a low RNA content. Within 12 hours or so following exposure to mitogens, lymphocytes enter the G_1 phase and begin to synthesize RNA. RNA content continues to increase during the S phase, beginning about 30 hours after stimulation, in which DNA synthesis occurs.

Analysis of DNA content alone cannot discriminate cells in G_0 (G_{1Q}) from cells in the **proliferative** G_1 state, because the DNA content remains at 2C until the S phase begins. Measurements of RNA content can be used to make this distinction and, in addition, to define different stages within G_1. Cells pass from G_{1Q} through a brief transitional phase called G_{1T}, in which RNA content is slightly increased, and then into G_{1A}, during which RNA content increases further, but remains lower than the RNA content of any S phase cell. They then enter G_{1B}, in which RNA content is at or above the lowest value seen in S phase cells. RNA content increases approximately linearly during S and G_2.

In exponentially growing cultures, which lack cells in G_{1Q}, cells appear to pass from S through G_2 and M back into G_{1A}. Normal cells, such as stimulated lymphocytes, when maintained in long-term culture, tend to revert back to a G_{1Q} state, although quiescent, low-RNA "S_Q" and "G_{2Q}" populations can appear transiently in cells deprived of nutrients or exposed to cold or to inhibitors of protein synthesis. Transition to quiescent (Q) states during S and G_2 appears to be somewhat more common in transformed and malignant cells.

The pattern just described, in which RNA content increases during proliferation and decreases during quiescence, has been observed in human and animal blood, connective tissue, and epithelial cells of normal and malignant origin, and thus appears to be reasonably general. In many of the cell types examined, e.g., blood cells and leukemic cell lines, RNA content decreases with **differentiation** or maturation of cells. In other cell types, particularly those in which mature, nonproliferating cells are actively involved in protein synthesis, differentiated cells may contain more RNA than is found in their less mature progenitors, and high RNA content may not identify proliferative states.

As is illustrated in the left portion of Figure 7-16, the patterns of cellular DNA and RNA content observed using AO staining can also be demonstrated when other dyes, in this instance Hoechst 33342 and pyronin Y, are employed to stain DNA and RNA. Other parameters can substitute for RNA content for the definition of cell cycle compartments; it is possible, for example, to use **DNA and nuclear protein content** to identify proliferative and quiescent cell subpopulations[749-53].

AO: Problems and Some Solutions

I mentioned previously that, when staining conditions are properly adjusted, the red and green fluorescence of AO provide good estimates of RNA and DNA content. It has not been easy for many people, myself included, to duplicate the results obtained by Darzynkiewicz et al[262-3] using AO. This is due to the fact that the staining depends on a rather

complex chemical equilibrium between AO bound to DNA, AO bound to RNA (and to other AO molecules), AO in solution in the sample (core) stream, and AO diffused into the sheath stream. The staining is therefore dependent, not only upon the concentration of dye and the concentration of cells used, but also upon the dimensions and flow rates of core and sheath fluid streams.

Most of the earlier work reported by Darzynkiewicz and his colleagues was done on Ortho Cytofluorograf flow cytometers. It was fairly easy to achieve similar results using these instruments, while adaptation of the AO staining procedures to other flow cytometers generally required some modifications of the staining protocol. As mentioned on p. 312, Pennings et al[734] reported that the stability and quality of staining were greatly improved when reagent was added continuously to the sample stream using a manifold and pump.

There are, however, other notable disadvantages associated with AO staining. The procedure used for DNA/RNA analysis requires membrane permeabilization by Triton X-100, and cannot, therefore, be used on living or intact cells. The orthochromatic (green) and metachromatic (red) fluorescence emissions of AO, between them, overlap the emission regions of fluorescein and almost every other material that can be used as a fluorescent antibody label with excitation near 488 nm. This makes it difficult to employ AO staining for DNA/RNA content analysis in conjunction with immunofluorescent staining to identify cells by phenotype or demonstrate expression of growth- or differentiation-related antigens. While UV-excited, blue fluorescent antibody labels could, in principle, be used in conjunction with AO, the antigens detected would have to retain their conformation at low pH following Triton X-100 treatment; this seems unlikely.

Finally, AO itself tends to adhere to the tubing and flow system components of flow cytometers and, unless great care is taken to remove residual dye from the instrument following analysis of AO-stained samples (e.g., by flushing with Clorox or another bleach), unstained or weakly stained cells (e.g., samples for immunofluorescence analysis) that are run thereafter will take up the dye and exhibit fluorescence, which may lead to misinterpretation of the data obtained.

Pyronin Y, Oxazine I, and Other Tricyclic Heteroaromatic Dyes as RNA Stains

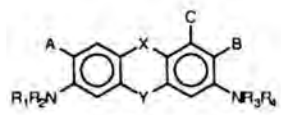
In attempting to develop alternative methods for flow cytometry of DNA and RNA content that could overcome the disadvantages associated with AO[113], I examined the properties of a number of tricyclic heteroaromatic dyes that are similar in structure to AO and that had been reported to stain DNA and/or RNA. These are summarized in Table 7-3. Among the dyes described in this table are **pyronin Y** and **methylene blue**, the xanthene and thiazine homologs, respectively, of AO, both of which are well known as RNA stains. Also included are the thiazine dye **new methylene blue** and the oxazine dye **brilliant cresyl blue**, both widely used in laboratory hematology to demonstrate the RNA in blood reticulocytes. Some of the dyes produce metachromatic staining; these tend to have higher dimerization constants than the dyes that do not exhibit metachromasia. However, dye binding to and staining of RNA can occur without metachromasia. All of the dyes bind to DNA, and were found by Müller et al to exhibit varying degrees of preference for G-C regions[266-7].

In the **methyl green-pyronin** technique for DNA/RNA staining[36], nuclei are stained green, while the cytoplasm is red, suggesting that DNA is stained predominantly by methyl green, while RNA is stained predominantly by pyronin. Methyl green, like the Hoechst dyes, binds without intercalation to DNA and exhibits a strong A-T preference[268]. These facts led me to try the combination of **Hoechst 33342 and pyronin Y**[113] for staining DNA and RNA in intact cells. While this approach has the disadvantage of requiring the use of dual-wavelength (UV and blue-green or green) excitation, the Hoechst/pyronin technique does produce results comparable with those obtained using AO (Figure 7-16). DNA content may be estimated with excellent precision (CVs of the G_1 peak below 2%) in intact cells stained with Hoechst 33342 in combination with pyronin Y. That the intensity of pyronin Y and fluorescence is largely representative of RNA content was established by the loss of up to 85% of this fluorescence when ethanol-fixed cells were treated with RNAse.

There is now good evidence that the absence of fluorescence from pyronin bound to DNA in cells stained with Hoechst/pyronin results from blocking of pyronin binding to DNA by the Hoechst dye. In 1982, Pollack et al[281] reported that methyl green, which, like the Hoechst dyes, binds to A-T sequences in the minor groove, blocks pyronin binding to DNA, even though pyronin binds intercalatively and has a G-C preference. In 1990, Loontiens et al[2611,12] reported that Hoechst 33258 displaces intercalators from DNA, and, in 1995, Toba et al[2343] noted that pyronin Y alone produced fluorescent staining of both DNA and RNA, and that both Hoechst 33342 and 7-AAD decreased pyronin fluorescence in RNAse-treated cells in a concentration-dependent fashion.

Darzynkiewicz and his colleagues[754-9] studied the interactions of pyronin with both cells and nucleic acids. With the Los Alamos group, and using the Los Alamos three-beam flow cytometer, it was shown that the combination of Hoechst 33342, pyronin Y, and fluorescein isothiocyanate (FITC) could be used to stain DNA, RNA, and protein in fixed cells[754-6].

The question remained as to the specificity of pyronin Y as an RNA stain in intact cells. Cowden and Curtis[760] reported in 1983 that the dye stained mitochondria of some live cultured cells. In my 1981 paper on Hoechst/pyronin staining[113], I had shown that RNAse treatment largely abolished pyronin fluorescence in fixed cells, and noted that pyronin fluorescence intensities were similar in fixed and unfixed cells. This suggested that most of the pyronin fluo-



CLASS	COMPOUND NAME	λ_{max} (nm)	R1	R2	R3	R4	A	B	C	A_{DNA} ($\times 10^4$)	K_D ($\times 10^4$)	Metachromatic?	Retic or RNA Stain?
ACRIDINES	proflavine	444	H	H	H	H	–	–	–	8.8			
X = CH	acridine orange (AO)	492	Me	Me	Me	Me	–	–	–	20.0	1.6	yes	yes
Y = NH	coriphosphine O	467	Me	Me	H	H	–	Me	–	3.2		yes	
AZINES	neutral red	540	Me	Me	H	H	–	Me	–	0.66		yes	yes
X = N													
Y = NH													
XANTHENES	3,6-diaminoxanthylium	496	H	H	H	H	–	–	–	1.8			
X = CH	acridine red		H	Me	H	Me	–	–	–				
Y = O	pyronin Y (G) (GS)	545	Me	Me	Me	Me	–	–	–	1.3	0.33		yes
	pyronin B	550	Et	Et	Et	Et	–	–	–				yes
THIOXANTHENES	3,6-diaminothioxanthylium	510	H	H	H	H	–	–	–	11.0			
X = CH	thiopyronin G	563	Me	Me	Me	Me	–	–	–	2.1	2.1		
Y = S													
OXAZINES	Capri blue GB (L)	643	Me	Me	Me	Me	–	–	–	0.28			
X = N	Capri blue GON		Me	Me	Et	Et	–	–	–			yes	
Y = O	oxazine 1	645	Et	Et	Et	Et	–	–	–				
	brilliant cresyl blue	636	Et	Et	H	H	Me	–	NH_2				yes
THIAZINES	thionin	598	H	H	H	H	–	–	–	3.7	2.2	yes	yes
X = N	azure C	609	Me	H	H	H	–	–	–				
Y = S	azure A	628	Me	Me	H	H	–	–	–			yes	yes
	azure B	647	Me	Me	Me	H	–	–	–	8.2	0.98	yes	yes
	methylene blue	665	Me	Me	Me	Me	–	–	–	8.1	0.71	yes	yes
	new methylene blue	636	Et	H	Et	H	Me	Me	–			yes	yes
	toluidine blue	636	Me	Me	H	H	–	Me	–	2.4		yes	yes

Table 7-3. Tricyclic heteroaromatic compounds usable for staining DNA and/or RNA. The general structure of these dyes is shown above the table. In the table, λ_{max} is the wavelength of maximum absorption, A_{DNA} the affinity for calf thymus DNA, in M^{-1}, and K_D the dimerization constant, also in M^{-1}. Affinities for DNA and dimerization constants are from Muller et al[2667]. The tabulated values for A_{DNA} and K_D should be multiplied by 10^4 to get the true values; for example, A_{DNA} for acridine orange is 8.8×10^4 M^{-1}.

rescence from intact cells was also accounted for by dye bound to RNA; it was impossible to prove the point, because I couldn't treat intact cells with RNAse.

What Does Pyronin Y Stain? Double-Stranded (Ribosomal) RNA and Sometimes Mitochondria

Darzynkiewicz et al[757-8] found that pyronin Y, at concentrations below 3.3 μM, produced primarily mitochondrial staining in live cells, while, at concentrations above 5 μM, the dye formed complexes with RNA; the interaction with RNA appears to be responsible for the irreversible toxicity of the dye which they noted at this concentration. They reported that the pyronin-DNA complex was not fluorescent, although a fluorescent complex with DNA could be formed when pyronin Y was added at high concentrations. They also found that complex of pyronin Y with single-stranded RNA was not fluorescent, and attributed the RNAse-sensitive fluorescence of pyronin Y in cells to dye bound to double-stranded RNA in polyribosomes[756,759,1350]. Schmid et al[2626] have since (1999) reported that 2 μg/mL pyronin Y produces stoichiometric staining of DNA in fixed, RNAse-treated cells.

Traganos, Crissman, and Darzynkiewicz[1350] found that the intensity of pyronin Y RNA staining varied with changes in conformation of RNA during mitosis and hyperthermia of CHO cells. Total RNA content detected after staining with AO increased in M as compared to G_2 phase cells, consistent with continued RNA synthesis during G_2. The content of double-stranded RNA, stained with ethidium (after DNAse treatment), was also somewhat higher in M cells. In contrast, stainability of RNA with pyronin decreased by 27% in M compared to G_2 cells, and stainability of RNA with pyronin was decreased in G_2 cells compared to cells in G_1. The effect was seen at a relatively narrow range of dye concentration (1.0-2.0 μg/ml), and was thought to involve selective denaturation and condensation of ribosomal RNA by pyronin in single ribosomes; this process does not occur in polyribosomes.

Since the ribosomal RNA content of cells generally parallels their total RNA content, at least in the context of rep-

resenting proliferative vs. quiescent states, Darzynkiewicz et al gave pyronin Y a clean bill of health as an RNA stain in fixed cells – they use the dye – but cautioned against its indiscriminate use in intact cells[756].

The caution relates specifically to the possibility that pyronin Y fluorescence measured in intact cells may reflect contributions from dye bound to mitochondria as well as from dye bound to RNA. In the rat and human lymphoid cells with which I have used the dye, mitochondrial fluorescence does not seem to be significant in intact cells stained with 5 μM pyronin Y. Cellular and mitochondrial uptake of pyronin Y and other cationic dyes, such as the cyanines and rhodamine 123, is driven in large part by the interior-negative electrical potential gradients across the cytoplasmic and mitochondrial membranes, as will be discussed at great length in the section on probes of membrane potential. I have already mentioned that pyronin Y fluorescence intensities are similar in intact and ethanol-fixed cells; in the latter, the RNAse sensitivity of pyronin fluorescence establishes that it comes predominantly from pyronin-RNA complexes.

If a substantial portion of pyronin Y fluorescence in cells originated from mitochondria, fluorescence should be greatly decreased in cells treated with proton ionophores and/or other uncouplers of oxidative phosphorylation, which decrease or abolish potential gradients across the mitochondrial and, in some cases, the cytoplasmic membrane. I have not noted more than a 5-10% difference in fluorescence between intact lymphoid cells stained in the presence and absence of a "cocktail" of uncouplers and ionophores that demonstrably eliminate mitochondrial uptake and retention of rhodamine 123 in cells such as fibroblasts. Thus, in intact or fixed rat and human lymphoid cells, it appears safe to interpret pyronin Y fluorescence as primarily indicative of RNA content.

In other cell types, containing more mitochondria, fluorescence from dye in these organelles might interfere with RNA content determination in intact cells using pyronin Y. However, such interference would be eliminated by addition of uncouplers. The mitochondrial-vs.-RNA fluorescence issue may be moot if RNA staining is being done to discriminate proliferating and quiescent cell compartments, since, as will be discussed in later sections, both cytoplasmic and mitochondrial membrane potential can serve, in lieu of RNA content and in combination with DNA content, as indicators of proliferative activity.

Surviving Vital Staining with Pyronin Y

I found that cells "vitally" stained with 5 μM pyronin Y could not be grown in culture, and elected to settle for other benefits of vital staining, i.e., relative ease of sample preparation and the elimination of any fixation artifacts that might interfere with immunofluorescent staining done concomitantly with RNA staining with pyronin Y and/or RNA/DNA staining with pyronin and Hoechst 33342[113]. Pyronin Y can be used with fluorescein- and/or PE/Cy5 tandem- or PerCP-labeled antibodies; since the dye is not well excited at 488 nm, fluorescence signals, even from 5 μM dye, are relatively weak. The emission filters generally used for phycoerythrin are well suited for measurement of pyronin Y fluorescence. While the Hoechst/pyronin technique has the disadvantage of requiring dual wavelength (UV and 488 nm) excitation, RNA content measurement alone in cells stained with both dyes may provide useful information and only requires a single 488 nm excitation beam.

Edward Srour, of the University of Indiana, who was interested in studying the cell cycle in human hematopoietic stem cells, decided to find out whether the Hoechst/pyronin DNA/RNA staining procedure would work at lower dye concentrations without killing the cells. It did; he and his colleagues[2340-2] now routinely sort and culture cells stained with Hoechst 33342 at a concentration of 1.6 μM (1 μg/mL) and pyronin Y at a concentration of 3.3 μM (also 1 μg/mL), adding 50-100 μM verapamil to block efflux of the dyes. They have recently published a detailed protocol for the staining procedure[2627]. I will have more to say about this in the section on stem cells in Chapter 10.

In my original procedure, intact cells were incubated with 5-10 μM Hoechst 33342 for about 5-10 min at 37 °C, after which concentrated Pyronin Y (Sigma-Aldrich and Polysciences both produce satisfactorily pure preparations of the dye) was added to a concentration of 5 μM and incubation continued for 30-45 min. Cells stained with this mixture can subsequently be stained with labeled antibodies, provided that the concentrations of both Hoechst 33342 and pyronin Y are maintained in all staining and washing solutions. When cells are stained with fluorescent antibodies and subsequently fixed, Hoechst/pyronin staining is considerably easier; dyes are added after the last wash step to achieve concentrations of 1 μg/mL Hoechst 33258 or 33342 and 3.3-5 μM (1-1.6 μg/mL) pyronin Y.

In a dual-beam (UV/488 nm) instrument, the fluorescence of Hoechst 33342, excited in the UV and measured in the range between 440-480 nm, is indicative of DNA content; pyronin Y fluorescence, measured between 570-600 nm, is indicative of RNA content. I have recommended leaving the Hoechst dye in the staining solution even if only RNA measurements are to be made, to block any artifacts due to pyronin Y binding to DNA; this may be unnecessary.

Other DNA Dyes Usable with Pyronin Y

Toba et al[2343-5] showed that a combination of 7-AAD and pyronin Y could be used to measure DNA and RNA content in fixed cells in a flow cytometer with a single 488 nm excitation beam; this technique also accommodates immunofluorescent staining with fluorescein-labeled antibodies. Schmid et al[2346] refined the staining procedure, and used an additional red laser to excite allophycocyanin-labeled antibody.

According to a March, 2002 posting to the Purdue Cytometry Mailing List from Derek Davies, DRAQ5 can also be used in combination with pyronin Y. I haven't tried.

For the record, Fred Kasten, who has headed the Biological Stain Commission and whose experience as a histochemist far exceeds mine, pronounces the "pyro" in pyronin to rhyme with "hero," which is the way I pronounce the "piro" in Shapiro. I had always thought the "pyro" rhymed with "my roe," which is how some Shapiros from Philadelphia pronounce the "piro." Fred's pronunciation more accurately reflects the Greek origin of pyronin's name, although I'm finding it hard to switch, not being enough of a pyromaniac to burn my bridges.

Tips on Tricyclics (Don't Get Depressed)

In general, it should be preferable to use tricyclic dyes with little or no metachromatic tendency as RNA stains in combination with dyes such as Hoechst 33342, since the orthochromatic absorption or fluorescence of RNA-bound tricyclic dye can provide an adequate estimate of RNA content under these circumstances. The laser dye **oxazine 1**, for example, gives no evidence of being metachromatic, but orthochromatic oxazine 1 fluorescence (excited at 633 nm; measured above 665 nm) in fixed cells stained with 5-10 μM dye is predominantly RNAse-sensitive, although not as much so as pyronin Y, and therefore may provide an estimate of RNA content.

There are, however, reasons for considering the use of metachromatic dyes other than acridine orange for simultaneous DNA/RNA content estimation. Among these, dyes such as methylene blue and the related azure dyes and toluidine blue may be of particular interest because their absorption maxima suit them to use in instruments with inexpensive He-Ne or diode laser sources operating in the 630-650 nm range. Methylene blue and toluidine blue are strongly metachromatic[205]; the absorption bands of concentrated solutions shift to shorter wavelengths, and it would be expected that polymeric forms of such dyes bound to RNA would therefore show metachromatic fluorescein emission at wavelengths longer than the 700-725 nm emission from the monomeric form[282]. Under suitable conditions, thiazine dyes can be employed to produce blue staining of nuclear DNA and selective, metachromatic purple staining of cytoplasmic RNA[283]. However, when I looked for metachromatic fluorescence in cells stained with these dyes, using an instrument with a red He-Ne laser source, I did not find any. It might be easier to discover suitable dyes by spectrofluorometry of dye complexes with various forms of nucleic acids.

At least one lot of dye I have encountered that was labeled pyronin Y wasn't, at least by thin layer chromatographic comparison to material from Aldrich and Polysciences. The funny thing was that the phantom dye was better excited at 488 nm than was pyronin Y, and produced staining with a degree of RNAse-sensitivity indicating that it was at least as specific as pyronin Y. I couldn't get the structure determined; I wish I knew what it was. 3,6-diaminoxanthylium and 3,6-diaminothioxanthylium, both shown in Table 7-4, might be worth a look as RNA stains excitable at 488 nm.

I have played briefly with **thiopyronin G**, usable with 532 nm YAG laser, 546 nm arc lamp or 543 nm green He-Ne laser excitation; this should work as a metachromatic dye. Unfortunately, I can't find a source for the dye; John Spikes, of the University of Utah, sent me a few milligrams in exchange for scientific song lyrics, which he collects. He, and others, have used thiopyronin as a photosensitizer, but it seems to be handed down from photobiologist to photobiologist. My interest in thiopyronin has waned, because I expect it to suffer from many of the same problems as does acridine orange; with the availability of Hoechst/pyronin, 7-AAD/pyronin, and, potentially, DRAQ5/pyronin, there seem to be several choices of two dyes that are better than one, especially when one wants to measure antigens as well as DNA and RNA.

Most tricyclic dyes do not increase fluorescence on binding to either RNA or DNA; on a mole-for-mole basis, the fluorescence of dye bound to nucleic acid is usually quenched relative to the fluorescence of free dye. The high local concentration of dye in dye-nucleic acid complexes accounts for the fluorescence of nucleic acid-containing structures being detectable above background, but background fluorescence is typically high. What you see in the fluorescence microscope is not always what you get in the flow cytometer; quenched dye, in this instance, dye bound to nucleic acid, bleaches more slowly than unquenched dye. Thus, when you look at AO-stained material under the microscope, much of the background fluorescence has already disappeared due to bleaching by the time your eyes focus, the green fluorescence from DNA-bound AO monomer fades rapidly, and the red fluorescence and phosphorescence from dye-RNA polymer persists the longest.

Tricyclics Gag on Mucopolysaccharides

Polyanionic cell constituents other than nucleic acids, notably **glycosaminoglycans (GAGs)** (formerly called **mucopolysaccharides**) such as **heparin** and **chondroitin sulfates**, bind tricyclic dyes and stain metachromatically with those dyes that do exhibit metachromasia. The metachromatic staining of GAG-containing granules in **blood basophils** and **tissue mast cells** was, in fact, noted by Paul Ehrlich, who gave both of these cell types their names, and has been used as an identifying characteristic since his time. It is sometimes possible to use tricyclic dyes to selectively stain GAGs in cells that also contain large amounts of RNA, by lowering the pH to the region of 1.0, at which point most of the phosphate groups of nucleic acids are not ionized while most of the sulfate groups of GAGs remain charged; the basic dye therefore binds to GAGs but not to RNA. Saunders has described the use of acridine orange for identification of GAGs[284]. Timar et al[761] have described a flow cytometric procedure for staining GAGs with AO; RNA staining is eliminated not by manipulating pH, but by altering electrolyte concentration.

There does not seem to be any easy way to use tricyclic dyes to selectively stain RNA in the presence of GAGs;

Darzynkiewicz et al have noted that heparin in mast cells interferes with RNA content estimation using AO because heparin-bound AO makes a significant contribution to the red fluorescence signal[262]. In most other cell types, however, in which large amounts of interfering GAGs are not found, the absorption or fluorescence of tricyclic dyes can give reasonable estimates of RNA content. Bauer and Dethlefsen[285] compared RNA content estimates in HeLa and CHO cells made by UV microspectrophotometry and by flow cytometry using a modification of the Darzynkiewicz AO staining procedure. They found a correlation coefficient of 0.93 between paired measurements made by the two methods following various RNAse treatments. They also reported some background contribution to red fluorescence due to DNA; it is not clear whether this might have been eliminated by further adjustment of staining conditions.

Reticulocyte Counting: Cyanines Beat Tricyclics; RNA in Nucleated Cells: Cyanines Don't

One of the more important applications of RNA content determination is in the detection and counting of reticulocytes in blood; the procedure and its flow cytometric implementation have been discussed on pp. 78 and 99. Under normal circumstances, red cells lose their nuclei before being released from the bone marrow into the blood, and neither young nor mature red cells contain DNA. Some RNA, a residue of the protein synthetic apparatus, remains in the young cells, and is lost during the cells' first day or two in circulation. If sufficient RNA is present in a red cell, an insoluble complex can be formed between this RNA and (tricyclic) basic dyes such as methylene blue; the netlike appearance of this precipitated material gives the name "reticulocyte" to this class of immature red cells.

The first flow cytometric approaches to reticulocyte counting, in the late 1970's and early 1980's, were based on the use of tricyclic dyes. Ortho received approval from the U. S. Food and Drug Administration (USFDA) for clinical use of a procedure using acridine orange[764,5], but there were problems with this dye due to high background fluorescence, although Schmitz and Werner reported improved results using optimized dye concentrations and logarithmic amplification on the AO red fluorescence channel[766]. Tanke et al described a method using pyronin Y[286,7], its major disadvantage was the requirement that cells be fixed. Later in the 1980's, the approach to reticulocyte counting shifted toward the use of basic dyes, different in structure from the tricyclics, which increase fluorescence by factors ranging from severalfold to several thousandfold on binding to RNA. These dyes, predominantly cyanines such as thiazole orange and related compounds such as thioflavin T and auramine O, stain both RNA and DNA. While they are nearly ideal for RNA detection in reticulocytes, from which DNA should be absent, they are poorly suited for demonstrating RNA in nucleated cells, unless the cells are treated with DNAse as described below.

Propidium Stains Double-Stranded RNA; What of Other Dyes?

Propidium iodide (PI) has been used by several investigators for analysis of RNA content. This dye binds by intercalation to double stranded nucleic acids, RNA as well as DNA. When PI is used for DNA content estimation in cells containing large amounts of RNA, broad fluorescence distributions are obtained due to the contribution of RNA-bound dye to the "DNA" fluorescence signal. The accuracy and precision of DNA measurements made with PI are improved when cells are treated with RNAse prior to analysis.

Frankfurt[293] described a complementary technique in which cells were treated with DNAse and stained with PI before flow cytometry was done; cellular fluorescence under these circumstances is due primarily to PI bound to double-stranded RNA. The contents of single- and double-stranded RNA in cells appear to follow one another; Wallen et al examined cultured mouse mammary tumor lines and reported good correlation between flow cytometric measurements of RNA using PI and AO and good correlation of both with RNA content estimated by UV microspectrophotometry[294].

Wright, Higashikubo, and Roti Roti[1351] combined propidium staining of double-stranded RNA with fluorescein isothiocyanate (FITC) staining of total protein (see the section on that) for flow cytometric studies of nuclear matrices prepared from nuclei by DNAse I digestion followed by NaCl extraction, and found that, while heat shock could protect some double-stranded RNA from RNAse digestion, propidium staining remained specific for double-stranded RNA.

Pyronin Y, as previously mentioned, forms fluorescent complexes primarily, if not exclusively, with double-stranded ribosomal RNA, and could presumably be used instead of propidium without the necessity for RNAse digestion. The monomeric and dimeric cyanines intercalate, and thus stain double-stranded RNA, but would require enzymatic removal of both DNA and single-stranded RNA to be useful.

An RNA-specific fluorochrome similar in structure and spectral characteristics (UV-excited, blue fluorescence) to DAPI was described by Wachtler and Musil[292]; I have not seen reports either of the use of this dye in flow cytometry or of whether it stains single- and/or double-stranded RNA.

7.5 FLUORESCENT LABELS AND PROTEIN DYES

More than half of the 37 spectra shown in Figure 7-9 (p. 296) are those of low and high molecular weight **labels** that are attached to other molecules to allow those molecules to be detected in or on cells or beads using cytometry. **Reactive** labels bind covalently to the molecules to be labeled; low molecular weight reactive labels can also be used as stains for cellular **proteins**, which can also be demonstrated using dyes, almost always acidic in character, which form ionic bonds with amino groups and other basic structures in proteins. Structures of a number of reactive labels are shown in Figure 7-17.

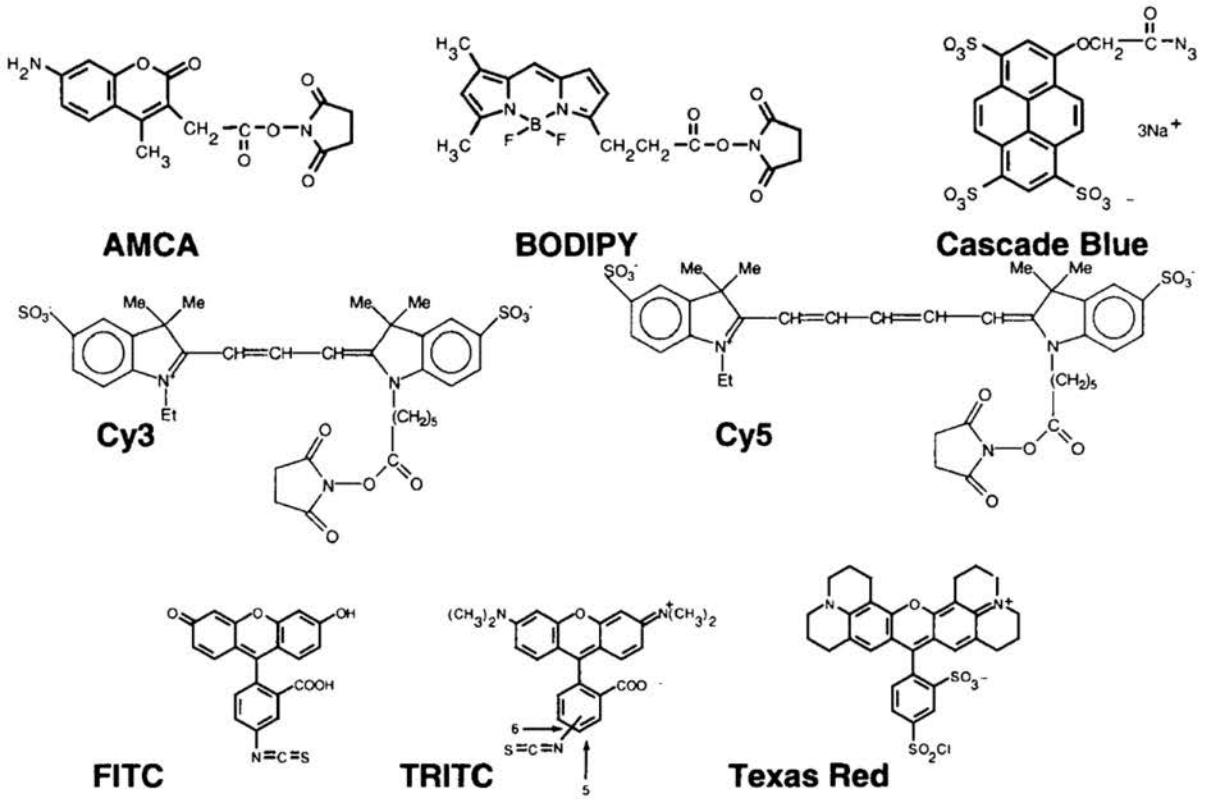


Figure 7-17. Chemical structures of some reactive labels. AMCA and BODIPY succinimidyl ester, Cascade Blue azide, FITC, TRITC, and Texas Red structures were provided by Molecular Probes, Inc.

Estimating Total and Basic Protein Content of Cells

Total protein content of fixed cells is estimated by staining with a variety of acid dyes that bind ionically or covalently to positively charged groups on proteins. It is difficult to establish the specificity of these dyes as protein stains, or how much dye is bound to materials other than proteins, because, while cells stained with DNA or RNA fluorochromes can be examined in the presence and absence of DNAse or RNAse, attempting to do the same trick with protein stains and proteolytic enzymes leaves you with samples containing stain in the presence and absence of cells. We thus have to be satisfied with a large body of indirect evidence that tells us that most of whatever isn't DNA or RNA in most cells is protein. By using acid dyes as protein stains, we increase the likelihood that what is being stained is actually protein, because these dyes are reacting predominantly with amino groups, which are considerably more abundant in proteins than in carbohydrates and lipids.

Total protein staining is useful both in monitoring growth and metabolism of otherwise homogeneous cell populations and in analysis of mixed populations containing cell types with different protein content, e.g., blood leukocytes. In most applications, protein stains are not used alone, but are combined with DNA fluorochromes. Most of the stains in common use have, therefore, been selected to have spectral characteristics complementary to those of ethidium or propidium on the one hand, or to those of DAPI or the Hoechst dyes, on the other.

Fluorescein Isothiocyanate (FITC)

Freeman and Crissman[295] examined several dyes suitable for argon ion laser excitation at 457 or 488 nm and selected fluorescein isothiocyanate (FITC) as a protein stain for use in combination with PI[217]. FITC was preferred to sulfonated dyes (e.g., brilliant sulfaflavine) because it binds covalently, leaving fluorescein moieties attached to cells after washing.

Because there is some overlap between the emission spectra of fluorescein and PI, fluorescence compensation may be required to eliminate contributions to the green fluorescence signal from PI and contributions to the orange or red fluorescence signal from fluorescein. When FITC is used for total protein staining, the fluorescein signal is usually relatively strong, and bleed into the orange or red channel is pronounced. This contrasts with the more common situation in which PI is combined with fluorescein-labeled antibodies; in this case, the effects of fluorescein spectral overlap on PI fluorescence are usually negligible, while those of PI spectral overlap on uncompensated fluorescein fluorescence are marked.

Sulforhodamine 101 (SR101)

Stöhr et al[296] examined various combinations of DNA and protein stains and selected one in which DAPI was used

to stain DNA and sulforhodamine 101 (SR101) was used to stain protein. These were used in an instrument with UV and 488 nm beams exciting DAPI and SR101, respectively; while it is also possible to excite both dyes with UV light, Heiden, Göhde, and Tribukait[1352] report that dual-beam excitation with UV and green is superior. There is relatively little spectral overlap between the emission spectra of DAPI and SR101 to begin with; when dual-beam excitation is used, any bleed of DAPI fluorescence into the SR101 measurement channel is eliminated.

SR101 binds ionically, rather than covalently, to proteins; staining with it and with other sulfonated dyes is an equilibrium process, and there is generally a considerable amount of free dye remaining in the background. Under some circumstances, background fluorescence of acid dyes used to stain protein may interfere with or prevent measurement of protein content (see "The Case of the Disappearing Leukocytes," pp. 220-1). However, this fluorescence may often be reduced considerably by lowering the ionic strength of the staining mixture[8,91,93].

Although, in theory, SR101 should be usable in combination with fluorescein-labeled antibodies in an instrument with 488 nm excitation, the much higher concentration of SR101 relative to fluorescein in this situation may result in more spectral overlap than can be compensated for by some instruments.

Hematoporphyrin (HP) as a Protein Stain

Takahama and Kagaya[1353] described a simplified simultaneous one-step staining method for DNA and cell protein using 0.001% DAPI or Hoechst 33342 as the DNA stain and 0.03% hematoporphyrin (HP) to stain protein. The fluorescence emission of HP is at 670 nm; the excitation spectrum of porphyrins suggests that HP would definitely be usable as a total protein stain with blue-violet excitation (436 nm arc lamp, 441 nm He-Cd laser, or 457 nm argon laser) and might well work with 488 nm excitation. If 488 nm excitation could be used, the large Stokes' shift of porphyrins should insure that emission in the green spectral region would be sufficiently low to permit simultaneous use of fluorescein-conjugated antibodies and HP. Tanaka et al[1354] compared staining with the DAPI/HP combination by flow and image cytometry and reported that it yielded more accurate results than did PI and fluorescein.

Rhodamine 101 (or 640) as a Vital Protein Stain

Since neither the covalent bonding nor the ionic bonding acid dyes penetrate membranes of living or intact cells to any appreciable extent, they can only be used for protein staining in fixed or permeabilized cells, nuclei, etc. In 1982, Crissman and Steinkamp reported that rhodamine 640 (i.e. rhodamine 101, the uncharged dye that is the chromophore of SR101 and of the reactive labels XRITC and Texas Red) could be used at concentrations of 1-5 μg/ml to stain living or intact cells, yielding fluorescence distributions nearly identical to the total protein content distributions obtained from fixed cells stained with XRITC or FITC[297]. One would expect that other uncharged rhodamine dyes with absorption and fluorescence at shorter wavelengths, e.g., rhodamine B, might also be suitable for "total protein" staining in intact cells.

What Do "Total Protein" Stains Stain?

Holme et al[1355] compared forward scatter and Coulter volume signals from platelets with fluorescein fluorescence values obtained when platelets were stained for total protein and found a high degree of correlation; since platelets are predominantly composed of protein, this provides further evidence in support of FITC as a total protein stain.

In fixed cells, measurements of orthogonal (90 °) light scattering may provide information similar to that obtained using protein stains[8,103,1255]; this was alluded to on p. 278. Figure 5-17 (p. 254) shows that in glutaraldehyde- fixed peripheral blood leukocytes, total protein content, as estimated from the UV-excited blue fluorescence of the acid dye "LN"[91,93] is tightly correlated, on a cell-by-cell basis, with orthogonal light scatter intensity in the several different classes of leukocytes[8]. Others (H. Crissman, personal communication; M. Pallavicini, personal communication) have also noted that fluorescent protein stains and side scatter measurements yield similar distributions. When beginning studies on a cell population, it is therefore advisable to examine the correlation between side scatter and total protein content as determined with a fluorescent dye. If the side scatter measurement appears to provide the same information as the protein stain, the scatter signal can then be used in the absence of the protein stain, allowing the fluorescence channel that would have been used for protein content estimation to be devoted to analysis of a more specific parameter, e.g., a surface antigen.

Staining to Demonstrate Basic Protein

Protein staining by acid dyes is dependent on the **ionization constants** of the dyes and of amino groups and other charged sites on proteins. Thus, binding of dyes to cells is affected by the pH of the staining solution. At alkaline pH, only the more strongly basic groups in proteins remain ionized and thus able to bind acid dyes; as pH decreases, more basic groups become ionized. Thus, the same basic dye can be used to stain **basic proteins** and total proteins at different pHs; brilliant sulfaflavine, for example, is used as a basic protein stain at pH 8 and a total protein stain at pH 2.8[298].

Covalent Labels for Antibodies and Other Molecules

The covalent bond forming dyes such as FITC, which has just been discussed as a stain for total protein content, are probably better known, and undoubtedly more widely used, as **fluorescent labels** for a variety of large and small molecules that can be bound strongly and specifically to various cellular constituents. Specific ligands thus labeled can be used as reagents for a number of structural and functional parameters, including **surface sugars** (demonstrated

using tagged lectins), **surface** and **intracellular antigens** (fluorescent antibodies), **surface charge** (fluorescent polycations), **surface** and **intracellular receptors** (fluorescent hormones, growth factors, neurotransmitters, viruses, etc.), **endocytosis** (fluorescent macromolecules, microorganisms, or plastic particles), **DNA synthesis** (fluorescent antibody to detect BrUdR in chromatin; fluorescent nucleotides), and **specific nucleic acid sequences** (fluorescent oligonucleotide probes). Spectral characteristics of the more important fluorescent labels are given in Figure 7-9 (p. 296) and Table 7-2 (p. 297).

Fluorescein Isothiocyanate (FITC) as a Label

Fluorescein, conjugated as its reactive isothiocyanate derivative (**FITC**), is by far the most popular fluorescent label; its excitation maximum is very close to the 488 nm argon ion laser wavelength available in almost all flow cytometers, its quantum efficiency is high, and it had been in use long enough before flow cytometers became available for conjugation and staining procedures to have become well established, particularly in immunology.

As was mentioned on p. 77, the fluorescent label used in the first description of the fluorescent antibody technique by Coons et al in 1941[44] was anthracene, which fluoresces blue when excited by UV light. The fluorescent antibody technique itself was developed after attempts to visualize the absorption of dye-labeled cell-bound antibodies in transmitted light[1087-8] had failed. It was possible to see concentrations of anthracene-labeled antibodies against the darker background of unstained tissue, but the UV-excited blue autofluorescence of pyridine nucleotides and other tissue components (see Figure 7-7 and text on pp. 290-1) limited the sensitivity of the fluorescent antibody method as originally described.

In 1950, Coons and Kaplan[45] reported that the use of **fluorescein-labeled antibodies** improved sensitivity; the green fluorescence of fluorescein made it easier to discern concentrations of antibody against the tissue background. Two major barriers to widespread use of the fluorescent antibody method remained; few labs had fluorescence microscopes, and most investigators were neither equipped nor willing to handle the phosgene gas used to prepare fluorescein isocyanate for conjugation. In 1958, Riggs et al[46] described the use of fluorescein isothiocyanate for labeling. The synthesis of FITC involves thiophosgene, which is less noxious and more manageable than phosgene, and FITC is stable enough to be marketed commercially in a form ready for conjugation.

The intensity of fluorescein fluorescence emission varies with pH within the range (6.5-8.0) likely to be encountered in samples; pH must therefore be controlled when quantification of results is important.

Labeling with Lissamine Rhodamine B and Tetramethylrhodamine Isothiocyanate (TRITC)

It was also in 1958 that Chadwick et al[299] described the use of **Lissamine rhodamine B 200**, or **sulforhodamine B**, for antibody labeling. This compound was conjugated by converting its sulfonic acid group to a sulfonyl chloride. Since the red fluorescence of rhodamine dyes and the green fluorescence of fluorescein can be readily distinguished by an observer, particularly when excitation filters are switched to allow selective excitation of first one dye and then the other, it became possible to examine material stained with two different antibodies, each with its own distinct fluorescent label. Once relatively easy-to-use fluorescein and rhodamine labels became available, immunology laboratories began to acquire fluorescence microscopes, which had been improved considerably between the 1940's and the 1960's. The stage was thus set for the relatively rapid acceptance of flow cytometry by immunologists, and it was not until flow cytometers came into widespread use in the late 1970's that significant further progress in the development of fluorescent labels for antibodies was to occur. By this time, an isothiocyanate derivative of rhodamine, **tetramethylrhodamine isothiocyanate (TRITC)** had also become available.

Multicolor Fluorescence I: FITC and TRITC

As was just noted, by the time flow cytometers became available to immunologists, many of them were using fluorescein and rhodamine labels to do two-color work under the fluorescence microscope, switching from a combination of a blue primary (excitation) filter and a yellow or green secondary (observation) filter for detection of fluorescein-labeled antibody to a combination of a green primary filter and a red secondary filter for detection of rhodamine- labeled antibody. It was also possible, although difficult, to look at the fluorescence from both labels at once, using blue-green excitation and a yellow secondary filter; this relied heavily on the human observer's ability to discriminate weak red fluorescence from strong green fluorescence.

The microscopes used for immunofluorescence work typically have mercury or xenon arc lamp sources; mercury lamps have strong emission lines at 436 nm (blue) and 546 nm (green) and put out considerably less light at intermediate wavelengths, while xenon lamps have a relatively flat emission spectrum in the blue and green regions. The absorption maximum of fluorescein is at about 490 nm; that of tetramethylrhodamine is at about 555 nm. Using a conventional blue (centered near 436 nm) excitation filter for fluorescein gives suboptimal excitation, while using a green filter centered near 546 nm for rhodamine gives near-optimal excitation. Using a 500 nm short-pass filter to excite both dyes doesn't give very good excitation of either, allowing the dark-adapted eye and its associated brain to resolve the relatively weak emission from both.

The 488 nm argon laser line commonly used for excitation in flow cytometers is essentially at the absorption maximum of fluorescein, while the absorption of tetramethylrhodamine at this wavelength is only about 5% of its maximum value. This factor alone dictates that, if equal amounts of fluorescein- and tetramethylrhodamine-tagged antibodies were present on a cell, the total fluorescence emission from the fluorescein antibodies would be 20 times that from the tetramethylrhodamine antibodies. When bound to antibodies, both fluorescein and tetramethylrhodamine usually have quantum efficiencies somewhere between 0.2 and 0.5 (roughly on the order of 50% of the quantum efficiencies of the free dyes); these are not different enough to balance out the very large difference in absorption. The differences in molar extinction coefficients between fluorescein and tetramethylrhodamine are also not great enough to overcome the differences in absorption at 488 nm. Thus, one can realistically expect at least an order of magnitude more fluorescence from fluorescein-tagged antibody than from an equivalent amount of tetramethylrhodamine-tagged antibody when 488 nm excitation is used. The resolution of the signals from the two dyes therefore depends upon the use of detectors equipped with optical filters chosen to take advantage of the difference in emission spectra between fluorescein and tetramethylrhodamine.

The emission maximum of fluorescein (Figure 7-9) is at about 520 nm, while that of tetramethylrhodamine is at about 570 nm; emissions from the two dyes should be well resolved using a green (515-550 nm) filter for the fluorescein fluorescence detector and a red-orange (560 nm long pass) filter for the tetramethylrhodamine fluorescence detector. This, however, does not take into account the large absorption difference at 488 nm. To do this, we have to imagine spectra in which we either increase the height of the fluorescein emission spectrum by a factor of 10 or decrease the height of the tetramethylrhodamine emission spectrum by a like factor. In this view, what seemed to be an insignificant "red tail" on the fluorescein emission spectrum, going out to 600 nm, now overshadows most of the tetramethylrhodamine emission. For best resolution of the tetramethylrhodamine emission, we really should use a long pass filter that cuts on at a wavelength of 590 nm or longer on the tetramethylrhodamine fluorescence detector. At that, we would have to use electronic or software fluorescence compensation to get rid of crosstalk from the longer wavelength fluorescein emission, and, if there is a lot more fluorescein than tetramethylrhodamine on a cell, even this won't help.

Loken et al[115], in the Herzenberg lab at Stanford, first did two-color immunofluorescence flow cytometry as just described, and also evened the balance between fluorescein and tetramethylrhodamine absorption by operating the argon laser to produce a mixture of visible lines (mostly 488 & 515 nm) or a 515 nm beam. The 515 nm line is not great for tetramethylrhodamine, but it's no better for fluorescein, and using this excitation wavelength forces you to employ a fluorescein detector filter that cuts on at a longer wavelength than you would otherwise use. Before phycobiliproteins were introduced as labels, this was about the best that could be done in the way of two-color immunofluorescence analysis with a single-beam cytometer; on a historical note, the fluorescein/rhodamine labeling work forced the Herzenberg group to develop fluorescence compensation.

Multicolor Fluorescence II: Rhodamine 101 Dyes

The most obvious alternative to the less than satisfactory single beam excitation method for cells labeled with fluorescein and rhodamine involved the use of separated excitation beams at different wavelengths, in essence imitating the observer at the fluorescence microscope switching filter combinations. There was no simple way to do this using fluorescein as the first label and tetramethylrhodamine as the second, because the only lines available from ion lasers well suited to tetramethylrhodamine excitation (528 nm from argon and 530 nm from krypton lasers) are in the region of fluorescein emission. Instead, derivatives of **rhodamine 101** were substituted for tetramethylrhodamine. In rhodamine 101, the ring structure of other rhodamine dyes is extended (see the structures of TRITC and Texas Red in Figure 7-17), leading to shifts in the absorption and emission spectra, which have maxima at wavelengths about 30 nm longer than the absorption and emission maxima of tetramethylrhodamine.

Adding a second beam, derived from a krypton laser emitting at 568 nm or a dye laser at 590 nm, to the existing 488 nm argon laser beam in a flow cytometer made it possible to examined cells simultaneously stained with antibodies labeled by conjugation with FITC and with X-rhodamine isothiocyanate (**XRITC**, Research Organics, Cleveland, OH) or the sulfonyl chloride derivative **Texas red** (from Molecular Probes, which was then located in Plano, TX), both bearing the chromophore of rhodamine 101[116,117]. Fluorescein fluorescence excited at 488 nm was measured at 510-550 nm, and rhodamine 101 fluorescence excited at 568 nm was measured at 590-630 nm; there was essentially no crosstalk between the signals.

While the rhodamine 101 derivatives solved some problems involved in two-color immunofluorescence flow cytometry, they precipitated others. People who used XRITC found it hard to remove unbound dye from protein conjugates, to which the hydrophobic dye adhered. Texas red became more popular, but had a tendency to inactivate antibodies (rat monoclonal antibodies in particular) and, sometimes, to part company with antibodies to which it had been conjugated. Rhodamine 101 supposedly has a quantum efficiency of 1.0, but Texas red-labeled antibodies don't seem to give as much of a fluorescence signal as do fluorescein-labeled antibodies. The people I know who have the best luck with Texas red immunofluorescence originally used the label almost exclusively in the forms of **Texas red-avidin** or **-streptavidin**, which will form extremely high-affinity bonds with biotin-conjugated antibodies[400]. Excitation of Texas red requires a krypton laser or an argon laser-pumped

tunable CW dye laser, neither of which is as easy to keep running as an argon laser. He-Ne lasers at 594 nm were not then powerful enough to present a viable option; the few milliwatts available at this wavelength might, however, do the job in modern instruments with efficient optics.

Early Problems with Multicolor Fluorescence

In addition to the difficulties presented by the rhodamine 101 derivatives, users faced some more general problems associated with two-color immunofluorescence measurements. As long as only a single antibody was used to stain cells, a significant enhancement of fluorescence signals could be obtained by using **indirect staining**, in which the fluorescent label is attached to a second **developing antibody** that binds to molecules of another antibody already bound to antigens on or in cells. It is, as a rule, not possible to put more than three molecules of fluorescein (or other dyes) directly on an IgG antibody molecule without either decreasing the specificity of the antibody reaction or decreasing the quantum yield of attached dye past the point of diminishing returns. It is, however, possible for more than three (usually 5 or 6) molecules of a developing antibody to bind to a single cell-bound antibody molecule. Thus, **direct immunofluorescent staining** will put no more than 3 dye molecules at each antigenic site, while indirect staining will put 15-18 dye molecules at each antigenic site, resulting in **amplification** of the fluorescence signal.

Most of the earlier single-color work with monoclonal antibodies was done using indirect staining, with something like a fluoresceinated goat anti-mouse Ig used as a developing antibody, since this *modus operandi* both eliminated the need for fluorochrome conjugation of each new monoclonal antibody and offered increased sensitivity as compared to direct fluorescent staining. Indirect staining of this kind, however, did not provide for labeling cells with two mouse monoclonal antibodies of the same immunoglobulin class.

When there were reasonably large numbers of antigenic sites present on cells, the obvious option in this instance was direct staining, using different labels (fluorescein and rhodamine 101) on each of the two antibodies. If some amplification was required, the use of **labeled avidin** and **biotinylated antibodies**[300], or of **hapten-conjugated antibodies** and differently labeled **anti-hapten antibodies**[301] resulted in more dye molecules being bound per antigenic determinant than would have been possible using direct staining.

What would have been most desirable, however, was a direct labeling technique that allowed more than three fluorescent molecules to be attached directly to each antibody molecule. The group at Block tried a "brute force" approach to such a method in which antibodies were conjugated to synthetic polymers bearing hundreds of fluorescein molecules (see p. 116); this didn't work, because the fluorescein fluorescence was quenched under those circumstances.

Shechter et al[302] had better luck with a procedure developed to produce highly fluorescent, physiologically active derivatives of insulin and other peptide hormones; they were able to attach 7 molecules of rhodamine to a molecule of **lactalbumin**, which was then conjugated to a molecule of hormone. As it turned out, however, when it came to designing fluorescent macromolecules suitable for antibody labeling, Nature had, as usual, outdone man.

Phycobiliproteins to the Rescue!

The **phycobiliproteins**[114,772,1356] are a family of macromolecules found in red algae and cyanobacteria (formerly called blue-green algae), in which they play critical roles in the function of the photosynthetic apparatus. Photosynthesis in green plants involves the direct interaction of light with chlorophyll, which has absorption maxima near 440 nm in the blue-violet and near 700 nm in the far red. Light in these spectral regions is not transmitted much beyond the surface layers of bodies of water, while green and blue light penetrate to greater depths. The survival of algae and cyanobacteria at these depths depends on the capacity of phycobiliproteins to absorb the shorter wavelength light and participate in a chain of nonradiative energy transfers that finally makes the light energy for photosynthesis available to chlorophyll.

The **phycoerythrins** absorb blue-green and green light, the **phycocyanins** green and yellow light, and the **allophycocyanins** orange and red light. While the function of phycobiliproteins in their natural environment is that of nonradiative energy transfer, these molecules are all highly fluorescent, and their particular fluorescence characteristics have been of great interest to users of flow cytometers since Oi, Glazer, and Stryer demonstrated the utility of phycobiliproteins as antibody labeling reagents[114].

The chromophores in phycobiliproteins are **bilins**, which are pyrrole pigments derived from the same building blocks as **porphyrins**; each phycobiliprotein molecule contains a large number of such chromophores. The extinction coefficients of phycobiliproteins are extremely high, and the quantum yields are also high. An antibody molecule directly labeled with fluorescein will have between 1 and 3 chromophores associated with it; an antibody molecule to which 6 fluoresceinated antibody molecules have been bound during an indirect staining procedure will have 6 to 18 associated chromophores. An antibody molecule directly labeled by conjugation with a phycobiliprotein may have as many as 34 associated chromophores, each with an absorbance and quantum yield roughly comparable to those of fluorescein. Spectra of R-phycoerythrin and allophycocyanin are shown in Figure 7-9 (p. 296); Figure 1-18 (p. 37) shows that, with excitation at 488 nm, a phycoerythrin-labeled antibody molecule will emit several times as much fluorescence as a fluorescein-labeled antibody molecule.

In addition to their high extinction coefficients and quantum yields, phycobiliproteins, and phycoerythrins in particular, are characterized by broad shoulders in their excitation spectra, allowing them to be excited effectively at wavelengths substantially below their emission maxima.

While the molecular weights of phycobiliproteins are sufficiently high so that conjugates may contain only one

molecule of phycobiliprotein per antibody molecule, the high extinction coefficients and quantum efficiencies of the phycobiliproteins insure that one molecule will get the job done.

Phycoerythrins: R-PE, B-PE, and Others

While the peak absorption of **R-phycoerythrin (R-PE)** is at 565 nm, with the emission maximum at 578 nm, the absorption at 488 nm is approximately 50% of maximum. This allows R-PE to be used very effectively in combination with fluorescein for two-color immunofluorescence flow cytometry; only a single excitation beam (e.g., 488 nm from an argon laser) is required. Fluorescein fluorescence is measured, as customary, in the green region around 530 nm, while R-PE fluorescence is detected in the orange-red region above 570 nm. If a 590 nm long pass filter is used instead of a 570 nm long pass filter, interference from the red tail of fluorescein emission can generally be minimized to the point at which fluorescence compensation[115] is not necessary; this was more practical years ago, when most instruments measured two-color fluorescence, than it would be now.

B-phycoerythrin (B-PE), like R-PE, has a molecular weight of about 240,000, and contains 34 bilin chromophores per molecule; its absorption maximum is at 545 nm, and it is less well excited at 488 nm than is R-PE. PE-labeled antibodies have been widely available since the late 1980's, and the combination of fluorescein-labeled and PE-labeled antibodies has been standard for two-color immunofluorescence measurements since that time. B-D licensed Stanford University's patent on phycobiliproteins, which was based on the work by Oi, Glazer, and Stryer[114], and controlled the market on phycobiliprotein-labeled antibodies until the late 1990's; since that time, PE-labeled antibodies have become available from an increasingly large number of manufacturers.

Ong, Glazer, and Waterbury[305] suggested that the phycoerythrin from the marine cyanobacterium *Synechococcus* WH8103 **(S-PE)** might be useful as a label because it contains more phycourobilin groups, which are responsible for the shorter wavelength absorption of phycoerythrins, than does any other known phycoerythrin. The absorption maximum of S-PE is at 492 nm; the emission maximum is at 565 nm. A solution of S-PE excited at 488 nm has a fluorescence intensity 19 times higher than that of an equimolar solution of fluorescein, and about twice as high as an equimolar solution of R-PE. S-PE would, if it could be produced in quantity, be the ideal phycobiliprotein to use alone or in combination with fluorescein for immunofluorescence measurements with 488 nm excitation. Since most of S-PE emission is at wavelengths between 555 and 585 nm, it is also likely that fluorescein- and S-PE-labeled antibodies could be used in combination with propidium iodide for simultaneous DNA content and two-color immunofluorescence analyses. The theoretical advantages of S-PE, to which I referred in previous editions of this book, have not been realized at this writing, because S-PE is too hard to come by and/or because R-PE is good enough for most purposes.

Allophycocyanin (APC) and APC-B

Allophycocyanin (APC) is of particular interest as a single label because it exhibits high (about 75% of the maximum value) absorption in the 633-638 nm range in which red He-Ne and diode lasers operate. The absorption maximum of APC is at 650 nm; its emission maximum is at 660 nm. APC contains 6 bilin chromophores and has a molecular weight of about 100,000. **Allophycocyanin B (APC-B)** emits at slightly longer wavelengths (maximum near 680 nm). My colleagues and I measured fluorescence from human leukocytes stained with an APC-conjugated antibody in a flow cytometer using a 7 mW He-Ne laser source[303]. Although we used a suboptimal long pass filter (665 nm cut on, which transmits less than 50% of the APC fluorescence) on the fluorescence detector, we obtained results that compared favorably with those from another instrument in which cells stained with fluorescein-antibody were illuminated with 200 mW at 488 nm.

Loken et al[644] found that 25-50 mW from a large He-Ne laser mounted on a B-D FACS, which has less efficient fluorescence collection optics than the Cytomutt I used, provided near-optimal excitation of APC-labeled antibodies; Doornbos et al[1136] were able to discriminate cells stained with APC-labeled antibody from unstained cells using a flow cytometer with a diode laser source emitting 3 mW at 635 nm.

If excitation in the 590-650 nm range usable with APC is available, this label offers advantages over PE and fluorescein for use with antibodies reactive with low surface density antigens in cells such as macrophages[1357], which exhibit high autofluorescence when excited at 488 nm.

Glazer and his associates[773-4,1356] studied the physical chemistry and spectral properties of APC, in the process uncovering and solving a potential problem with its use as an antibody label. Native phycobiliproteins are composed of subunits; B-PE and R-PE each contain 13 subunits, while APC is made up of 3. Although phycobiliproteins are stable under most conditions associated with their use as labels, APC tends to dissociate into subunits at concentrations below 10^{-8} M, and APC concentrations might fall below this range in washed samples stained with APC-labeled antibody or ligand. Cross-linking the subunits while APC is in the trimeric state prevents dissociation, stabilizing the labeled antibody.

Phycocyanins

C-phycocyanin (C-PC), with an absorption maximum at 620 nm and an emission maximum at 650 nm, has been used as an antibody label by Hoffman et al[646], who were able to detect and resolve fluorescence from C-PC-labeled and APC-B-labeled antibodies, using a 642-657 nm bandpass filter for the former and a 675-695 nm bandpass filter for the latter, in an Ortho flow cytometer equipped with a 7 mW, 633 nm He-Ne laser source. Taking advantage of the

small, but not insignificant absorption of C-PC at 488 nm, Daley et al[775] used a PC-avidin conjugate with biotinylated antibodies and fluorescein- and PE-labeled antibodies to do three-color immunofluorescence measurements on a Coulter EPICS instrument with a single 488 nm laser source.

R-phycocyanin II (R-PC-II)[776], a phycocyanin found in some species of *Synechococcus*, might be useful as a third label; it has absorption peaks at 533, 554, and 615 nm and an emission peak at 646 nm. However, as is the case with S-PE, it may be impractical to produce R-PC-II in quantity.

Phycobiliprotein Tandem Conjugates: PE-APC, PE-Texas Red, PE-Cy5, PE-Cy5.5, PE-Cy7, etc.

Glazer and Stryer[306] (1983) were the first to prepare a **tandem conjugate** of B-PE and APC in which energy transfer between these proteins, with the phycoerythrin molecule the donor and the allophycocyanin molecule the acceptor, results in strong emission at 660 nm on excitation at wavelengths between 470 and 560 nm. This material was shown by B-D to be usable as a third antibody label in combination with fluorescein and a phycoerythrin, permitting 3-color immunofluorescence measurements with 488 nm excitation. The PE-APC tandem conjugate, however, had two notable disadvantages; first, the chemistry involved in its preparation and conjugation was nontrivial, and, second, energy transfer was not complete, resulting in substantial emission from the conjugate in the same spectral range as phycoerythrin emission. In 2001, Tjioe et al[2628] found it somewhat easier to prepare and use PE-APC tandem conjugates.

The phycobiliprotein tandem conjugates now in widest use incorporate only a single phycobiliprotein molecule, namely, phycoerythrin, to which are conjugated several molecules of a lower molecular weight fluorochrome. The first widely used conjugates prepared in this fashion incorporated **phycoerythrin and Texas Red**; antibodies labeled with such conjugates, are available from a number of manufacturers, each using its own trade name for the conjugate. While most of the emission from PE-Texas Red conjugates is in the 610-620 nm emission region of Texas Red, incomplete energy transfer results in substantial emission from the conjugates in the PE emission region around 580 nm, and PE itself has substantial emission in the 610-620 emission range. As a result, a lot of fluorescence compensation must be applied to separate the fluorescence signals from a PE-labeled antibody and another antibody labeled with a PE-Texas Red tandem conjugate; while the spectra of PE and PE-Texas Red are shown in Figure 7-9 (p. 296); the spectral overlap problem is best appreciated from Figure 1-18 (p. 37) and the related discussion (pp. 36-7).

PE-Cy5 tandem conjugates, introduced by Waggoner et al[1359], incorporating a single phycoerythrin molecule and several molecules of the cyanine dye label **Cy5**, are now widely preferred over PE-Texas Red conjugates as a third label for immunofluorescence analyses using 488 nm excitation; they emit at the emission maximum of Cy5, near 660 nm.

Lansdorp et al[1360] took an intermediate step on the road to PE-Cy5 conjugates by preparing Cy5-labeled anti-PE antibodies, which could be complexed with PE-labeled antibodies; they observed that energy was transferred efficiently from PE to Cy5 in such complexes, enabling them to be used as a third label in combination with fluorescein- and PE-labeled antibodies, provided uncombined anti-PE antibody sites were blocked. Energy transfer is at least as efficient in PE-Cy5 conjugates as in complexes; Figure 7-9 (p. 296) and Figure 1-18 (p. 37) demonstrate that there is much less emission spectral overlap between PE and a PE-Cy5 conjugate than there is between PE and a PE-Texas Red conjugate. Accordingly, less fluorescence compensation is required. PE-Cy5-labeled monoclonal antibodies are widely available.

The list of phycoerythrin tandem conjugates has expanded considerably since the last edition of this book was written; it now includes PE-Cy5.5 (emission maximum near 700 nm) and PE-Cy7 (emission maximum near 770 nm). As you will find in Chapter 8, there are now flow cytometers on the market that will allow you to make simultaneous measurements of the fluorescence of fluorescein, PE, PE-Texas red, PE-Cy5, PE-Cy5.5, and PE-Cy7, and side scatter to boot, using a single 488 nm excitation beam. Don't look for hardware compensation in those puppies.

Allophycocyanin Tandem Conjugates: APC-Cy7 and APC-Cy5.5

In the last edition, I suggested that "It might...be desirable to prepare tandem conjugates of APC that could be used in conjunction with APC itself for multicolor immunofluorescence measurements employing a 633 nm He-Ne or 635 or 650 nm diode laser source." It didn't take long for this to happen; in 1996, Roederer et al[2629] and Beavis and Pennline[2630] contested priority for APC-Cy7, when the paper that had been accepted first was published second[2630]. APC-Cy5.5 seems to have just come along out of the blue (or the far red); I couldn't find a claimant on MEDLINE. APC-Cy7 emits maximally near 770 nm, and APC-Cy5.5 near 700 nm; both are now available from a number of companies, conjugated to a variety of monoclonal antibodies.

Mercy Me! PerCP!

The first new reference added to the Third Edition, reference 1027, by Mandy, Bergeron, Recktenwald, and Izaguirre, was a tandem in its own way. It introduced the concept of T cell gating for lymphocyte subset analysis (see pp. 30-4 and 277); it also described the use of a new third label, **peridinin chlorophyll protein**, or **PerCP**. This material is a component of the photosynthetic apparatus in a dinoflagellate; as illustrated in Figure 7-9, it has an absorption maximum near 490 nm and a relatively sharp emission peak at about 680 nm. The sharpness of the emission peak minimizes crosstalk between PerCP and PE, and therefore also minimizes the amount of fluorescence compensation needed.